EXPLORING THE ROLE OF SELENOCYSTEINE BIOSYNTHESIS ENZYME SEPHS2 IN CANCER

A Dissertation Presented

By

ANNE ELISABETH CARLISLE

Submitted to the Faculty of the

University of Massachusetts Graduate School of Biomedical Sciences, Worcester

in partial fulfillment of the requirements for the degree of

DOCTOR OF PHILOSOPHY

NOVEMBER 6, 2020

CANCER BIOLOGY PROGRAM

EXPLORING THE ROLE OF SELENOCYSTEINE BIOSYNTHESIS ENZYME SEPHS2 IN CANCER

A Dissertation Presented By

ANNE ELISABETH CARLISLE

The signatures of the Dissertation Defense Committee signify completion and approval as to style and content of the Dissertation

_____
Dohoon Kim, Ph.D., Thesis Advisor

_____
Leslie Shaw, Ph.D., Member of Committee

_____
David Guertin, Ph.D., Member of Committee

_____
Arthur Mercurio, Ph.D., Member of Committee

_____
Nada Kalaany, Ph.D., External Committee Member

The signature of the Chair of the Committee signifies that the written dissertation meets the requirements of the Dissertation Committee

_____
Eric H. Baehrecke, Ph.D., Chair of Committee

The signature of the Dean of the Graduate School of Biomedical Sciences signifies that the student has met all graduation requirements of the school

_____
Mary Ellen Lane, Ph.D., Dean of the Graduate School of Biomedical Sciences

Cancer Biology Program
November 6, 2020

DEDICATION

To my late father

Thomas Craig Tacha, Ph.D.

I have thought of my dad more times than I can count in the past few years of my life in graduate school. Many times, I was encouraged by the idea that if he could complete his Ph.D., then I can too. Countless times I wished for his advice. My dad taught me to live my best life, and to love and appreciate those you care about fiercely, because you never know which day might be your last.

I love you Pops, and I know you're here with me.

ACKNOWLEDGEMENTS

Here we are! I have so many people to thank for all their help in the last 5 and a half years of my Ph.D. journey. It really takes a village, just like they say. Maybe they originally said that about raising children, but I think it applies here too.

First, I want to sincerely thank my mentor Dohoon Kim, Ph.D. He took a chance on me when he invited me to join his lab, and I will forever be grateful. He has been a patient and kind mentor to me. I appreciate how much he has trusted me to help him develop the Kim Lab from the beginning. I know that I could be challenging, as I was always asking questions and asking for justification. He guided me through this project and the past 4+ years in lab. He always asked how my weekend was in our Monday meetings, because he knew how important a life outside of lab was. Thank you for teaching and guiding me as I learned to grow into a scientist.

The Kim lab members have also been very important in my grad school journey. Namgyu Lee Ph.D., Mihir Doshi, Austin Peppers, and Meghan Spears as the current lab members as well as lab alum Kevin Krupczak– all of you have helped shape who I am as a scientist and a person today. Namgyu, I could not have done this without you! Thank you for contributing so much to my project, and for being a great mentor. You always made time to help me. I know you will be an amazing P.I. one day. Mihir and Austin, thank you so much for helping me with experiments along the way. You both made the lab environment a fun place to be. Kevin taught me so much in the beginning. Even though we only worked together for 6 months, you taught me virus making and tissue culture techniques that I used for the rest of my thesis. Thank you so much for being so

welcoming in the beginning. I would also like to thank the colleagues who are not in the Kim Lab that contributed to my thesis study and don't have another section later –Sung Jin Park Ph.D., Daniel Youkana, Rui Li Ph.D., Alexander B. Joseph, Miles Smith Ph.D., Karl Simin Ph.D., Julie Zhu Ph.D., and Paul Greer Ph.D. And of course, I didn't forget about Meghan – she has her own section later.

I also want to mention how thankful I am for my mentorship committee. Eric Baehrecke Ph.D., Leslie Shaw Ph.D., Dave Guertin Ph.D. and Arthur Mercurio Ph.D. – thank you all so much for your guidance over the years. Most of you served on my Qualifying Exam Committee and have been with me since the beginning. Thank you for all of your meaningful comments and advice. Leslie, thank you and your lab for your help and advice as I learned *in vivo* techniques in mice. Eric, thank you for your patience with me as I tend to plan way in advance and have a million questions.

I would also like to thank my other colleagues in the Molecular, Cell and Cancer Biology department, past and present. Jenny Janusis, Justine Roderick, Matija Zelic, Liz Allen, John Amante, Shauna Dandy, Andy Melber—thank you for all of your help and advice through the years. A big thank you to Caitlin Brown, Kevin O'Connor, Sharon Briggs and Peter Chhoy for your help as well. Kevin and Peter, I appreciate our long talks and I'm thankful to have had those times as a break from the experiments. I'd also like to thank anyone else I may have missed, especially those on the fourth floor LRB. Thank you for lunches on the couches in the lobby and for pie baking contests and wing eating adventures. I appreciate you all.

I would also like to thank the GSBS Dean, Mary Ellen Lane Ph.D., for all of her advice and support through the years. Your personal messages of encouragement were so very kind. I am thankful to have been able to work with you through my student leadership positions. A big thank you also to Morgan Thompson, who was always looking out for us and helped so much with student leadership. What strong and amazing women leaders I have had as role models! Of course, I must thank the ladies who keep it all running – Mindy Donovan, Annette Stratton and Barbara Buccagalia. It was always a pleasure to see your smiling faces in the GSBS office. I will miss saying, "Hello ladies."

A very, very important part of my time in graduate school has been experiencing it with the friends I have made along the way. We got through the first year together and spent many late nights studying, and also not studying. My crew from the beginning—Meghan Spears, Kristin Abramo Ph.D., Kevin Luk, Jake Gellately, Kayleigh Gallagher Ph.D., James Gilbert, Mike Jones, Gordie Lockbaum Ph.D. – I'm so thankful to have experienced grad school alongside you. And also, Suzy Xu, Jooyoung Lee Ph.D., and David Stelter Ph.D.—I'm so thankful that I have gotten to know you all as well. I look forward to many more drinks, brunches, dinners, barbecues and ski trips. Some of us have taken our next steps already, and now it's my turn. I am extremely proud of you all. I can't wait to see what's next for all of us. There aren't enough words so just...thank you for everything. I love you all.

Also, a huge shoutout to the MD/Ph.D. friends who are so important to me. Asia Matthew-Onabanjo Ph.D. and Peter Cruz Gordillo Ph.D., both of you impress me so much in both your careers and your lives. I am so grateful that you are a part of my

village, and I am a part of yours. Asia, I very realistically could not have done this without you. Thank you for your endless support and for teaching me everything I know about mouse work. Peter, I think one of the very few good things that 2020 has given me so far is getting to know you better and becoming your friend. I was, and am, so proud of you both. Thank you for your never-ending light, optimism and encouragement. I love you.

I want to give a special shout-out to my girls. Kristin, you were my first friend here at UMMS. I was so lucky to have you in those first few months, and I still am very grateful to have you in my life. I loved living just down the street from you, when we could pop over for a drink or a movie night. I cherish those memories, and all of the others. I love you. Thank you for inviting me to years of Thanksgivings and Easters with your family. Paul and Lorraine, thank you for all of the generosity over the years.

Meghan, Meg, buddy, bestie – wow, here we go. We've been a pair for so long that I still can't wrap my head around taking the next step and not being able to turn my chair and talk to you, 6 feet away. How many times have people asked one of us where the other is, on the off chance we wander out of lab without one another? Being in lab with your best friend for 4 and a half years has presented a couple challenges, but they have been vastly outweighed by how amazing this experience has been. The entire time, I knew I had someone right there with me who I could talk to about the big ups and downs of grad school and life, just as easily as I could check some quick dilution math with you. There is something very special in having a best friend that you can share so much with. I am endlessly grateful for you. I can't wait to experience what comes next, just as we have

the past few years—maybe not physically together as much, but there for each other just the same. I look forward to Sunday dinners. I love you.

I have been so lucky to have spent these past few years knowing how much my family supports me. You are all always in my corner and for that I am forever grateful. Momma, Susan, Bill – we may only be able to see each other a few times a year but those moments mean everything to me. Thank you, Gramma for always supporting me. You have told me so many times that you are proud, and it means so much to me. Aunt Sylvia and Uncle Denny, thank you for making it clear that I'm welcome any time at your house— I'm there so often that it's become like a second home. Being with you while taking a break from school and lab has meant everything to me. Thank you for opening your home to me. Uncle Tom, Aunt Barbara, Uncle Bill, Aunt Kathy – I have loved seeing you almost every October for the past few years. Spending time together means so much to me, especially now when I don't get to see you for the first time in years. It was also so special to be able to see all my cousins last year – thank you all for your support. To all of you, my dear Carlisles, I could write pages and pages in your honor. For the sake of brevity, I will just say thank you and love you very much.

I would also like to take a moment to extend the dedication of this thesis to the family members I have lost. To Ethlyn and Bill Tacha, Frank Jefferson Carlisle Jr. (Grampa), and Frank Jefferson Carlisle III (Uncle Jeff) – your support meant everything to me while you could give it. I know you're here with me now.

A special thank you goes out to my immediate family. To my mom's wife, Susan Sullivan—without a doubt, I wouldn't be where I am today without you. If you hadn't lit

a fire under my butt as an aimless teenager, I never would have had the drive to pursue graduate school and push through these last years. You have been a role model for me for the majority of my life. Your work ethic has always been a great example. I'm so glad we're family. And Bill, big bro, thank you for always being in my corner. Even if it's just a quick reply to a Snapchat, I'm so glad every time we get to talk. I love you both, very much.

Finally, and perhaps most importantly, I huge thank you to my mom, Martha Carlisle. My momma is the first person I call after a tough day or to celebrate an achievement. There aren't enough words to tell you how much your endless support means to me. You have been my cheerleader every step of the way! You help me through the lows and celebrate the highs. In part, this thesis is also for you, because I couldn't have done this without you. I'll love you forever, I'll like you for always. Thank you for everything.

ABSTRACT

Selenium is a micronutrient that is used by the selenocysteine biosynthesis pathway to produce the amino acid selenocysteine, which is required in selenoproteins. Many of the 25 human selenoproteins, such as glutathione peroxidases and thioredoxin reductases, play important roles in maintaining cellular redox homeostasis. In this study we characterize how this metabolic pathway is upregulated in cancer cells and how this increase in activity creates a unique vulnerability. We have outlined the evidence and underlying mechanisms for how many metabolites normally produced in cells are highly toxic, and we describe this concept as illustrated in selenocysteine metabolism.

My thesis explores how SEPHS2, an enzyme in the selenocysteine biosynthesis pathway, is essential for survival of cancer, but not normal cells. SEPHS2 is required in cancer cells to detoxify selenide, an intermediate that is formed during selenocysteine biosynthesis. Breast and other cancer cells are selenophilic, owing to a secondary function of the cystine/glutamate antiporter SLC7A11 that promotes selenium uptake and selenocysteine biosynthesis, which, by allowing production of selenoproteins such as GPX4, protects cells against ferroptosis. However, this activity also becomes a liability for cancer cells because selenide is poisonous and must be processed by SEPHS2. These results show that SEPHS2 is a cancer specific target and indicates the therapeutic potential of SEPHS2 inhibition in the treatment of cancer. Collectively, this thesis identifies SEPHS2 as a targetable vulnerability of cancer cells, defines the role of selenium metabolism in cancer, and outlines a roadmap for future studies regarding toxic metabolites and cancer.

TABLE OF CONTENTS

LIST OF TABLES AND FIGURES

LIST OF ABBREVIATIONS

KEGG – Kyoto Encyclopedia of Genes and Genomes

CRISPR/Cas9 – Clustered regularly interspaced short palindromic repeats/CRISPR

KO – knock out

gRNA – guide RNA

SEPHS2 – selenophosphate synthetase 2

Sec-tRNA – selenocysteinyl-tRNA

PSTK – including phosphoseryl-tRNA kinase

SEPSECS – selenocysteine synthetase

SECIS – selenocysteine insertion sequence

SBP2 – selenium binding protein 2

eEFSec – selenocysteine-specific eukaryotic elongation factor

SCLY – selenocysteine lyase

SEPHS1 – selenophosphate synthetase 1

SPS – selenophosphate synthetase

HSDB – Hazardous Substance Data Bank

ROS – reactive oxygen species

Mg^{2+} – magnesium

SARS-CoV-2 – severe acute respiratory syndrome coronavirus-2

SIRS – systemic inflammatory response syndrome

NIOSH – National Institute for Occupational Safety and Health ()

GPX – glutathione peroxidase

H_2O_2 – hydrogen peroxide

GSH – glutathione

TXNRD – thioredoxin reductase

SEPP1 – selenoprotein P

SELI –selenoprotein I

SELM – selenoprotein M

NPC – Nutritional Prevention of Cancer

SELECT – Selenium and Vitamin E Cancer Prevention Trial

CIN1 – cervical intraepithelial neoplasia grade 1

RCC – renal cell carcinoma

MRPs – multidrug resistance proteins

TOXNET – NIH Toxicology Data Network

CTRL – non-targeting control gRNA

CC3 – Cleaved caspase 3

UCM – unconditioned medium

TBH – tert-butyl hydroperoxide

Ferr – Ferrostatin-1

CAT – Catalase

LC-MS – liquid chromatography– mass spectrometry

PVP – polyvinylpirolidone

ICP-MS – inductively coupled plasma mass spectrometry

OE – overexpression

DTNB – 5,5′-dithiobis-(2-nitrobenzoic acid)

IACUC – Institute Animal Care and Use Committee

IRB – Institutional Review Board

ISH – in situ hybridization

NRF2 – NF E2 Related Factor 2

KEAP1 – Kelch-like ECH-associated protein 1

HIF-1 – Hypoxia-inducible factor 1

RNAi – RNA inhibition

GEPIA – Gene Expression Profiling Interactive Analysis

OD – optical density

IPTG – isopropyl β- d-1-thiogalactopyranoside

FPLC – fast protein liquid chromatography

Q column – quaternary amine column

COPYRIGHT INFORMATION

The following figures are reproduced from publications with permission.

Figure Number	Publisher	License
Figure 1.3	Elsevier	4927250032872
Figure 1.4	PNAS	No permission required

PREFACE

All of the work presented in this thesis was performed at the University of Massachusetts Medical School in the laboratory of Dohoon Kim.

Parts of this dissertation have been published as:

Carlisle, A. E. et al. Selenium detoxification is required for cancer-cell survival. **Nat Metab** 2, 603-611, doi:10.1038/s42255-020-0224-7 (**2020**).
Publisher: Springer Nature
License: 4927260045666

Lee, N., Spears, M. E., **Carlisle, A. E.** & Kim, D. Endogenous toxic metabolites and implications in cancer therapy. **Oncogene** 39, 5709-5720, doi:10.1038/s41388-020-01395-9 (**2020**).
Publisher: Springer Nature
No permission needed

CHAPTER I:

INTRODUCTION

Portions of this chapter are adapted from:

Lee, N., Spears, M.E., Carlisle, A.E. *et al.* Endogenous toxic metabolites and implications in cancer therapy. *Oncogene* **39,** 5709–5720 (2020). (https://doi.org/10.1038/s41388-020-01395-9)

N.L. and D.K. conceived the review; M.E.S. designed the figures. N.L., M.E.S. A.E.C and D.K. wrote the manuscript with consultation from all of the authors.

Cancer

The National Cancer Institute Surveillance, Epidemiology and End Results Program (SEER) reports that the average age adjusted all-sites cancer incidence rate across all sexes, ages and races for the years 2013-2017 to be 442.4 out of 100,000. Additionally, SEER reports that the 5-year age adjusted mortality rate of cancer for the years 2014-2018 to be 155.5 out of 100,000[1]. Not only is cancer a prevalent and deadly disease, but many of the leading drug and radiation-based therapies are highly cytotoxic, leading to extreme side effects. Therefore, it is necessary to work towards developing therapies that are specific to cancer cells without damaging normal cells. It may be beneficial to target cancer-specific hallmark characteristics, such as altered metabolism, to enhance the specificity of chemotherapeutics and decrease unwanted cytotoxic effects[2].

Toxic metabolite approach to cancer therapy

Metabolism is an aspect of cancer biology that is attractive in terms of therapy. First, it has been known for a long time that the metabolism of cancer cells differs from that of normal cells in many ways. A widely known metabolic alteration in cancer cells is high glucose consumption and high levels of lactate production with a lack of oxidative phosphorylation, referred to as the Warburg effect[3,4]. Another commonly observed metabolic perturbation in cancer cells is the deregulated uptake of amino acids[5]. In particular, many cancer cells are highly dependent on glutamine for their survival and proliferation[5]. In addition, lipid metabolism is also modified in cancer cells[6] because

rapidly proliferating cells require fatty acids for the synthesis of signaling molecules and membranes[7]. The identification of such cancer-specific metabolic changes provides the opportunity to develop novel therapeutic strategies to treat cancer. The "druggability" of enzymes further adds to the appeal of cancer metabolism as a therapeutic avenue. Druggable enzymes have small, hydrophobic pockets in regions required for their activity. Enzymes are, by their catalytic nature, highly druggable, due to their pockets for their substrates and coenzymes[8,9]. Even if cancer-selective targets are identified by characterizing the role of the targets in cancer, it can be difficult to translate the basic research into the clinic if the targets are not easily druggable.

Much of cancer metabolism research has centered on the idea of targeting the "cellular building blocks" that cancer cells require, and there are notable examples of clinical efficacy (Fig. 1.1a). Cancer cells upregulate a variety of metabolic pathways involved in the production of cellular building blocks that support the increased demand for the biosynthesis of proteins, lipids, and nucleic acids[10]. While the approach of starving a cancer cell of these essential metabolites is both logical and proven[11-13], there are also some important factors that can limit the effectiveness of this strategy in killing a cancer cell. First, when the biosynthetic pathway for an essential metabolite is disrupted, there may be mechanisms by which a cell can salvage it through a secondary route (Fig. 1.1b). This can occur by compensatory production of the metabolite through an alternative pathway, uptake from the extracellular environment, or breakdown of existing macromolecules in the cell[10]. Therefore, the potential for multiple sources of essential

building blocks can make targeting a biosynthetic enzyme insufficient to limit a metabolite adequately to kill a cancer cell.

Second, a metabolic enzyme that appears to be essential in tissue culture may not end up being essential in a more physiological (*in vivo*) context, as typical culture media conditions do not accurately reflect the diversity and quantity of metabolites that are available in the human bloodstream[14]. Uric acid, pyruvate, taurine and various other metabolites are present at higher levels in human serum than in culture media[14]. Consequently, disrupting a biosynthetic pathway may sufficiently deprive cells of an essential metabolite in tissue culture, while *in vivo* the cells may be able to obtain the metabolite from the bloodstream.

As illustrated, there are multiple reasons why targeting a particular enzyme that produces cellular building blocks may not be effective to kill a cancer cell. Thus, even when this enzyme appears to be important to a cancer cell, either due to the product it makes or due to it being increased in expression and/or activity, targeting it may not translate to effective therapy. Fig. 1.1 outlines an alternative approach: the notion of killing cancer cells not by impairing the production of biosynthetic building blocks, but rather by inducing an accumulation of toxic intermediates that lie within metabolic pathways. Assuming a standard linear metabolic pathway that involves the stepwise chemical conversion of a series of metabolites, the loss of an enzyme that converts toxic metabolite “b” to a nontoxic metabolite “c” may result in the accumulation of “b” to toxic levels in the cell (Fig. 1.1c). This approach may overcome some of the aforementioned limitations of the building block deprivation approach. Even if alternate synthesis or

uptake routes exist for the building block synthesis, it cannot remedy the issue of accumulated toxic metabolites. Importantly, if this metabolic pathway is more active in a particular type of cancer cell compared with a normal cell, then the accumulation of “b” should occur at a greater rate in the cancer cell, providing a therapeutic window. The more toxic metabolite “b” is, the more likely it is that the disruption of the downstream enzyme will be detrimental to the cancer cell.

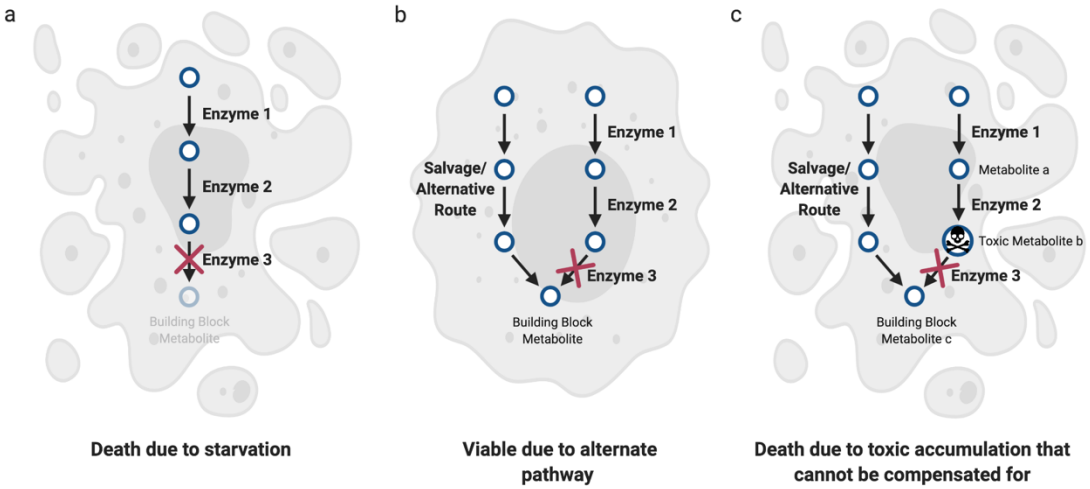

Figure 1.1 – Scenarios for targeting metabolic enzymes that produce essential cellular building blocks in cancer

a. Targeting a metabolic enzyme to disrupt the production of a metabolite that is essential to a cancer cell can be an effective therapeutic strategy.

b. When there are alternate means for production or acquisition of an essential metabolite, targeting the synthesizing enzyme may be inadequate to kill a cancer cell.

c. An alternative approach is to target an enzyme directly downstream of a toxic metabolite, which will result in accumulation of the upstream toxic metabolite. Even if there are alternative routes for producing the building block metabolite, this strategy should still work to exert toxicity in a cancer cell.

Figure adapted from:

Lee, N., Spears, M.E., Carlisle, A.E. *et al.* Endogenous toxic metabolites and implications in cancer therapy. *Oncogene* **39,** 5709–5720 (2020).

It may seem counterintuitive that endogenously produced metabolites, which in many cases form the building blocks of the cell, can be poisonous. However, when cross referencing known metabolites with toxicity databases such as TOXNET[15] or HSDB[16], it becomes clear that many metabolites have toxic profiles. As a striking example, the commonly utilized toxic fixative formaldehyde is produced naturally in the brain via oxidative breakdown of the folate backbone[17]. It can be inferred that under normal physiological conditions, the levels of potentially toxic metabolites in the cell are maintained at nontoxic levels either via further metabolism by detoxifying enzymes or efficient secretion mechanisms. Demonstrating this notion, many inborn metabolic disorders such as phenylketonuria or maple syrup urine disease, which involve loss of function mutations in amino acid breakdown genes, are thought to be caused by toxic accumulation of amino acid degradation pathway metabolites, as dietary amino acid restriction can ameliorate or prevent the pathology[18,19]. Here, endogenous metabolites are defined as those that are annotated by Kyoto Encyclopedia of Genes and Genomes (KEGG)[20] as substrates or products of the ~1900 metabolic enzymes encoded in our genome[21]. By cross-referencing the KEGG list of endogenous metabolites with the aforementioned toxicity databases, we developed a working list of endogenous metabolites with reported toxic properties. We call this categorization the “endotoxome.”

These metabolites that are normally produced in cells and have toxic properties suggest that their accumulation would be deleterious to a cell. This has an important implication for the function of metabolic enzymes—that enzymes that process a toxic metabolite in a pathway may serve an important detoxification function, as they prevent

accumulation of toxic metabolites. This suggests that it may be possible to induce poisoning of cancer cells with an accumulation of toxic metabolites that they themselves have produced, by targeting such “detoxification enzymes”. Thus, the detoxifying enzymes represent novel and druggable targets for killing cancer cells.

But how can a therapeutic window exist for such a mechanism, so that the toxicity occurs primarily in cancer cells? In theory, the detoxification requirement would be in proportion to the production of the toxic metabolite in the first place. This can be analogized as a “kitchen sink” model (Fig. 1.2), where the faucet represents the upstream metabolic enzymes or transporters that are responsible for formation or import of the toxic metabolite, and the drain represents the “detoxifying” enzyme preventing the overflow of the sink with the toxic metabolite (Fig. 1.2a). In this model, the drain is only required in cells in which the faucet is on, i.e., the toxic metabolite is appreciably being produced. Thus, if certain cancer cells produce a particular toxic metabolite at a greater rate than normal cells (Fig. 1.2b, c), they should be more dependent on the detoxifying enzyme than normal cells, and drugs that target this detoxifying enzyme should be selectively toxic toward these cells. Also, disruption of the upstream toxic metabolite producing step should rescue against the effects of detoxifying enzyme KO, if the detoxifying enzyme was required for detoxification rather than what it produces (Fig. 1.2d).

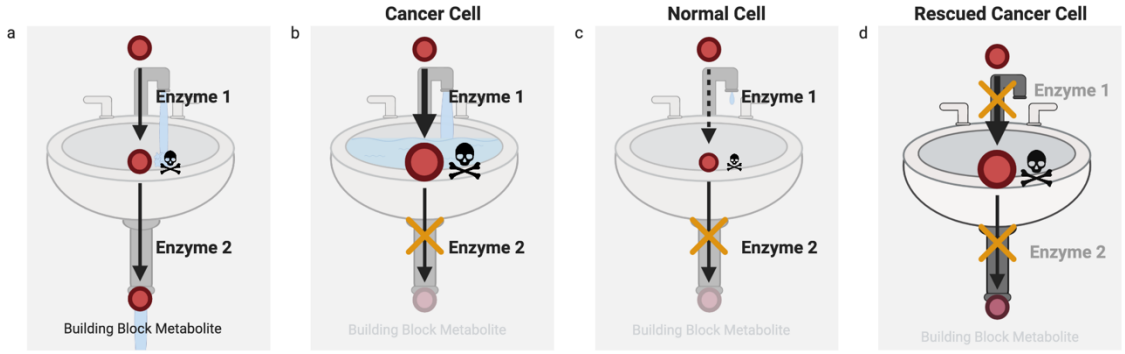

Figure 1.2 – Kitchen sink model for metabolic pathway containing toxic metabolite
Red dots and arrows represent metabolites and enzymatic reactions, respectively. Faucet and drain of kitchen sink are analogies of enzymatic reactions of upstream and downstream metabolic enzymes, respectively; the basin represents the accumulation level of the toxic metabolite.
a. The level of toxic metabolite candidate is constantly maintained at a nontoxic level as both faucet and drain are opened (active), balancing metabolite production and removal.
b. Example of toxic metabolite accumulation by targeting the downstream detoxification enzyme. Enzyme 1 and Enzyme 2 are the faucet and drain for toxic metabolite buildup in the pathway. Many cancer cells have elevated Enzyme 1 expression relative to normal cells and are able to import precursors and produce toxic metabolites at an elevated rate. Thus, their faucet is wide open, and disrupting Enzyme 2 is akin to blocking the drain, resulting in toxic overflow.
c. However, in normal cells, disrupting Enzyme2/blocking the drain is not a problem as the faucet is relatively "closed". In both **b** and **c**, building block metabolite cannot be produced, yet only **b** is toxic, indicating that the toxicity must have come from toxic metabolite accumulation rather than consequences of downstream building block production.
d. Similarly, in a cancer cell such as in scenario **b**, the preemptive KO of the upstream Enzyme 1 rescues the cells against the toxic effects of Enzyme 2 KO, further demonstrating that toxicity in **b** was due to toxic metabolite accumulation.
Created with BioRender.com.

Figure adapted from:
Lee, N., Spears, M.E., Carlisle, A.E. *et al.* Endogenous toxic metabolites and implications in cancer therapy. *Oncogene* **39,** 5709–5720 (2020). (https://doi.org/10.1038/s41388-020-01395-9)

CRISPR/Cas9 as an Investigative Tool

Clustered regularly interspaced short palindromic repeats/CRISPR associated gene 9 (CRISPR/Cas9) is a robust method for investigating the buildup of toxic metabolites *in vitro*. This system can be superior to others, especially in the study of metabolism. Gene silencing techniques such as shRNA result in a "knock down" of the gene of interest[22]. It is true that in many cases, a substantial decrease in protein expression results in a significant phenotype. The study of metabolism may be one of the areas of study that instead benefits from the use of CRISPR/Cas9. CRISPR/Cas9 techniques commonly result in a complete "knock out" (KO) of the protein of interest[23,24]. In the case of enzyme disruption, KO is superior to knock down due to the variable activity of metabolic enzymes. For example, if a shRNA was used to knock down an enzyme with a very high activity, it is possible that the remaining levels of enzyme have enough activity to result in a similar phenotype to control cells. The complete elimination of enzyme using CRISPR/Cas9 guarantees that one can observe the metabolic consequences of removing an enzyme from the cell.

Using CRISPR/Cas9, it is possible to systematically knock out detoxifying enzymes of interest and investigate the effects on viability of cancer cells. We developed a method for determining essential detoxifying enzymes by using lentivirally transduced CRISPR/Cas9 to systematically KO enzymes downstream of potentially toxic metabolites in a panel of multiple cancer cell lines. This method was developed to take into account the varying infectability and growth rates of different cancer cell lines. We compare the viability of cells infected with CRISPR/Cas9 and the guide RNA (gRNA) of

interest to the same cells that are infected with a non-targeting guide. These cells were assayed for viability over 5 days of growth with the KO and compared to control. Candidates for essential detoxifying enzymes were deemed promising if KO of the enzyme with multiple gRNAs resulted in significantly decreased cancer cell viability when compared to the control non-targeting gRNA. It was particularly important to observe a differential toxicity across the cancer cell line panel, i.e. some cell lines were harmed by the gene KO and some were not. This indicated to us that the enzyme was not pan-essential for all cell survival.

Selenocysteine Biosynthesis Pathway

Selenium is an essential micronutrient in humans that is taken up in the diet[25-27]. Although selenium content varies widely due to different selenium levels in soil and water sources, foods generally high in selenium include eggs, meat, fish and legumes[28,29]. Selenium can be found in multiple different forms in these foods, including organic forms selenocysteine and selenomethionine, and inorganic forms selenite (SeO_3^{2-}) and selenate (SeO_4^{2-}) (Table 1.1). These compounds are readily absorbed via the small intestine, enter the bloodstream and are taken up by cells and metabolized to selenocysteine[30,31].

The *de novo* selenocysteine metabolism pathway is a multi-step process. In the case of selenite, one of the common dietary forms of selenium, selenocysteine metabolism begins with its reduction to selenide (H_2Se)[32]. This occurs in the reducing environment that is created by reactive thiols in the extracellular space[33]. Selenide is likely the source of selenium that is taken up by the cells and processed by

Name	Structure
Selenate	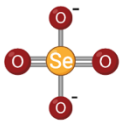
Selenite	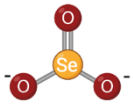
Selenide	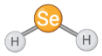
Selenophosphate	
Selenocysteine	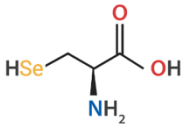
Selenomethionine	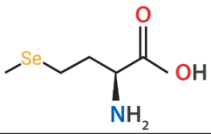

Table 1.1 – Inorganic and organic selenocompound structures
Created with BioRender.com

selenophosphate synthetase 2 (SEPHS2)[34]. SEPHS2 uses ATP and selenide as substrates for the formation of selenophosphate[35]. Selenophosphate is then converted to selenocysteinyl-tRNA (Sec-tRNA) in a multistep process including phosphoseryl-tRNA kinase (PSTK), which provides the phosphoseryl intermediate tRNA and serves as a substrate for selenocysteine synthetase (SEPSECS)[36]. SEPSECS processes the phosphoseryl-tRNA and selenophosphate, which acts as the selenium donor for the production of Sec-tRNA[36]. This specialized amino acid is then incorporated into the production of selenoproteins.

An interesting facet of selenoprotein synthesis is the unique mechanism for selenocysteine incorporation. Sec-tRNA is integrated at a UGA codon[37,38]. Selenoprotein mRNA is unique in that it has a *cis*-acting 3' UTR stem-loop region called a selenocysteine insertion sequence (SECIS)[38,39]. This hairpin motif is necessary for recognition of the UGA codon as a selenocysteine insertion site and not a stop codon. Selenoprotein mRNA that has been mutated to take out the SECIS results in prematurely truncated proteins[40].

Additional translational regulation of selenoproteins occurs in the form of multiple cofactors. For example, selenium binding protein 2 (SBP2) is a positive regulator of selenoprotein expression that binds to the SECIS element and aids in the recognition of the UGA codon[41,42]. The selenocysteine-specific eukaryotic elongation factor (eEFSec) recruits Sec-tRNA and works in tandem with SBP2 to insert selenocysteine into nascent polypeptide chains at the UGA codon[43,44]. Multiple additional factors have been reported to have positive or negative regulation of selenoprotein

production, such as ribosomal protein L30[45-47]. This underlines the complex and highly regulated nature of the selenoprotein biosynthesis pathway.

Although organic forms of selenium, selenocysteine and selenomethionine, are ingested and taken into the bloodstream, these cannot be directly incorporated into selenoproteins. Instead, selenomethionine can be randomly incorporated into all proteins as a replacement for methionine, in which selenium replaces sulfur[48]. It has been reported that the main biological function of selenomethionine is as an unregulated pool of organic selenium[48]. For that selenium to be useful, selenomethionine must be converted to selenocysteine via the trans-sulfurization pathway[32]. Selenocysteine is then recycled into selenide via selenocysteine lyase (SCLY), processed by SEPHS2 and from there follows the *de novo* selenocysteine metabolism pathway[49,50]. Interestingly, SEPHS2 itself is a selenoprotein, so there is a feedback loop involved in SEPHS2 function and production.

It is important to note that SEPHS2 is not the only human enzyme named selenophosphate synthetase. Selenophosphate synthetase 1 (SEPHS1) is inappropriately named, however, as SEPHS1 does not produce selenophosphate[51]. Both SEPHS1 and SEPHS2 were identified after they were reported as homologous to the bacterial selenophosphate synthetase (SPS), encoded by the gene *SelD*[34]. Both SEPHS1 and SPS have cysteine containing active sites and therefore are not selenoproteins like SEPHS2. SEPHS1 has ATP hydrolysis activity and has been reported to play an essential role in redox homeostasis[52]. SEPHS1 is highly expressed in rapidly dividing cells, including during development and in cancer[52]. It has been reported that SEPHS1 is involved in intracellular redox homeostasis by regulating the expression and activity of proteins

participating in redox homeostasis such as glutaredoxin 1 in mice[52]. SEPHS1 does not function in the selenocysteine synthesis pathway. Knockdown of SEPHS1 with siRNA does not impair selenoprotein biosynthesis, and transfection of SEPHS1 into SEPHS2 knockdown cells also does not restore selenoprotein biosynthesis[51]. This indicates that SEPHS1 cannot functionally compensate for a lack of SEPHS2.

Selenide as a Toxic Metabolite

Selenide became a potential toxic metabolite of interest due to its reported toxic properties in multiple model organisms. According to the PubChem Hazardous Substance Data Bank (HSDB), hydrogen selenide gas is toxic when inhaled in as low a dose as 300 ppb for guinea pigs and 6.04 ppm in mice[16]. The mechanism for this toxicity has been reported as an increase in reactive oxygen species (ROS). Hydrogen selenide reacts with oxygen to create elemental selenium and hydroxyl radicals[53]. Reactive oxygen species have been reported to react with proteins and DNA and cause oxidative stress and cellular dysfunction, leading to cellular damage that signals for cell death[54].

SEPHS2 Structure

Study of the primary structure of SEPHS2 helps to elucidate its function. UniProt (Q99611) categorizations of key features include the selenocysteine active site at amino acid position 60[55]. Other important amino acids are the ATP binding sites at positions K63, D138, and D161[55]. Additionally, magnesium (Mg^{2+}) is a cofactor that

binds at residues D120, D161, and D316. Most of these amino acid sites are inferred by similarity to various SEPHS2 orthologs, including human SEPHS1 and bacterial SPS[56,57].

The secondary structure for human SEPHS2 enzyme has not been solved via x-ray crystallography. However, it is possible to infer the potential structure of SEPHS2 from the structure of bacterial SPS. SPS functions in the same manner as human SEPHS2 by using ATP and selenide as substrates for the production of selenophosphate[57]. Noinaj *et al.* reported that the SPS mutant C17S, a mutation that was required to solve the crystal structure, crystalizes as a homodimer due to the association of the N-terminal domains of each of the monomers. The two domains connect to form the active site, which sits within a long, narrow channel that runs the length of the protein[57].

The human SEPHS2 structure has been molecularly modeled *in silico*[58]. This report did not define whether SEPHS2 would form a homodimer similar to bacterial SPS, but instead reported a model structure for a single SEPHS2 protein using sequence analysis and a series of molecular modeling software packages. This group states that human SEPHS2 structure includes an N-terminal domain with an alpha-helix and a long, disordered loop, a central core with an alpha-beta 2-layer sandwich architecture and a disordered c-terminal domain. Conclusions from this model include that the Sec 60 active site is exposed on the surface of the protein at both a neutral and acidic pH and is stabilized by pi-cation and H-bond interactions of multiple key residues[58].

Toxic Consequences of Selenium Deprivation and Excess

The World Health Organization recommends that adult humans take in at least 25-35μg of selenium per day to support maximal production of selenoproteins[59]. Selenium content in food varies widely and multiple regions of the world including New Zealand, Finland, and parts of China contain soil that is low in selenium[60]. Selenium deprivation is evident in diseases that occur in livestock that are farmed in these areas such as skeletal myopathies in calves, cardiomyopathies in swine, and vascular disorders in poultry[61]. This deprivation is most severe in the Sichuan province of China and is associated with the higher incidence of human Keshan disease, an endemic cardiomyopathy that is common in children under 15 years of age and has a high mortality rate[62]. The relevance of selenium deprivation was confirmed by noting the lack of serum and hair selenium in patients with Keshan disease, as well as the decrease of incidence rates when children were given a selenite supplement[62].

Additionally, lack of selenium has been associated with an increase in pathology associated with infection. A report has shown that mice infected with a mild strain of influenza A and fed a selenium deficient diet had a much more severe pathology than mice fed a diet with normal levels of selenium[63]. Interestingly, it has recently been reported that selenium deficiency is associated with mortality risk from COVID-19, the disease that stems from severe acute respiratory syndrome coronavirus-2 (SARS-CoV-2) infection, which is the cause of the current global pandemic[64]. Patients that are suffering from systemic inflammatory response syndrome (SIRS) and have low serum selenium levels at admission suffered three times higher frequency of ventilator-associated pneumonia, organ system failure, and mortality in comparison to other patients[65].

However, it is not only selenium deprivation that results in damaging effects. Excess selenium can have pathological consequences. Interestingly, Marco Polo may have provided some of the first records of selenium toxicity sometime in the thirteenth century, as he wrote,

> "…they cannot venture amongst the mountains with any beasts of burden excepting those accustomed to the country, on account of a poisonous plant growing there, which, if eaten by them, has the effect of causing the hoofs of the animal to drop off."[66]

It has been reported that this effect, now referred to in the livestock trade as alkali disease, was due to the animals consuming the plants from the genus *Astragalus* that are common in parts of western China[67]. Many species of this plant have been deemed toxic due to their ability to concentrate selenium taken up from the soil[67]. The cause of this disease is likely the same as many other reports regarding selenium toxicity— that the buildup of hydroxyl and other oxygen radicals results from selenide reacting with oxygen.

Exposure to high levels of selenium, identified by the term selenosis, has been shown to result in many varied symptoms in humans including hair loss, garlicky breath, gastrointestinal disturbances, and upper airway irritation[68,69]. Selenosis can occur by accidental ingestion of gun-bluing agents, which have significant levels of selenious acid, as well as misformulated dietary supplements[70,71]. Direct hydrogen selenide gas exposure is rare but has been reported to occur in both research and industrial settings[72,73]. The National Institute for Occupational Safety and Health (NIOSH) defines the hydrogen

selenide gas exposure limit for humans as 0.05ppm. Hydrogen selenide is described as "a colorless gas with an odor resembling decayed horseradish" [74]. Although it has been established that hydrogen selenide inhalation can be very damaging, there are no reported cases of fatalities. This is likely due to the fact that hydrogen selenide can be oxidized to harmless colloidal red selenium at the mucous membranes of the nose and throat[75].

Selenocysteine and Selenoproteins

Selenocysteine is an analog of cysteine, where a selenium atom is substituted for sulfur[76,77] (Table 1.1). Selenocysteine provides a benefit to selenoprotein enzymes due to its lower pKa in comparison to cysteine, which allows the enzyme to have a higher reactivity at physiological pH[78]. In comparison to cysteine, selenocysteine is a more active nucleophile and therefore has a higher reactivity. The electrophilicity of the selenium atom itself may allow selenoproteins to resist irreversible oxidation, in contrast to cysteine which is difficult to reduce if over-oxidized[79]. These account for the multiple advantages that enzymes in the selenoproteome have over traditional cysteine containing enzymes.

The human genome encodes 25 selenoproteins. Many organisms have the required machinery to produce selenoproteins, although the number of selenoproteins in an organism's genome can vary from one (*Caenorhabditis elegans*) to 59 (*Aureococcus anophagefferens*)[80,81]. Interestingly, selenoproteins are completely lost in fungi and a number of higher animal species such as the silkworm and numerous insects[82]. Aquatic species trend toward having a more abundant selenoproteome, while most terrestrial

animals are comparatively conservative in their use of selenium in proteins[83]. The majority of these proteins function as enzymes with various roles within the cell and have a selenocysteine in their active site. However, some selenoproteins have analogous enzymes in other species where the active site selenocysteine is replaced with cysteine. Although most identified selenoproteins work in some red-ox related manner, they have a variety of biological roles[84,85].

An important subset of selenoproteins consists of various antioxidant enzymes. There are two families of selenoprotein antioxidants that have multiple isoforms—glutathione peroxidases and thioredoxin reductases. Glutathione peroxidases, of which there are 5 selenoprotein isoforms (GPX1/2/3/4/6), function to reduce hydrogen peroxide (H_2O_2) in a glutathione (GSH) dependent manner[86]. Reduction of H_2O_2 by glutathione peroxidase 1 (GPX1), converts the active site selenocysteine to selenic acid (-Se-OH). Selenic acid is then reduced by one molecule of GSH, leading to a glutathionylated selenol intermediate (-Se-SG). This selenol intermediate reacts with a second GSH molecule, restoring the active site selenocysteine and producing a single molecule of oxidized glutathione (GSSG)[87]. There are also 3 thioredoxin reductase isoforms, all of which are selenoproteins. Cytosolic thioredoxin serves as a substrate for thioredoxin reductase 1 (TXNRD1), and this pairing makes up the major disulfide reduction system of the cell[88]. Each one of these antioxidant selenoenzymes contains one selenocysteine moiety in its active site[84].

GPX1 and TXNRD1 are particularly abundant cytosolic antioxidants, while other isoforms tend to be organelle or tissue specific. For example, glutathione peroxidase 2

(GPX2) is expressed mostly in the gastrointestinal tract, and thioredoxin reductase 2 (TXNRD2) is located in the mitochondria[89,90]. Glutathione peroxidase 4 (GPX4) is a particularly well-studied selenoprotein, especially for its role in ferroptosis. Ferroptosis occurs when iron-dependent ROS leads to an increase in lipid peroxides[91]. It was first reported by Yang, *et al*. that GPX4 was a regulator of ferroptotic cell death. GPX4 can directly regulate this mechanism because of its specificity for reducing phospholipid hydroperoxides[92]. Further regulation comes from the cystine/glutamate antiporter xCT. xCT imports cystine, the rate limiting ingredient for glutathione synthesis[93,94]. As glutathione is necessary for the function of GPX4, the activity of xCT then also regulates GPX4 function and ferroptosis. xCT, selenium import and GPX4 will be further discussed in later sections.

Another subset of selenoprotein enzymes function in thyroid metabolism. These selenoproteins are three paralogous forms of iodothyronine deiodinases, DIO1/2/3, which function in regulating thyroid hormones via reductive deiodination[95]. These deiodinases have a specific sub-cellular localization— DIO1 and DIO3 are located in the plasma membrane, and DIO2 in the ER[96]. DIO2 is unique in the fact that it is one of the only selenoprotein enzyme that has an additional selenocysteine residue outside of the active site— the function of which is unknown[95]. Thyroxine, a major thyroid hormone, is secreted in its inactive form. DIO1 and DIO2 function to convert thyroxine to its active form 3,3’,5-triiodothyronine, while DIO3 catalyzes the removal of an inner ring iodine, deactivating the hormone again[97]. Therefore, the 3 selenoproteins in the thyroid function to balance the level of active secreted hormone.

There are a variety of selenoproteins that have been identified, most commonly with bioinformatic approaches that search for the specialized in-frame UGA codons and SECIS elements, that have not been well characterized. These selenoproteins are named with letters— examples include selenoprotein I (SELI) and selenoprotein M (SELM). Work continues on categorizing these selenoproteins, and many have putative reported roles. Selenoproteins H, T, V, and W are characterized as thioredoxin-like, and have reported functions in redox regulation and age-related degeneration[98]. Selenoprotein O plays a role in chondrocyte viability and proliferation[99]. Other lettered selenoproteins such as K, S, and N have putative roles in ER-associated degradation and oxidative stress, muscle development and inflammatory response[100,101].

The final categorization of the selenoproteome consists of secreted proteins. Both glutathione peroxidase 3 (GPX3) and selenoprotein P (SEPP1) are secreted from cells and function as antioxidants in plasma[102]. SEPP1 is particularly important for regulating pools of selenium throughout an entire organism, as it is abundantly expressed and accounts for 50% of selenium in plasma[103,104]. The function of SEPP1 is two-fold— it is both an antioxidant enzyme and a carrier for selenium, which is directly related to its abundance of selenocysteine residues[105]. SEPP1 contains 10 selenocysteine residues which can be broken down and recycled via SCLY in the recipient cell to produce selenocysteine *de novo*. Deletion of SEPP1 results in an increase of selenium in the liver as well as excreted selenium metabolites, and a sharp decrease of selenium levels in the brain and testis[106]. Therefore, it has been suggested that the liver is the main tissue for

uptake of selenium from the blood and SEPP1 secretion. SEPP1 then functions to carry selenium to peripheral tissues such as the brain.

Selenium and Cancer

While very little was known about the relevance of selenium metabolism enzymes to cancer before the study described in Chapter II, there has been extensive research into the relationship between selenium and cancer risk. Using a modification of a literature search and analysis method established by Vincenti, *et al.*, a PubMed search was conducted to provide an updated overview of the research on selenium and cancer[107]. This search, using the MeSH terms "selenium," "humans," and "cancer," and then choosing "Clinical Trials" as the Publication Type, identified 4,363 results with 279 (6%) of these results pertaining directly to clinical trials. Randomized control trials, in which patients are nutritionally supplemented with approximately 200μg of selenium per day, have been conducted in an attempt to understand the epidemiology of selenium supplementation and cancer incidence. Many of these trials, including the Nutritional Prevention of Cancer (NPC) and the Selenium and Vitamin E Cancer Prevention (SELECT) trials have had conflicting results that lead researchers to conclude that 200μg of selenium per day does not reduce the risk of overall cancer[107].

Interestingly, there are more promising results for the use of selenium as a cancer therapy. For example, women given 500μg of selenium (as sodium selenite) per day during radiation therapy for cervical and uterine cancers demonstrated a higher 5 year overall survival rate (91.9%) than those given a placebo (83.1%)[108]. Another study

showed that women diagnosed with cervical intraepithelial neoplasia grade 1 (CIN1) and treated with 200μg/day of selenium (as selenized yeast) for 6 months showed a higher regression rate of 88% versus 56% in those treated with placebo[109]. A search of the U.S. National Library of Medicine database ClinicalTrials.gov with the terms "selenium" and "cancer" shows multiple clinical trials that are openly recruiting as of October 14, 2020. These trials are seeking to use varying forms of selenium to prevent breast neoplasms, prevent chemotherapy-induced neuropathy, and treat renal cell carcinoma (RCC) in combination with chemotherapy. Although further research is necessary, the cervical and uterine cancer studies show selenium compounds as promising antineoplastic or adjuvant agents. It is important to note that while there is a lot of evidence of selenium toxicity in cancer, it has not yet led to a successful clinical application despite many attempts through the years.

Some selenoproteins have been highly studied in relation to cancer[85]. Because many selenoproteins have antioxidant functions, and altered redox homeostasis is implicated in tumor initiation and progression, it is reasonable that selenoproteins would play a role in cancer[110]. Overexpression of GPX1 has been linked to higher tumor burden in mouse models of skin cancer, as well as resistance to chemotherapy and radiation[111,112]. The siRNA mediated decrease of SEPP1 has been reported to increase ROS in prostate cancer cells[113]. However, the relationship between oxidative stress, selenoproteins, and cancer is complex. Increased oxidative stress can enhance tumorigenesis through genomic instability and mutation, but excess can be toxic and induce tumor cell death[114] (Figure

1.3). The relationship between oxidative stress and cancer is highly relevant to the study of selenium in cancer that is reported in Chapter II.

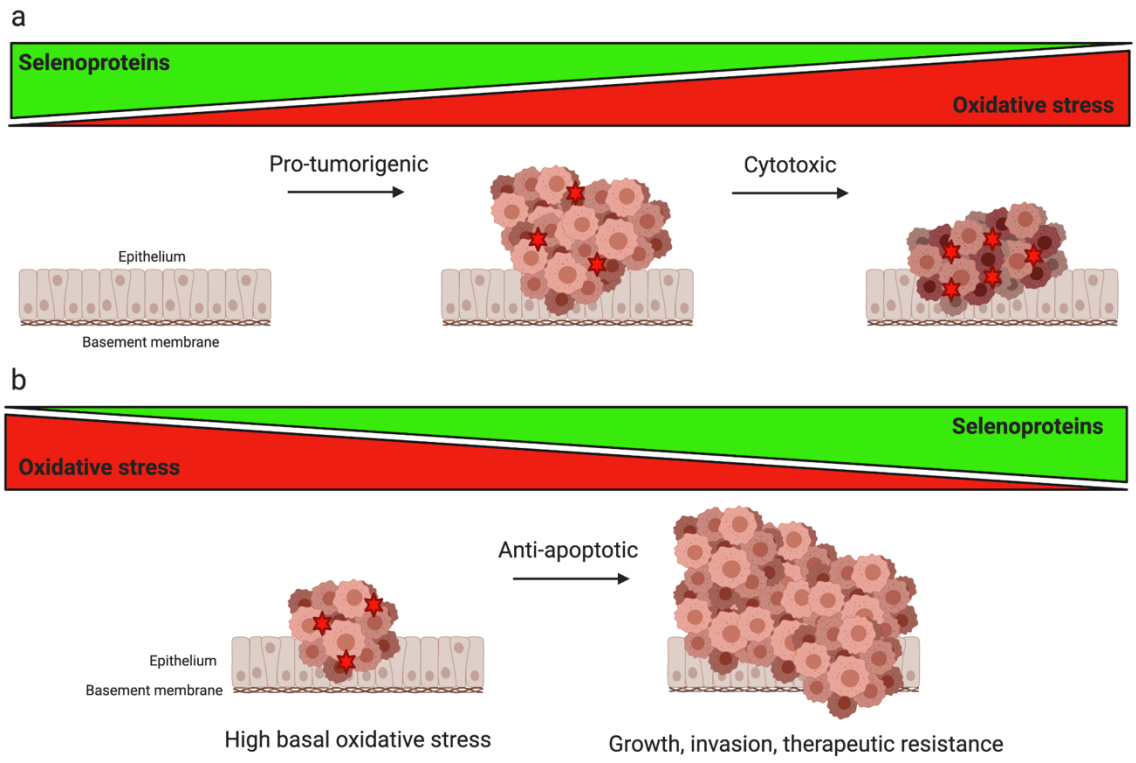

Figure 1.3 – Context-dependent effects of selenoprotein expression on oxidative stress and tumorigenesis

a. In normal epithelium, selenoprotein loss induces a moderate increase in oxidative stress which can increase DNA damage and favor tumor initiation, although high levels of oxidative stress can promote cytotoxicity resulting in tumor cell clearance.
b. In tumor cells with higher baseline levels of oxidative stress, increased expression of selenoproteins can protect from cytotoxic effects and can lead to increased tumor growth, progression, and therapeutic resistance.
Created with BioRender.com

Figure adapted from:
Short SP, Williams CS. Selenoproteins in Tumorigenesis and Cancer Progression. Adv Cancer Res. 2017;136:49-83.

xCT as a Regulator of Selenium Uptake

As far back as the 1960s, selenium has been shown to have an affinity for tumors. Cavalieri, *et al.* published a paper using Se^{75}, a radioactive isotope of selenium, as a tumor tracer in autoradiographs of lung cancer patients[115]. This affinity is likely explained by a phenomenon we call "selenophilicity." Cancer cells have a higher demand for selenoprotein antioxidants to maintain redox homeostasis, therefore they take up more selenium to produce antioxidant selenoproteins. xCT (also referred to as xc-) has been implicated as an essential mediator for selenocompound reduction and has been reported to play a role in selenium import[33,116].

xCT has been highly studied for its role in maintaining intracellular glutathione levels before the link between selenium and the transporter was suggested. The xCT transporter consists of two subunits that create a heterodimer that is linked by a disulfide bridge[93,117]. The gene *SLC7A11* encodes light subunit which is a functional transporter that has 7 transmembrane domains and is referred to both as xCT and SLC7A11. The gene *SLC3A2* encodes the heavy subunit 4F2hc, which is involved in trafficking the heterodimer to the plasma membrane[117]. These two subunits work in tandem to import cystine, the oxidized doublet form of cysteine, and export glutamate at a 1:1 ratio[93,94].

The cystine that xCT imports is readily reduced intracellularly to cysteine, which is then used for the production of glutathione and other functions. Cysteine is also exported out of the cell via multidrug resistance proteins (MRPs). Extracellular cysteine is readily oxidized into cystine, and this mechanism increases the levels of reduced thiol groups in the extracellular space[33]. A relationship between xCT function and selenium uptake has

previously been reported in which the authors suggest that xCT function and the resulting cysteine export and cystine import promotes selenium uptake related to the reduction of selenite to selenide[33] (Figure 1.4). The direct mechanism of physical selenide import is currently unknown.

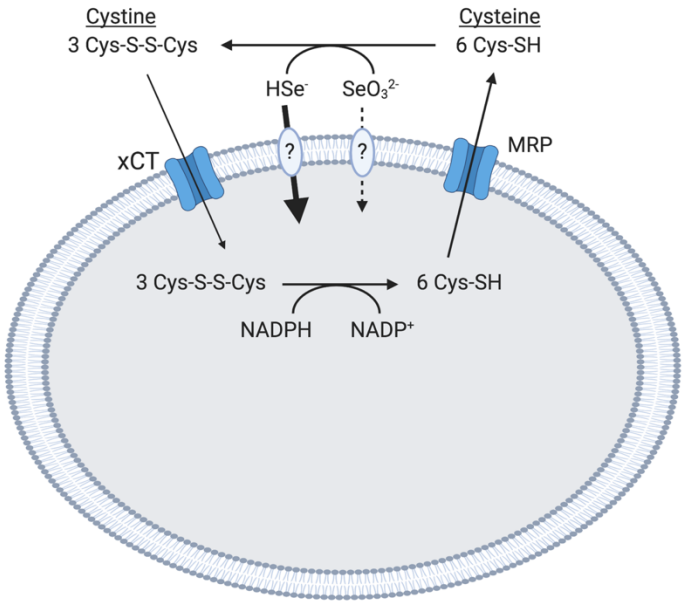

Figure 1.4 – Model for selenite cytotoxicity
The xCT cystine/glutamate antiporter facilitates the uptake of cystine, which is reduced intracellularly to cysteine by NADPH-dependent redox systems. A significant fraction of intracellular cysteine is re-secreted into the extracellular compartment by MRPs, causing a reductive extracellular microenvironment. Extracellular reduction of selenite leads to a high-affinity uptake of a reduced form of selenite, selenide, causing selenium accumulation and toxicity.
Created with BioRender.com.

Figure adapted from:
Olm E, Fernandes AP, Hebert C, Rundlöf AK, Larsen EH, Danielsson O, Björnstedt M. Extracellular thiol-assisted selenium uptake dependent on the x(c)- cystine transporter explains the cancer-specific cytotoxicity of selenite. Proc Natl Acad Sci U S A. 2009 Jul 7;106(27):11400-5.

The relationship between xCT and cancer has been well studied. One report states that the upregulation of xCT in pancreatic cancer cells promotes cell growth and survival when treated with oxidative stressors such as chemotherapeutics[117]. Another study suggests that increased xCT expression promotes tumor invasion in glioblastoma[118]. A particularly interesting study shows how the expression of xCT increases alongside the tumorigenesis of melanoma, from low expression in normal skin to higher expression in primary melanoma and even more increased expression in metastatic melanoma cells[119]. These studies establish that xCT expression is upregulated in cancer cells. This leads us to hypothesize that increased xCT expression allows cancer cells to take up more selenium, an idea that will be discussed thoroughly in Chapters II and III.

Rationale for Thesis Project

Cancer cells upregulate metabolic pathways to preferentially fuel cancer specific processes such as unchecked growth and cellular transformation. We have previously shown that cancer cells can be killed with endogenous metabolites by disrupting key detoxifying enzymes[120]. To determine whether this concept can be applied to other metabolic pathways, we created a list of enzymes that were directly downstream of potential toxic metabolites. We hypothesized that disruption of some of these enzymes may be harmful to cancer cells due to loss of detoxification capacity and the resulting buildup of a toxic metabolite. We performed a small-scale CRISPR/Cas9 based screen to determine the essentiality of these candidate detoxifying enzymes, and we determined SEPHS2 is selectively essential in a subset of cancer cell lines. SEPHS2 is the

downstream enzyme that processes selenide, a candidate toxic metabolite. We hypothesized SEPHS2 is essential to cancer cells due to its role in the detoxification of selenide. Also, SEPHS2 may be more important in cancer cells due to the detoxification demand that occurs with increased selenium uptake[115]. We hypothesized that SEPHS2 may be a promising cancer target due to these factors.

The aim of this doctoral thesis was to determine whether SEPHS2 plays an important role in detoxifying selenide in addition to its previously reported function of producing selenocysteine and antioxidant selenoproteins in cancer cells. Therefore, we examined the essentiality of SEPHS2 in cancer, normal immortalized, and primary cell lines as well as orthotopic tumor xenografts. We observed that the cystine-glutamate antiporter xCT is a necessary facilitator of selenium uptake into cells. We also examined whether SEPHS2 could directly detoxify selenide gas. The results of these studies are summarized in Ch. II of the thesis.

CHAPTER II:

SELENIUM DEXTOXIFICATION IS REQUIRED FOR CANCER CELL SURVIVAL

This chapter is reproduced from:

Carlisle AE, Lee N, Matthew-Onabanjo AN, Spears ME, Park SJ, Youkana D, et al. Selenium detoxification is required for cancer-cell survival. Nat Metab. 2020;2:603–11. (https://doi.org/10.1038/s42255-020-0224-7)

A.E.C. and D.K. conceived the project; A.E.C., N.L. and D.K. designed the research. A.E.C. and N.L. performed most of the experiments with assistance from A.N.M.-O., M.E.S., M.B.D., D.Y., A.B.J. and A.P. In situ hybridization and immunohistochemistry experiments were carried out by S.J.P., N.L. and P.L.G. ICP-MS-based experiments for selenite measurements were conducted by M.S. R.L., N.L., M.B.D. and L.J.Z. conducted mining and analyses of TCGA and other large-scale datasets. A.N.M.-O. and L.M.S. assisted with mouse xenograft studies. K.S. assisted with human sample studies. A.E.C., N.L. and D.K. wrote the manuscript with consultation from all of the authors.

ABSTRACT

The micronutrient selenium is incorporated via the selenocysteine biosynthesis pathway into the rare amino acid selenocysteine, which is required in selenoproteins such as glutathione peroxidases and thioredoxin reductases[84,121]. Here, we show that SEPHS2, an enzyme in the selenocysteine biosynthesis pathway, is essential for survival of cancer, but not normal cells. SEPHS2 is required in cancer cells to detoxify selenide, an intermediate that is formed during selenocysteine biosynthesis. Breast and other cancer cells are selenophilic, owing to a secondary function of the cystine/glutamate antiporter SLC7A11 that promotes selenium uptake and selenocysteine biosynthesis, which, by allowing production of selenoproteins such as GPX4, protects cells against ferroptosis. However, this activity also becomes a liability for cancer cells because selenide is poisonous and must be processed by SEPHS2. Accordingly, we find that SEPHS2 protein levels are elevated in samples from people with breast cancer, and that loss of SEPHS2 impairs growth of orthotopic mammary tumor xenografts in mice. Collectively, our results identify a vulnerability of cancer cells and define the role of selenium metabolism in cancer.

INTRODUCTION

Altered metabolism is a hallmark of cancer[2], and enzymes that produce metabolites required by cancer cells are attractive targets for therapy. However, targeting these enzymes may have limited efficacy when the same metabolites are available in the tumor environment, or can be produced through alternative routes[122]. As an alternative therapeutic approach, we sought to identify metabolic enzymes that may be required in cancer cells to prevent the buildup of toxic metabolites (Fig 2.3a). To first identify endogenously produced toxic metabolites, we cross-examined the metabolites in the human metabolic network with toxicological data from the NIH Toxicology Data Network (TOXNET)[15]. The enzymes that use these toxic metabolites as substrates according to the Kyoto Encyclopedia of Genes and Genomes (KEGG)[20] were designated as putative detoxifying enzymes, and a panel of these were examined for their role in cell viability (Figure 2.1).

Toxic metabolite	Chemical structure	Proof of compound toxicity (PMID)	Pathway	Detoxifying enzyme
Cysteamine		2253283, 8616813	Taurine/hypotaurine metabolism	ADO
Inosine monophosphate	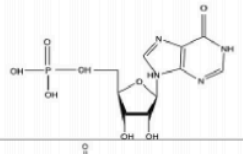	7271444	Purine metabolism	ADSS, IMPDH2
Arachidonic acid, Linoleic acid	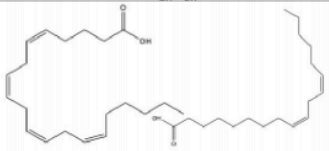	7898670, 1582681, 11042099	Arachidonic acid metabolism	ALOX15B
2-hydroxyestradiol	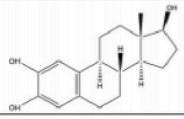	15513894	Tyrosine metabolism	COMT
2'-deoxyuridine 5'-triphosphate	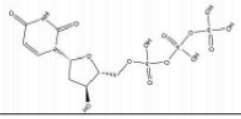	2015598	Pyrimidine metabolism	DUT
Glycerophosphocholine	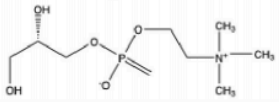	9202319	Glycerol metabolism	GDPD5
Methylglyoxal	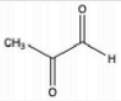	25855294	Glycine metabolism	GRHPR
Nicotinamide	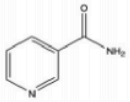	4271091	Nicotinate and nicotinamide metabolism	NAMPT
2-Phosphoglycolate	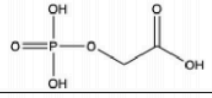	27731369	Glyoxylate and dicarboxylate metabolism	PGP
Retinal	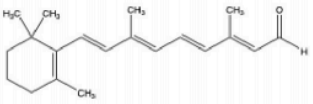	19553623	Retinol metabolism	RDH8
Hydrogen selenide	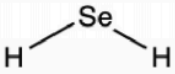	7357982	Selenocompound metabolism	SEPHS2

Figure 2.1 – Panel of toxic metabolites and putative detoxifying enzymes tested.
A panel of metabolites that have documented toxic properties, and the downstream enzymes which use them as substrates, designated as 'detoxifiers', are listed. Chemical structures and PMID of references which document the toxicity of each metabolite as a compound are shown.

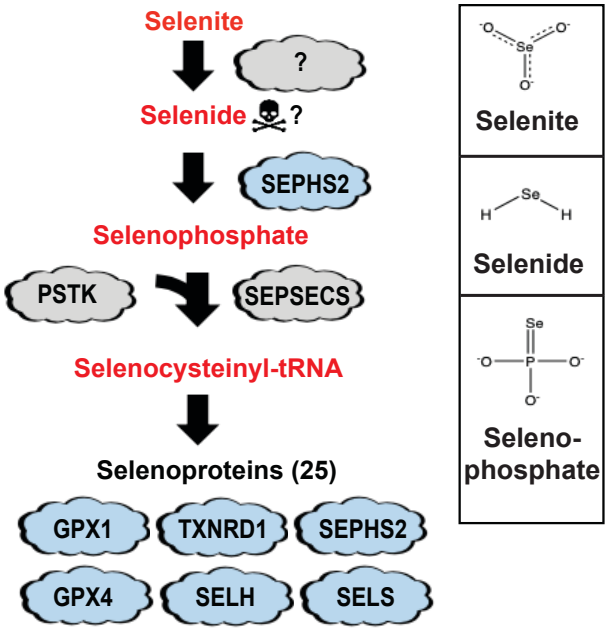

Figure 2.2 — Diagram of selenocysteine biosynthesis pathway and chemical structure of selenite, selenide and selenophosphate

RESULTS

Identification of SEPHS2 as an enzyme that is selectively essential to cancer cells and is a potential therapeutic target

CRISPR/Cas9-based gene disruption[23] of several of these enzymes impaired cell viability in one or more of the tested cell lines (Fig. 2.3b). Loss of SEPHS2 was particularly detrimental, causing a loss of viability of over 40% in 6 of the 11 cell lines tested, including the breast-cancer line MDAMB231 and the glioma line U251 (Fig. 2.3d). We designated SEPHS2 as a candidate detoxifier because its annotated substrate is selenide (H_2Se), a compound that has been reported to be toxic in accidental industrial- or laboratory-exposure cases[72,73]. After expanding our testing to additional cancer lines and to non-transformed cells, we found that SEPHS2 knockout (KO) was toxic to 12 of 22 cancer cell lines but none of the 7 tested normal lines (Fig. 2.3c). SEPHS2 KO in cancer cells induced loss of cell proliferation (Fig. 2.3d), loss of colony-forming capacity (Fig. 2.5c) and cell death (Figs. 2.3e and 2.4a–d). Notably, loss of SEPHS2 was non-toxic to all normal (non-transformed immortalized or primary) lines that we tested, such as the mammary epithelial lines MCF10A and MCF12A, as well as primary lung and colon fibroblasts (Fig. 2.5b), despite efficient KO (Fig. 2.22a). Furthermore, MCF10CA1h cells, which are HRAS-transformed, phenotypically malignant versions of MCF10A cells[123], are sensitive to SEPHS2 KO (Figs. 2.5a), providing an isogenic model for SEPHS2 dependency in transformation and malignant progression. Importantly, overexpression of a mutant form of SEPHS2 (SEPHS2-U60C) that is

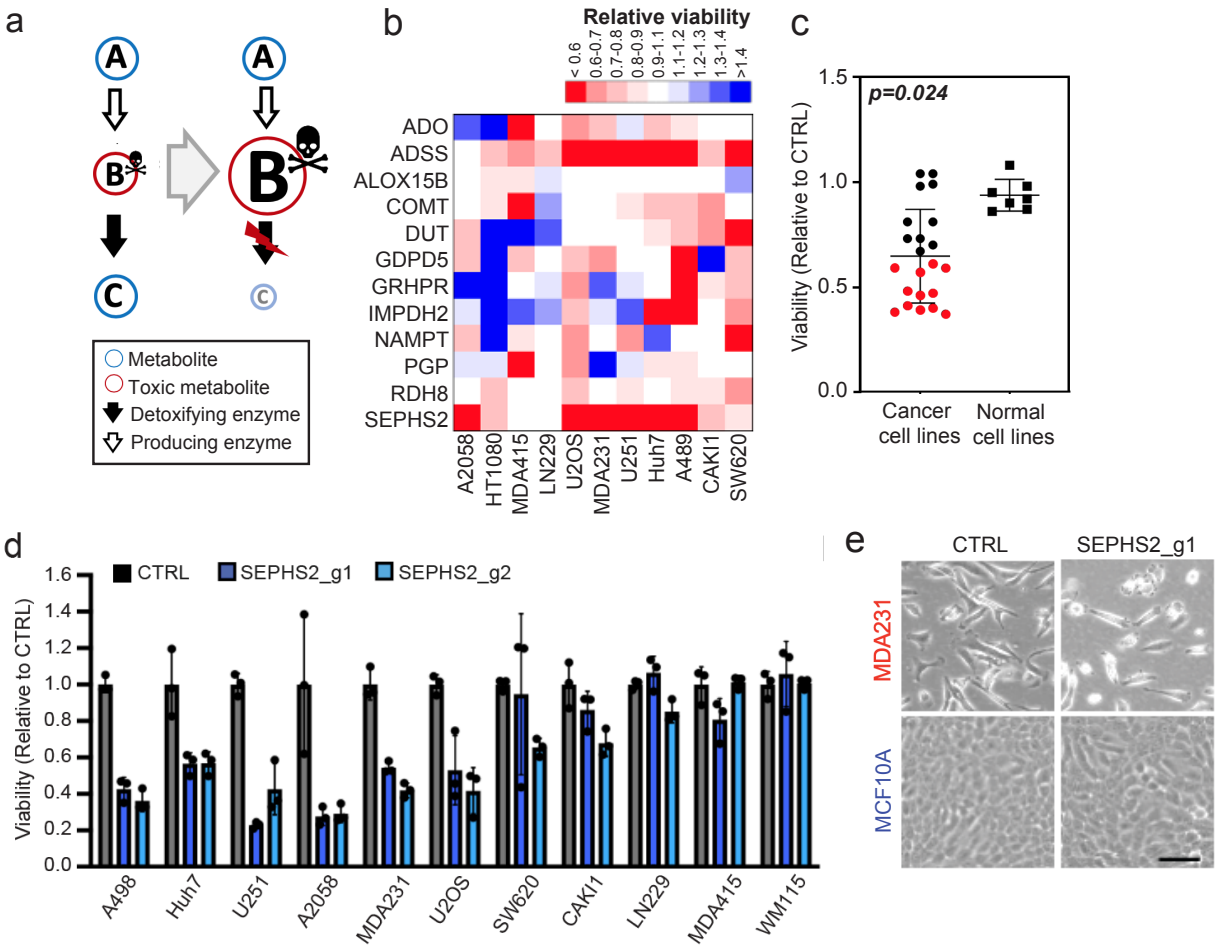

Figure 2.3 – Identification of SEPHS2 as an enzyme that is selectively essential to cancer cells

a. Toxic-metabolite poisoning strategy. If B is a toxic metabolite, and the downstream (detoxifying) enzyme is disrupted, toxic accumulation of B, rather than the loss of metabolite C, may cause toxicity.

b. Heat map representing the impact of KO of each putative detoxifying enzyme (rows) on viability (measured as described in the Methods) of cancer cell lines (columns). Values are relative to expression of a non-targeting gRNA in cells from the same line (which was set at 1; red indicates a decrease and blue indicates an increase in viability MDAMB231 is abbreviated to MDA231, and MDAMB415 to MDA415.

c. Dot plot of effect of SEPHS2 KO on the viability of 22 cancer cell lines and 7 non-cancer cell (non-transformed and primary) lines of varying tissue origin, with each dot representing one cell line. Values are relative to expression of a non-targeting control gRNA (CTRL) in cells from the same line.

d. Viability of cell lines following KO with guides against SEPHS2 for 9 days. Values are relative to the same cell lines expressing nontargeting (CTRL) guide (=1.0). SEPHS2_g1 and SEPHS2_g2 are two different gRNAs targeting SEPHS2.

e. Light microscope images of MDAMB231 and MCF10A cells subjected to CTRL or SEPHS2 KO. Scale bar=25μm

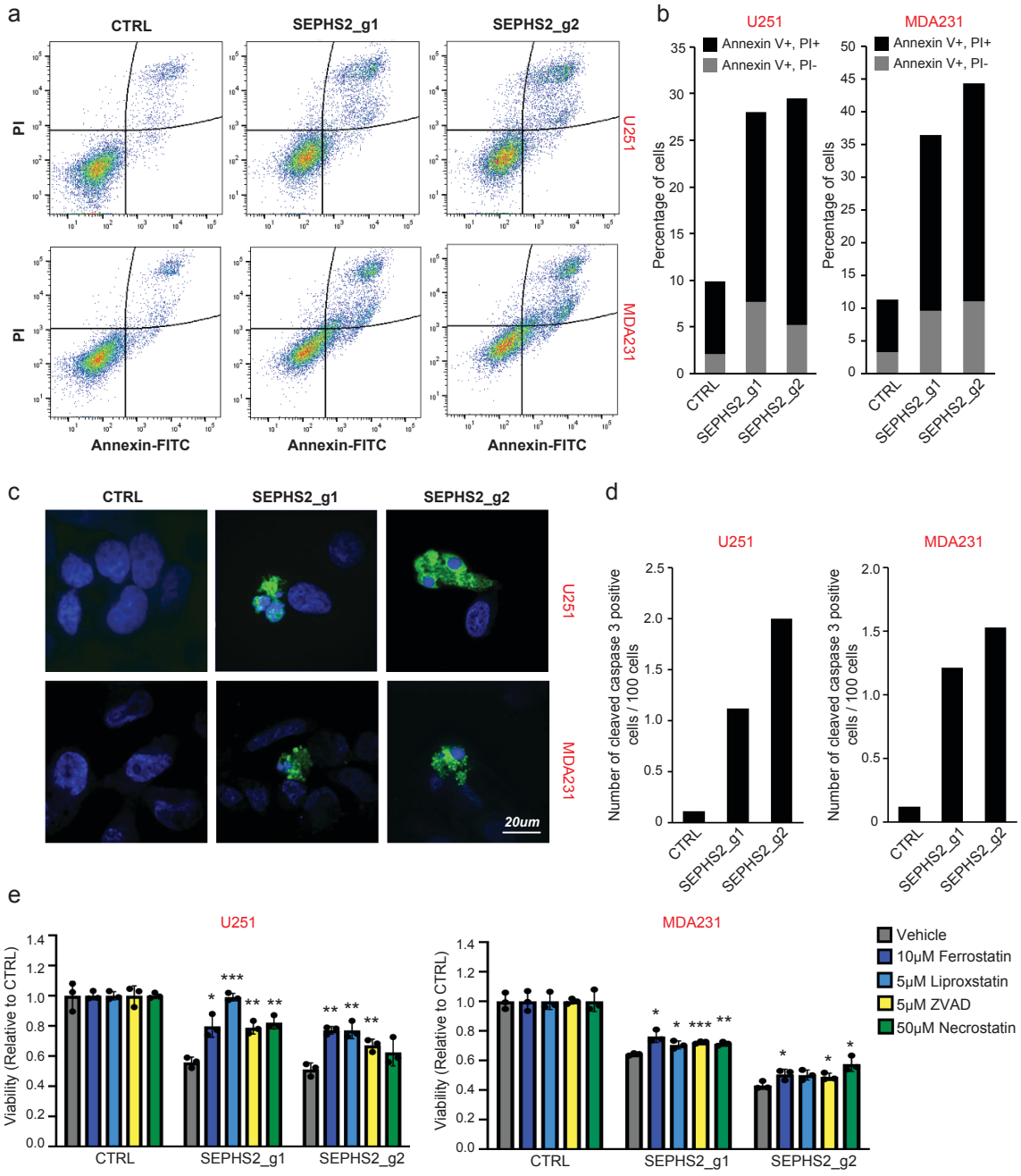

Figure 2.4 – Induction of cell death by SEPHS2 KO in cancer cells
a. Raw flow cytometry of PI and Annexin V double-stained U251 and MDAMB231 cells following KO with guides against SEPHS2 at 10 days after viral infection.
b. Percentages of Annexin V + /PI- and Annexin V + /PI + cells.
c. Cleaved caspase 3 (CC3) staining in MDAMB231 and U251cells following KO with guides against SEPHS2 at 10 days after viral transduction. Scale bar=20μm. **d**.

Quantification of CC3 positive cells over total cells in CTRL and SEPHS2 deficient MDAMB231 and U251. Counts are from random fields.
e. Viability of control and SEPHS2 deficient U251 and MDAMB231 cells treated with vehicle or the indicated drugs for 4 days. Values are relative to the cell lines expressing nontargeting (CTRL) guide, set at 1.0.
For all panels, *$p < 0.05$, **$p < 0.01$, and ***$p < 0.001$ (student's two-tailed t test).

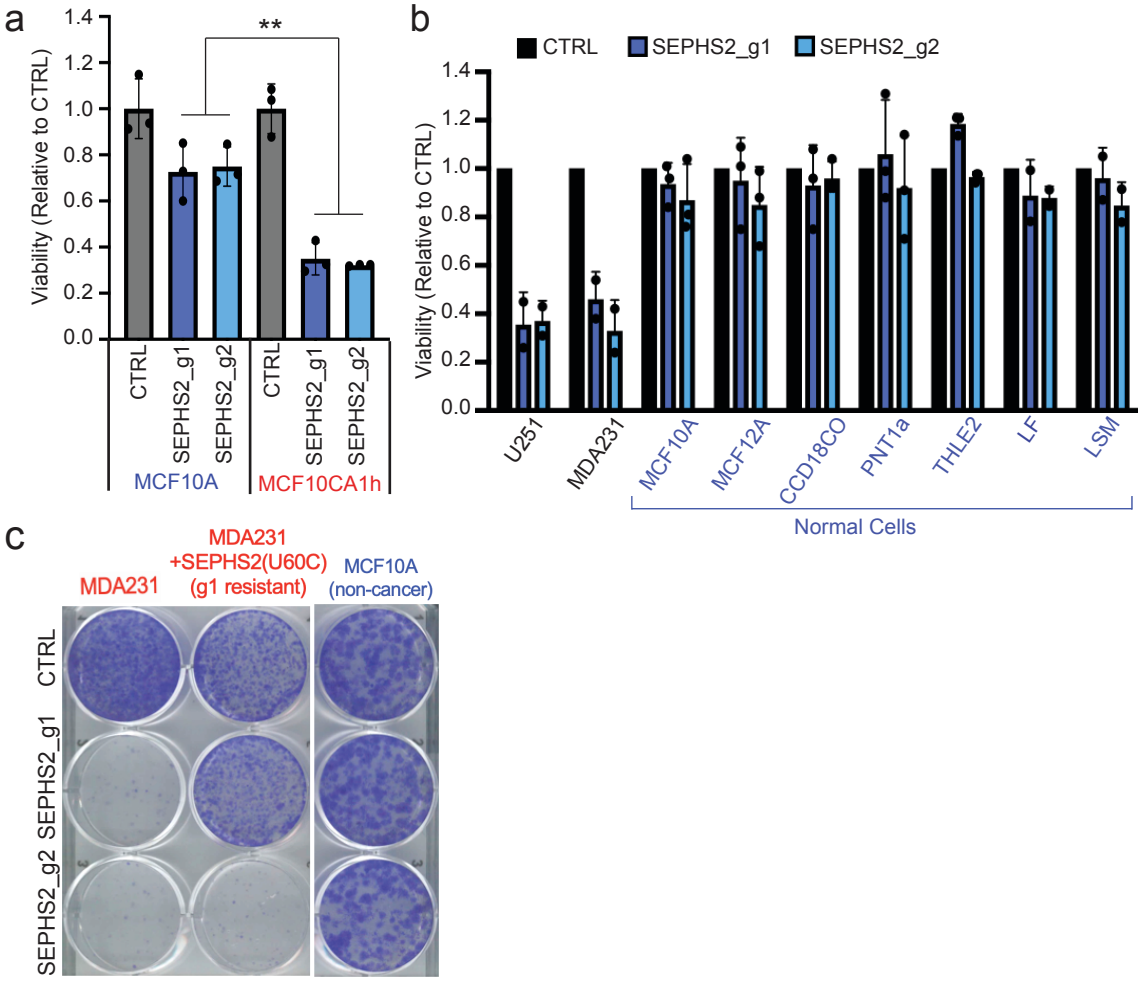

Figure 2.5– SEPHS2 is not essential for normal cells

a. Viability of cell lines following KO with guides against SEPHS2 for 11 days. Values are relative to the same cell lines expressing nontargeting guide (=1.0).

b. The viabilities of non-cancer lines following KO, with gRNAs against SEPHS2 (blue bars), for 9 d. Values are relative to expression of a non-targeting gRNA in cells from the same line (black bars). SEPHS2 KO efficiency for each line is shown in Figure 2.22.

c. Crystal violet staining showing the colony-forming ability of MDAMB231 cells, MDAMB231 cells overexpressing g1-resistant SEPHS2-U60C and MCF10A cells, following SEPHS2 KO via g1 and g2.

For a, $^{**}p < 0.01$ (student's two-tailed t test).

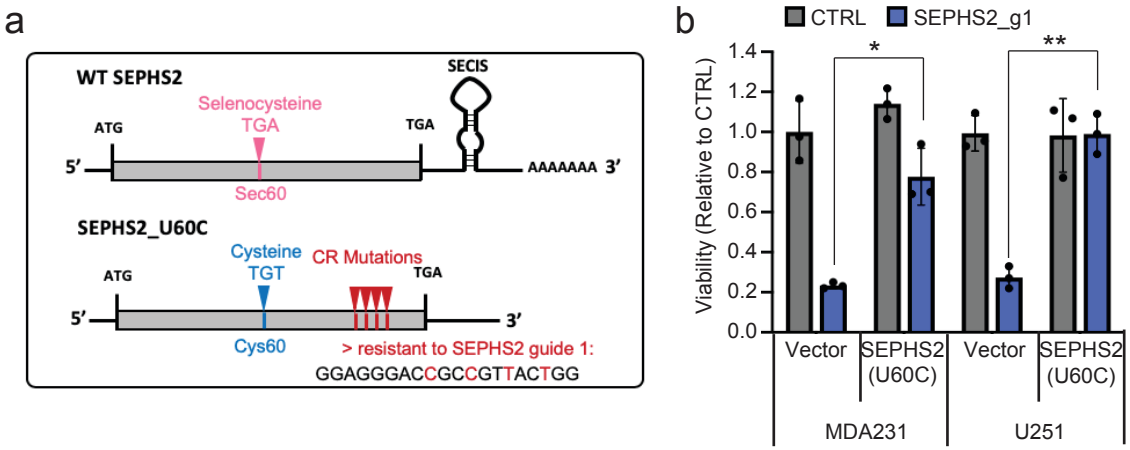

Figure 2.6 – Overexpression of CRISPR-resistant SEPHS2 confirms that the effects of SEPHS2 KO is on target

a. Map of wild type SEPHS2 and CRISPR resistant mutant SEPHS2_U60C. Details of features are provided in Methods.

b. Viability of vector and SEPHS2_U60C overexpressing cell lines subjected to CTRL and SEPHS2 g1 KO.

For b, *$p < 0.05$ and **$p < 0.01$ (student's two-tailed t test).

resistant to one of the guide RNAs (guide 1, g1) rescued cells from the toxic effects of SEPHS2 KO from the corresponding gRNA, demonstrating that the observed toxicity was not due to off-target effects of CRISPR (Figs. 2.5c and 2.6). Furthermore, we verified that SEPHS1 does not carry out an analogous function to that of SEPHS2 (Fig. 2.7), as has been previously indicated[51]. Thus, SEPHS2 is an enzyme that is essential for survival in many cancer cells but is surprisingly dispensable in normal cells. To validate these findings in vivo, we disrupted SEPHS2 in an orthotopic xenograft model for breast carcinoma. Loss of SEPHS2 resulted in a substantial improvement in tumor-free survival of the host (Fig. 2.8a), which appeared to be due to a combination of reduced tumor formation (Fig. 2.8b) and average tumor volume and weight (Fig 2.8c,d). The few SEPHS2-KO tumors that did form showed varying expression of SEPHS2 protein levels, suggesting both an expansion of cells that escaped KO and adaptation of KO cells to allow survival (Fig. 2.8e). Meta-analyses of SEPHS2 gene expression in cancer and normal tissues revealed that SEPHS2 was overexpressed at the messenger-RNA level across many types of tumors, including breast cancer, relative to its expression in their normal tissue counterparts (Fig. 2.9). SEPHS2 protein was also substantially upregulated in human breast-cancer tissues compared with normal breast tissue (Fig. 2.10a,b). Notably, SEPHS2 expression was associated with poor survival in people with breast cancer (Fig. 2.10c). These results demonstrate that SEPHS2 is an enzyme that is both overexpressed in and required for the survival of breast cancer cells. Collectively, these findings indicate that SEPHS2 is a highly attractive target for cancer therapy, which may

be druggable because SEPHS2 is a metabolic enzyme with hydrophobic substrate pockets[57].

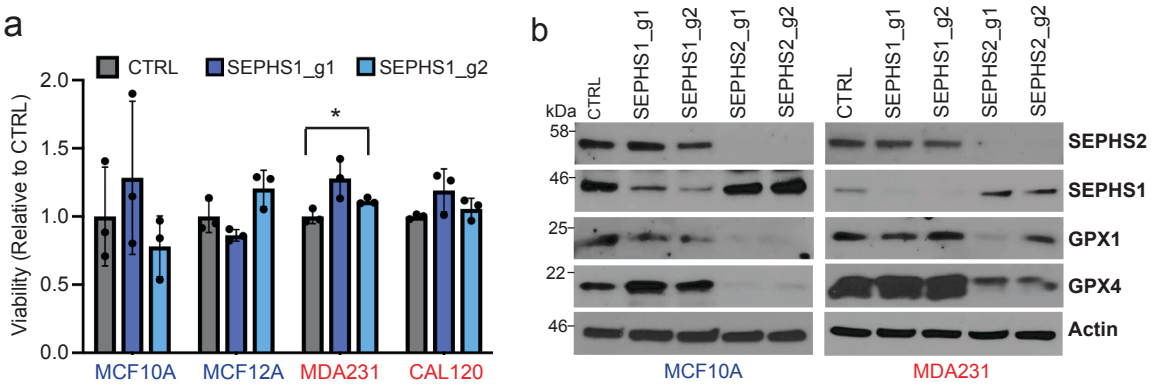

Figure 2.7– SEPHS1 is functionally distinct from SEPHS2 and does not play a role in selenoprotein production

a. Viabilities of noncancer (immortalized) and cancer lines following KO with guides against SEPHS1 (blue bars) for 9 days. Values are relative to the same cell lines expressing nontargeting guide (black bars), set at 1.0.

b. Immunoblots of selenoprotein expression in MCF10A and MDAMB231 cells subjected to (CRISPR/Cas9-induced) KO with guides against SEPHS1, SEPHS2, or control guides for 11 days.

For a, *$p < 0.05$ (student's two-tailed t test).

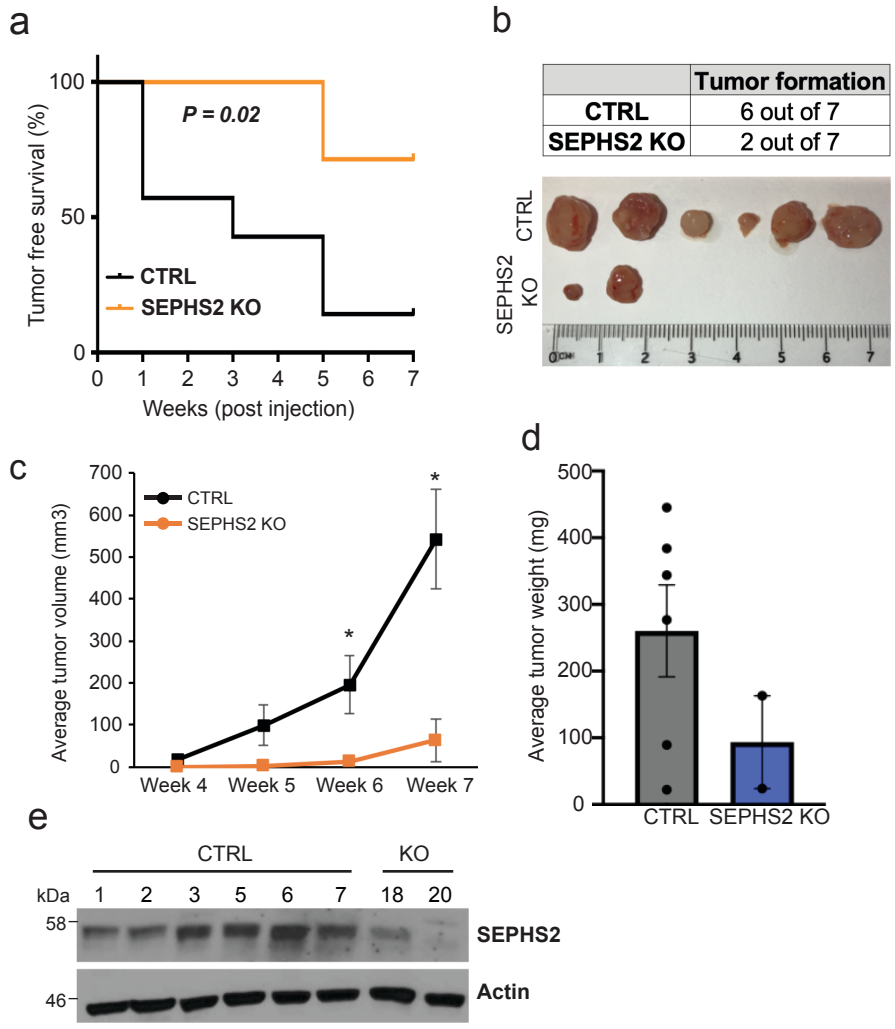

Figure 2.8 – Disruption of SEPHS2 reduces tumor formation and growth in an orthotopic xenograft model for breast cancer

a. Kaplan–Meier plot of tumor-free survival for mice orthotopically injected with SEPHS2 KO or control KO MDAMB231 cells. n = 7 mice for each condition. P value is student's two-tailed t test.

b. Tumor-formation data and ex vivo images of the tumors at the endpoint.

c. In vivo tumor volume measurements for CTRL and SEPHS2 KO MDAMB231 orthotopic xenograft tumors. For c and d, if no tumor has formed, tumor weight and volume was designated 0 for CTRL, n = 6 and for SEPHS2 KO n = 2.

d. Weight measurements for ex vivo CTRL and SEPHS2 KO MDAMB231 orthotopic xenograft tumors.

e. Immunoblot of SEPHS2 in CTRL and SEPHS2 KO MDAMB231 orthotopic xenograft tumors. Number is an animal identifier number.

For c, *p < 0.05 (student's two-tailed t test).

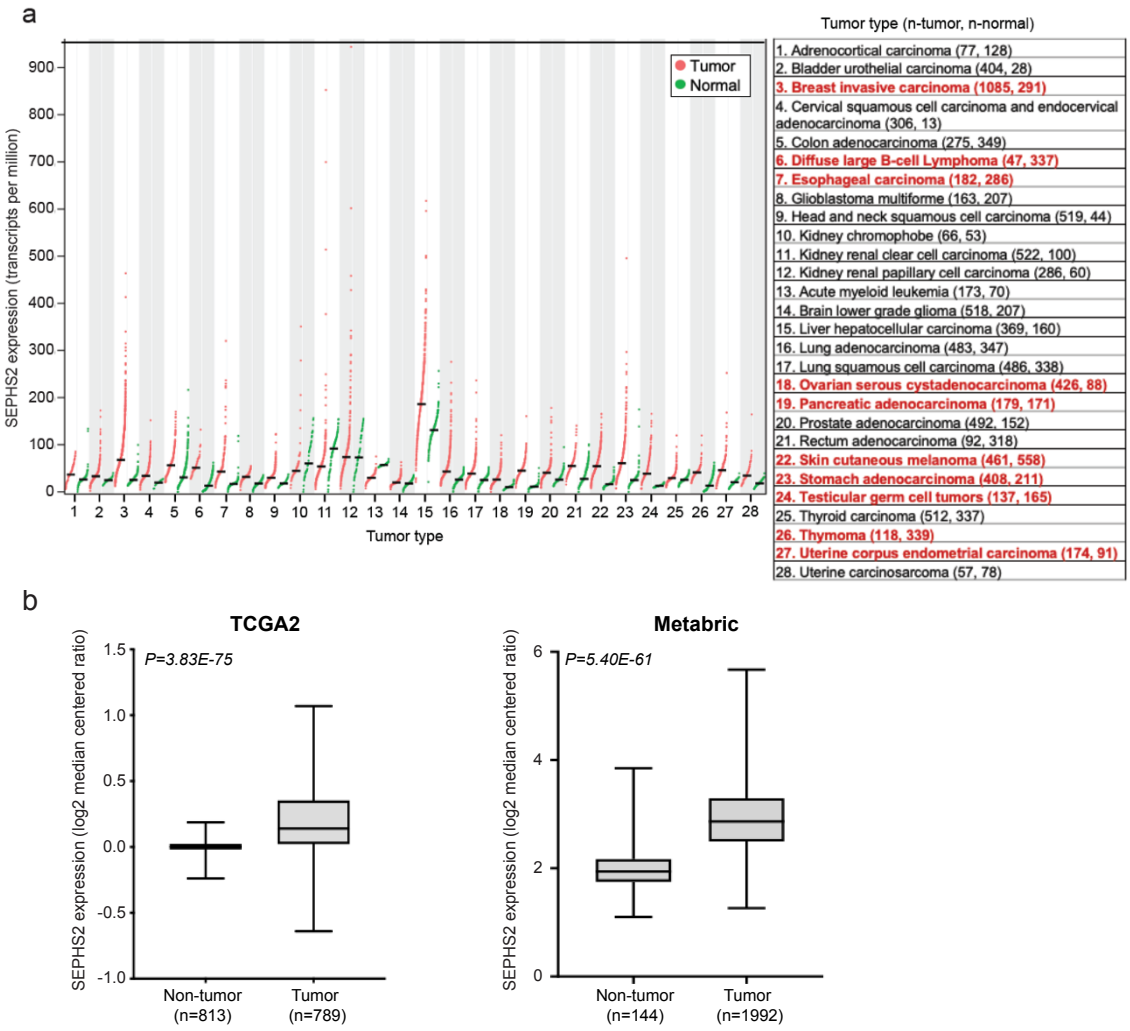

Figure 2.9 – Expression of SEPHS2 in various types of tumor and normal tissues
a. Expression profiles of SEPHS2 in 28 types of normal and tumor tissues. Normalized mRNA-Seq expression profile data from patient tumor tissues and normal tissues was obtained from GEPIA (Tang, Z. et al. (2017) GEPIA: a web server for cancer and normal gene expression profiling and interactive analyses. Nucleic Acids Res, 10.1093/nar/gkx247). Tumor subtypes having over 2-fold SEPHS2 expression in tumor than normal and q-value less than 0.01 indicated with red. q values are have been determined by ANOVA and adjusted for FDR (false discovery rate).
b. Box plots of SEPHS2 mRNA expression levels in patient tumors and normal breast tissue. SEPHS2 expression was compared in tumor and normal breast samples from TCGA and METABRIC datasets. For TCGA2 data, minimum is non-tumor (-0.239), tumor (-0.6386), maximum is non-tumor (0.1874), tumor (1.0702) and median is non-tumor (0.0014), tumor (0.1402). For Metabric data, minimum is non-tumor (1.10097), tumor (1.26305), maximum is non-tumor (3.85158), tumor (5.67272), and median is non-tumor (1.941515), tumor (2.86621).

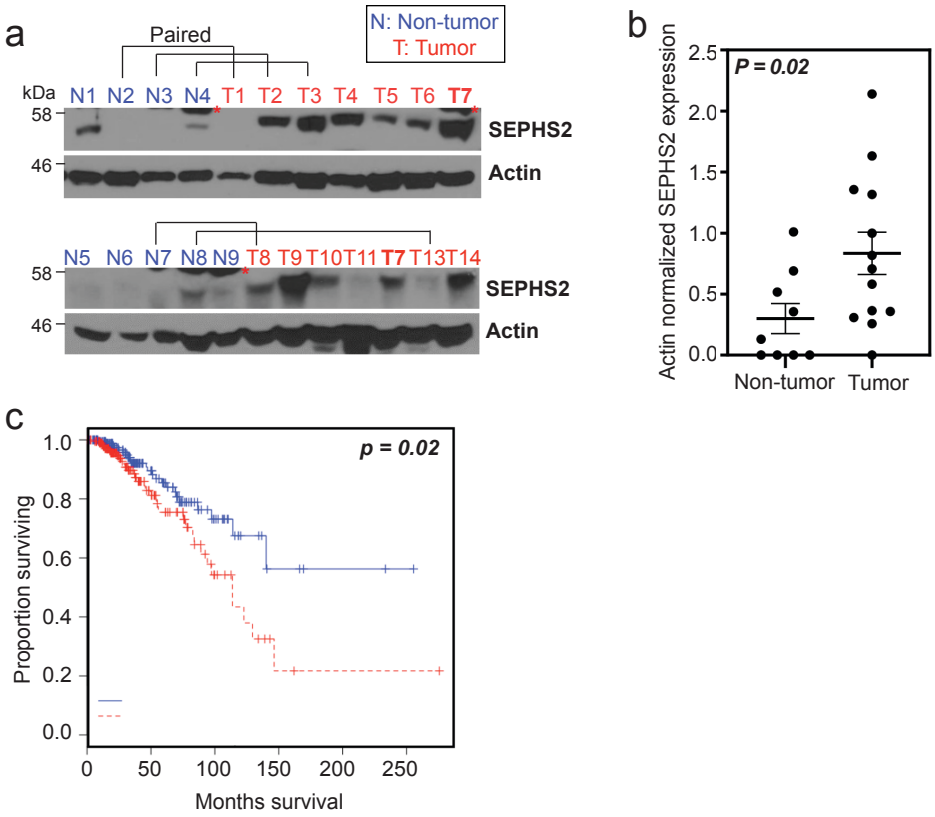

Figure 2.10– *Ex vivo* patient sample investigation of SEPHS2 as a potential therapeutic target

a. SEPHS2 immunoblots from cancer tissue and normal breast tissue from people with breast cancer. Paired samples from the same person are indicated. Red asterisks indicate non-specific bands present in mammary tissue.

b. Quantification of SEPHS2 band intensities from a, normalized to that of actin; each dot represents one sample from a. P value is from student's two-tailed t-test.

c. Overall survival estimates for people with breast carcinoma in TCGA based on SEPHS2 expression (SEPHS2 low, n = 180; SEPHS2 high, n = 191).

P values are from student's two-tailed t-test.

SEPHS2 is dispensable to non-transformed cells despite being required to produce selenoproteins

SEPHS2 is required for production of selenoproteins, a group of 25 proteins containing selenocysteine residues, which include antioxidant enzymes such as glutathione peroxidase 4 (GPX4) and thioredoxin reductase 1 (TXNRD1)[51,84,121]. Thus, it was surprising that SEPHS2 was not essential for the survival of normal cells. SEPHS2 phosphorylates selenide to form selenophosphate, which serves as the selenium donor for the biosynthesis of selenocysteinyl tRNA by phosphoryl-tRNA kinase (PSTK) and O-phosphoserine tRNA-selenocysteine tRNA synthase (SEPSECS) (Fig. 2.2). Disruption of any of these enzymes resulted in a dramatic decrease in selenoprotein levels (Fig. 2.11a), including that of SEPHS2 itself as it is also a selenoprotein. Strikingly, the non-transformed MCF10A cells subjected to SEPHS2 KO maintained their growth rate for 28 d, despite having lost SEPHS2 and the capacity to express selenoproteins (Fig. 2.11b,c). However, SEPHS2 KO in MDAMB231 cancer cells produced a severe reduction in growth rate, which ultimately recovered around day 20 (Fig. 2.11b). SEPHS2 and several selenoproteins were initially depleted in the population, but then recovered between days 16 and 20 (Fig. 2.11c). This indicated that SEPHS2 KO cells were strongly selected against and died out, with the population being replaced by wild-type cells which escaped CRISPR KO. Collectively, these results indicate that normal cells require neither SEPHS2 nor selenoprotein production for their survival and proliferation under basal conditions.

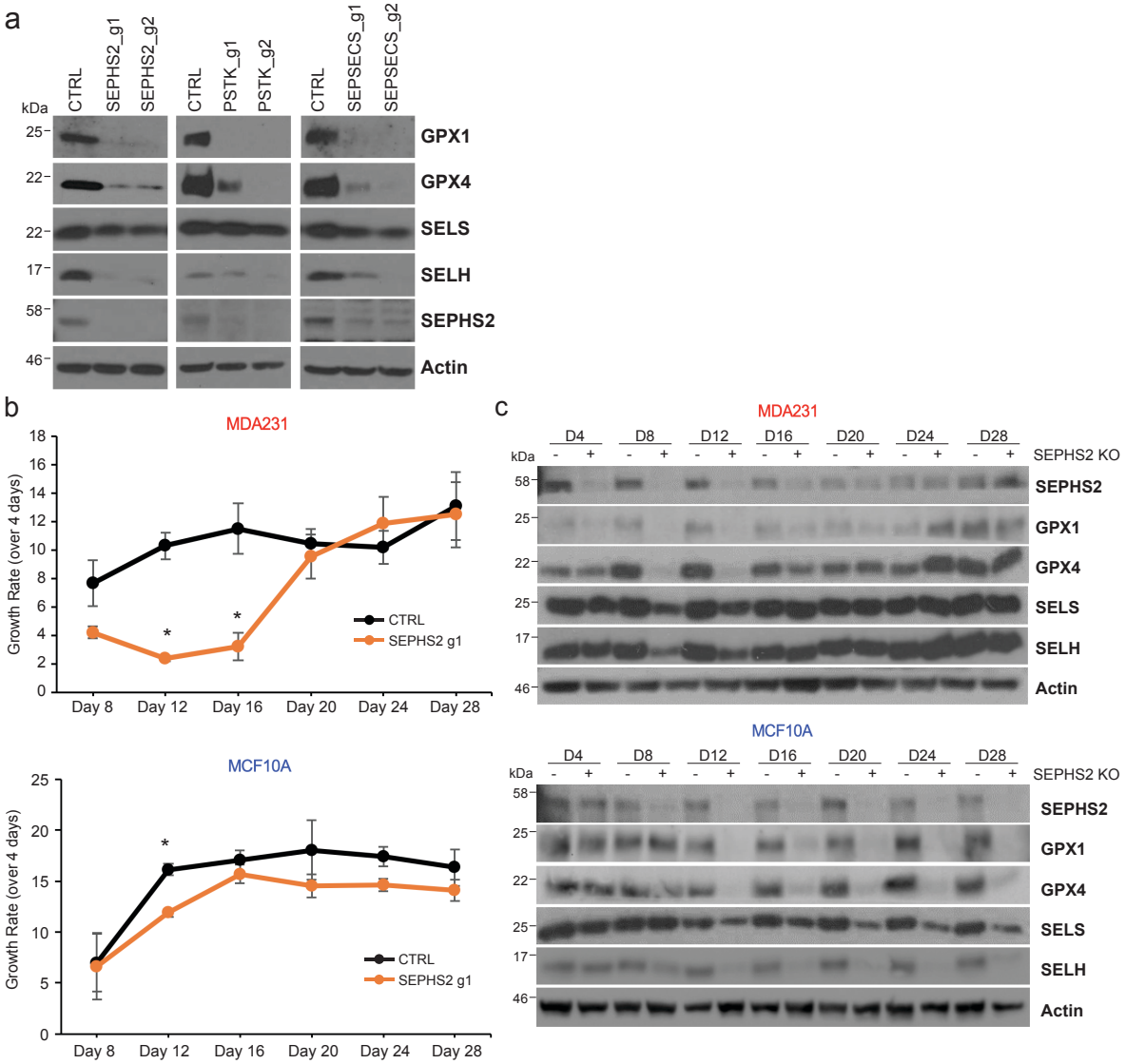

Figure 2.11 - SEPHS2 is dispensable to non-transformed cells despite being required to produce selenoproteins

a. Immunoblots of selenoprotein expression in MDAMB231 cells subjected to CRISPR–Cas9-induced KO with gRNAs against genes encoding enzymes in the selenocysteine biosynthesis, SEPHS2, PSTK and SEPSECS, or control gRNAs for 11 days.

b. Long-term monitoring of growth rates of MDA-MB-231 cells and MCF10A cells subjected to CRISPR–Cas9-induced KO with gRNAs against SEPHS2 or control, over the course of 28 days. Each point represents the fold change of growth over the previous 4 days.

c. Immunoblots of selenoproteins expressed by MDAMB231 and MCF10A cells, taken at each time point from b.

For b, *P < 0.05 (two-tailed Student's t-test).

xCT-mediated reduction of selenite is the initial step of the selenocysteine biosynthesis pathway in cancer cells and protects against ferroptosis

As selenoprotein production by SEPHS2 per se was not essential for cell survival, we considered the hypothesis that cancer cells may have a selenium-detoxification demand that normal cells do not have. Interestingly, in the 1960s, it was observed that radioactive selenite (SeO_3^{2-}), a common dietary form of selenium, preferentially accumulated in tumors, and this was briefly explored as a tumor-labelling strategy[115,124]. Therefore, we examined whether we could recapitulate this selenium uptake in cancer cell lines, as this may determine the detoxification requirement. As excessive selenite is toxic to cells[125], we carried out a focused CRISPR screen to identify genes required for selenium import, assuming that KO of genes necessary for either selenite import or selenide production would prevent selenite toxicity. The 21 candidate genes were selected on the basis of a literature search and on homology from selenium transporters in other species (Fig. 2.12). KO of SLC7A11 and SLC3A2, the two components of the xCT cystine–glutamate antiporter[93,94], ameliorated selenite sensitivity (Figs. 2.13a and 2.15a,b), and SLC7A11 KO prevented selenium accumulation in cells treated with selenite (Fig. 2.13b). In examining a panel of breast cancer and non-transformed lines, we found that cells that expressed elevated levels of SLC7A11 took up more selenium (that is, they were ‘selenophilic’) than did normal and cancer cells with little or no SLC7A11 (Fig. 2.13c,d). Thus, SLC7A11 is required for selenium import and for the toxic effects of selenite in cancer cells.

Candidates	Rationale for being a candidate transporter	Reference (PMID)
IMPDH1	Non-transporter metabolic enzyme used as negative control	N/A
DBH	Non-transporter metabolic enzyme used as negative control	N/A
SLC26A11	Homologue of yeast selenate transporter (Sul1p and Sul2p)	18789529, 12626430
SLC4A1	Reported selenite transporter	8238316, 22580993
SLC4A3	SLC4A1 homologue	8238316, 22580993
SLC7A11	Reported indirect modifier of selenium uptake; enriched in selenite-sensitive lines	19549867
SLC39A10	Homology/functional overlap with SLC39A8	29927321, 27166256
SLC39A14	Homology/functional overlap with SLC39A8	29927321, 27166256
SLC39A6	Homology/functional overlap with SLC39A8	29927321, 27166256
SLC39A8	Reported selenite transporter	29927321, 27166256
SLC26A10	Evidence for overlap between sulfur and selenium transport	23148951
SLC26A4	Evidence for overlap between sulfur and selenium transport	23148951
SLC26A9	Evidence for overlap between sulfur and selenium transport	23148951
SLC26A2	Evidence for overlap between sulfur and selenium transport	23148951
SLC26A5	Homologue of yeast selenate transporter (Sul1p and Sul2p)	18789529, 12626430
SLC1A4	Candidate due to high enrichment in selenite-sensitive cell lines	N/A
STARD8	Candidate due to high enrichment in selenite-sensitive cell lines	N/A
SLC13A3	Homologue of putative selenium transporter in rat; enriched in selenite-sensitive lines	16129486
GABRA3	Candidate due to high enrichment in selenite-sensitive cell lines	N/A
KCNE4	Candidate due to high enrichment in selenite-sensitive cell lines	N/A
ABCB4	Homologue of bacterial selenite/selenate transporter	18789529
SLC26A1	Evidence for overlap between sulfur and selenium transport	23148951
SLC26A7	Evidence for overlap between sulfur and selenium transport	23148951

Figure 2.12 – Candidate transporters tested
A list of selenium transporter candidates examined in the focused screen, rationale for candidacy, and references.

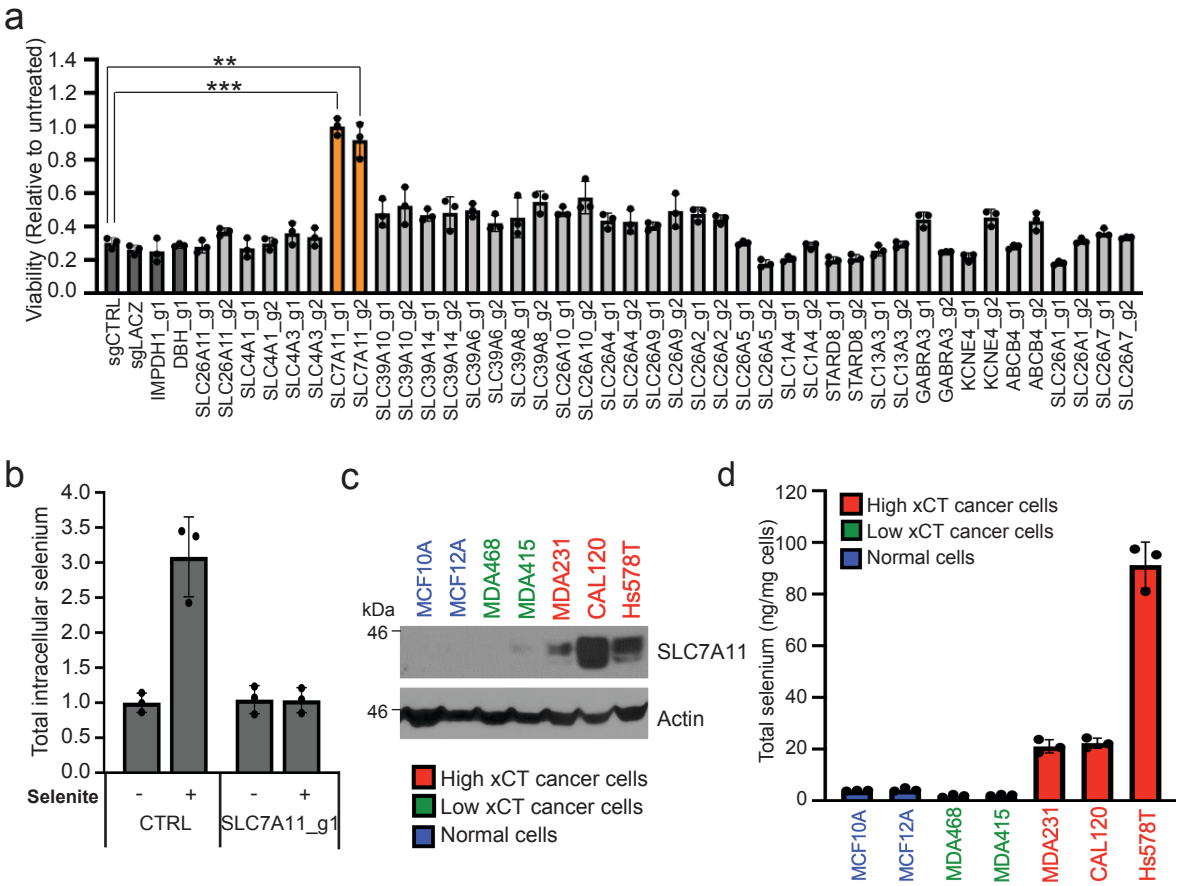

Figure 2.13 – SLC7A11 mediates selenium uptake in cancer cells

a. Viability of U251 cells subjected to KO with gRNAs against various control genes (dark grey bars) or against candidate selenium transporters, and then 48 h of treatment with 12 µM sodium selenite. Values are relative to viability of KO cells from the same line treated with vehicle.

b. Selenium uptake in U251 cells either with or without SLC7A11 depletion. Total intracellular selenium was quantified following 12 µM selenite supplementation of for 2 h in U251 cells. Values are relative to that in control cells from the same line treated with vehicle.

c. Immunoblots of SLC7A11 in a panel of breast cancer and normal breast lines. Non-cancer lines are in blue, cancer lines with low SLC7A11 expression are in green and cancer lines with high SLC7A11 expression are in red here and in subsequent histograms.

d. Selenium uptake in the same panel of cell lines. Total intracellular selenium levels were measured following treatment with 12 µM selenite for 2 hours.

For a, $^{**}p < 0.01$ and $^{***}p < 0.001$ (student's two-tailed t test).

It has been shown that import of cystine by xCT results in its intracellular reduction to cysteine and subsequent export; this increases extracellular reduction potential in the form of reduced thiol groups from cysteine, which may be involved in selenium uptake[33]. Indeed, selenophilic cells had increased extracellular thiols (Fig. 2.14a), and this was dependent on xCT (Fig. 2.14b and Fig. 2.15c,d). xCT allowed selenium uptake via extracellular reduction of selenite, rather than by acting as its physical transporter, as providing extracellular thiols by adding glutathione to medium sensitized cells to selenite toxicity even in the absence of functional xCT (Fig. 2.14c). We hypothesized that the reduction of selenite to selenide through this mechanism would be sufficient for selenium import, as selenide is highly volatile. The reduction of selenite is key to its toxicity, as we could completely prevent or induce toxicity by modulating extracellular thiol levels (Figs. 2.13a and 2.14c). Disruption of SLC7A11 resulted in reduced selenoprotein expression (Fig. 2.14d), demonstrating its role in promoting selenoprotein production. Collectively, these results show that SLC7A11 is involved in the following model (Fig. 2.14e): the elevated expression of SLC7A11 in selenophilic cancer cells results in increased cystine import, reduction of cystine to cysteine in the cell and export via an undetermined exporter. This results in the extracellular accumulation of thiols (from cysteine), which can reduce selenite to volatile selenide and can induce both its import into the cell and cellular toxicity. It has been known that upregulation of SLC7A11 results in increased glutathione production via cystine import in cancer[126]. The ‘moonlighting’ role of SLC7A11 and xCT in allowing selenium uptake and selenocysteine biosynthesis provides an elegant mechanism for the coordination of

increased glutathione production with increased production of the selenoprotein enzymes (GPXs) that utilize it. Furthermore, this mechanism explains the decades-old observation of increased selenium uptake in cancer cells[115,124] and suggests that selenium uptake has a role in cancer-cell biology, particularly involving the selenoproteins that are produced as a result. SLC7A11 is regulated by crucial cancer genes such as p53[127], and we speculate that these canonical cancer pathways may thus affect selenocysteine biosynthesis.

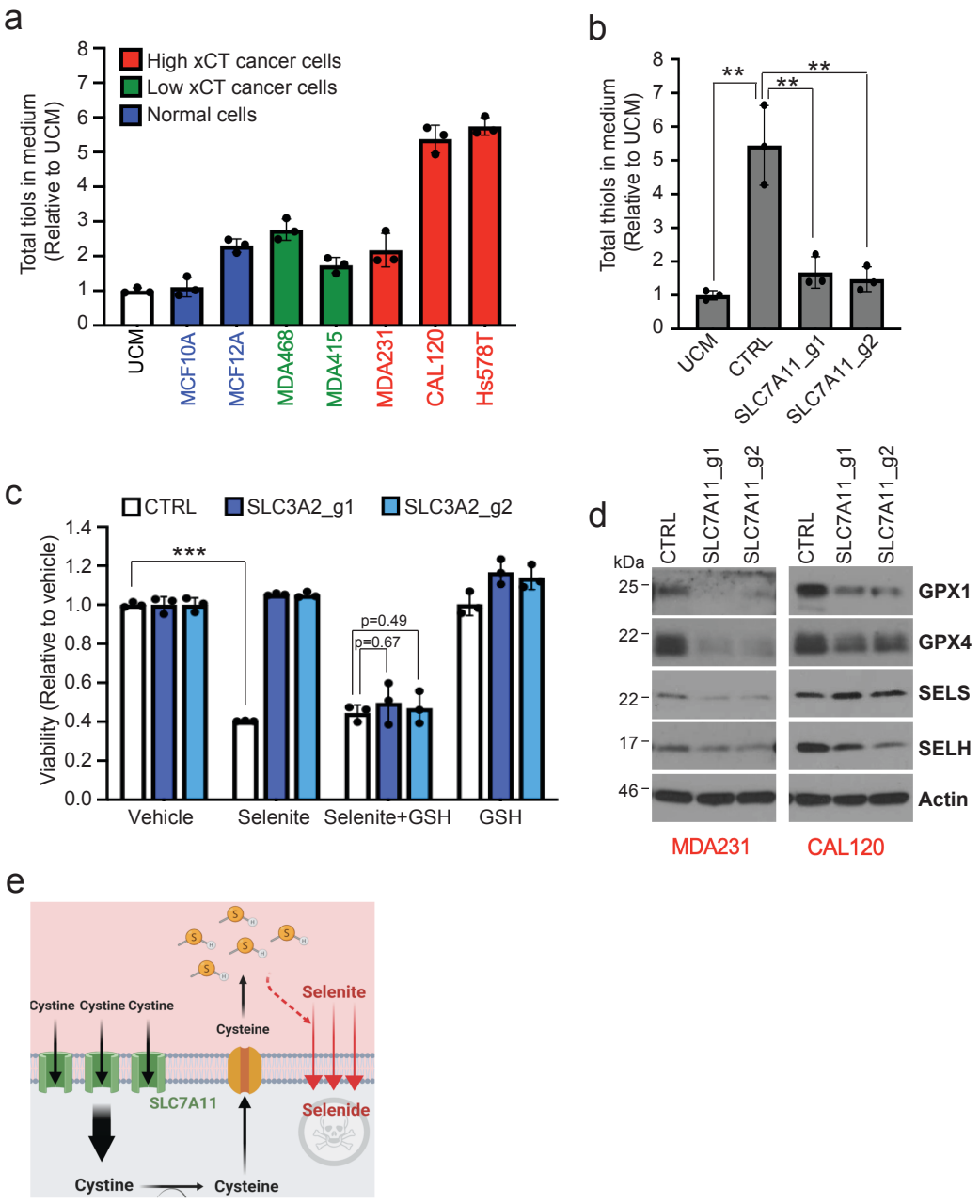

Figure 2.14 – SLC7A11-mediated reduction of selenite is important for selenium uptake and is the initial step of selenocysteine biosynthesis

a. Total thiol quantification of media from the panel, conditioned for 24 hours. Each value was normalized to that of unconditioned medium (UCM) for every thiol-quantification assay.

b. Total thiol quantification of media from control KO and SLC7A11-KO MDAMB231 cells that were conditioned for 24 hours.

c. Viability of control and SLC3A2-KO MDAMB231 cells treated with vehicle, 12 μM sodium selenite and/or 75 μM reduced L-glutathione (GSH) for 72 hours. Values are relative to viability of cells from the same line treated with vehicle.
d. Immunoblots of selenoproteins in triple-negative breast-cancer cells subjected to KO with gRNA against *SLC7A11* for 11 days.
e. Representation of the model revealed by the results in Fig. 2.14.
For all panels, $^{**}P < 0.01$ and $^{***}P < 0.001$ (Student's two-tailed *t*-test).

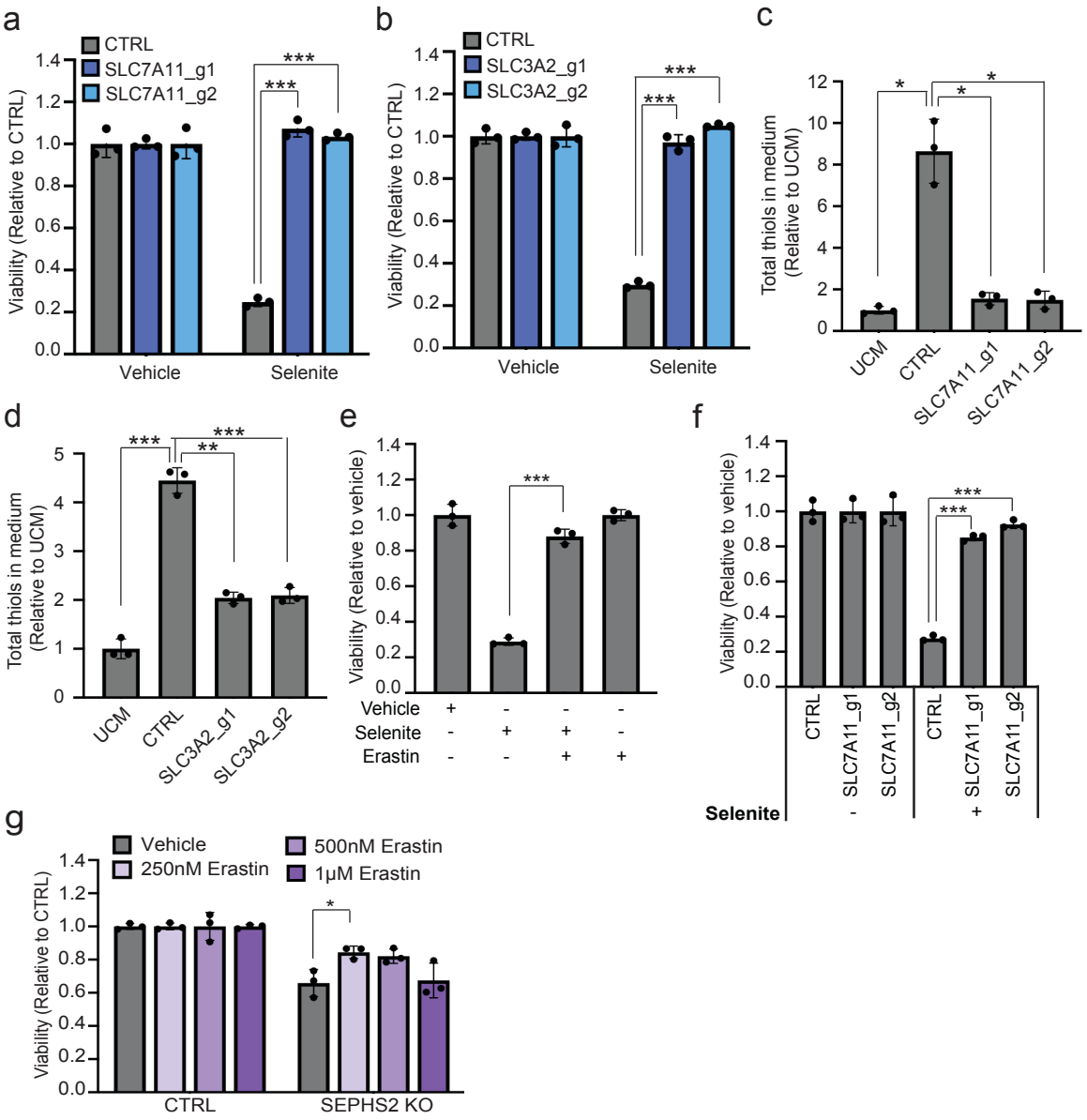

Figure 2.15 – Functional characterization of xCT

a. Viability of control and SLC7A11 KO U251 cells treated with 12 μM of sodium selenite for 48 hr. Values are relative to that of the same cells treated with vehicle (=1.0).

b. Viability of control and SLC3A2 KO U251 cells treated with 12 μM of sodium selenite for 48 hr. Values are relative to that of the same cells treated with vehicle (=1.0).

c. Total thiol quantification of 24 hr conditioned media from control and SLC7A11 KO U251 cells.

d. Total thiol quantification of 24 hr conditioned media from control and SLC3A2 KO U251 cells. Each value was normalized to that of unconditioned medium.

e. Viability of U251 cells treated with vehicle, 12 μM sodium selenite, and/or 10 μM Erastin for 72 hr. Values are relative to the cells treated with vehicle (=1.0).
f. Viability of control and SLC7A11 KO U251 cells treated with vehicle or 12 μM sodium selenite for 72 hr. Values are relative to the control cells treated with vehicle (=1.0).
g. Viability of control and SEPHS2 KO CAL120 cells treated with vehicle or indicated doses of Erastin for 4 days. Values are relative to each untreated cells (=1.0). For b-h, n = 3 biological replicates; error bars are S.D. For all panels, the measure of center is mean. For all panels, *$p < 0.05$, **$p < 0.01$, and ***$p < 0.001$ (student's two-tailed t test).

Selenoproteins, such as GPX4, have been implicated in the protection of cancer cells against various insults, such as ferroptosis or chemotherapeutic drugs[92,128] so we examined whether selenophilicity is associated with increased resistance to such insults. We found that selenophilic breast-cancer cells had increased resistance against the ferroptosis-inducing prooxidant tert-butyl hydroperoxide (TBH), as well as against nutrient starvation and hypoxia, in contrast to the non-selenophilic normal cells (Fig. 2.16a,b and Fig. 2.17a,b). We did not note any association of SEPHS2 or GPX4 expression with any tumor environmental features (Fig. 2.18a–f) or with hypoxia in culture (Fig. 2.18g). Knockout of SEPHS2 or GPX4 did not sensitize the selenophilic cancer cells to hypoxia or nutrient starvation, suggesting that other mechanisms downstream of SLC7A11 are involved in their protection against these insults (Fig. 2.17c,d).

In contrast, disruption of selenocysteine biosynthesis via SEPHS2, PSTK or SEPSECS KO, or KO of GPX4 itself, sensitized cells to TBH (Fig. 2.16c,d), suggesting a role for the selenocysteine biosynthesis pathway in protection against ferroptotic insults in selenophilic cancer cells. Furthermore, the cell death induced by SEPHS2 KO was partially rescued by the ferroptosis inhibitors ferrostatin and liproxstatin, suggesting that loss of GPX4 and sensitization to ferroptosis may facilitate the toxicity of SEPHS2 KO (Fig. 2.4e). Recently, FSP1 was identified as an endogenous inhibitor of ferroptosis[129,130]. KO of FSP1 in the MCF10A cells, which were normally resistant to SEPHS2 KO toxicity, rendered them sensitive (Fig. 2.16e,f). The function of FSP1 explains how these cells can tolerate SEPHS2 KO, even though it results in loss of GPX4. Collectively, these

results indicate that upregulation of the selenocysteine pathway is advantageous to cancer cells by protecting against ferroptosis, whereas its loss is tolerable to non-transformed cells owing to the presence of anti-ferroptotic mechanisms. Furthermore, the toxicity of SEPHS2 KO in cancer cells is facilitated by their hypersensitization to ferroptosis.

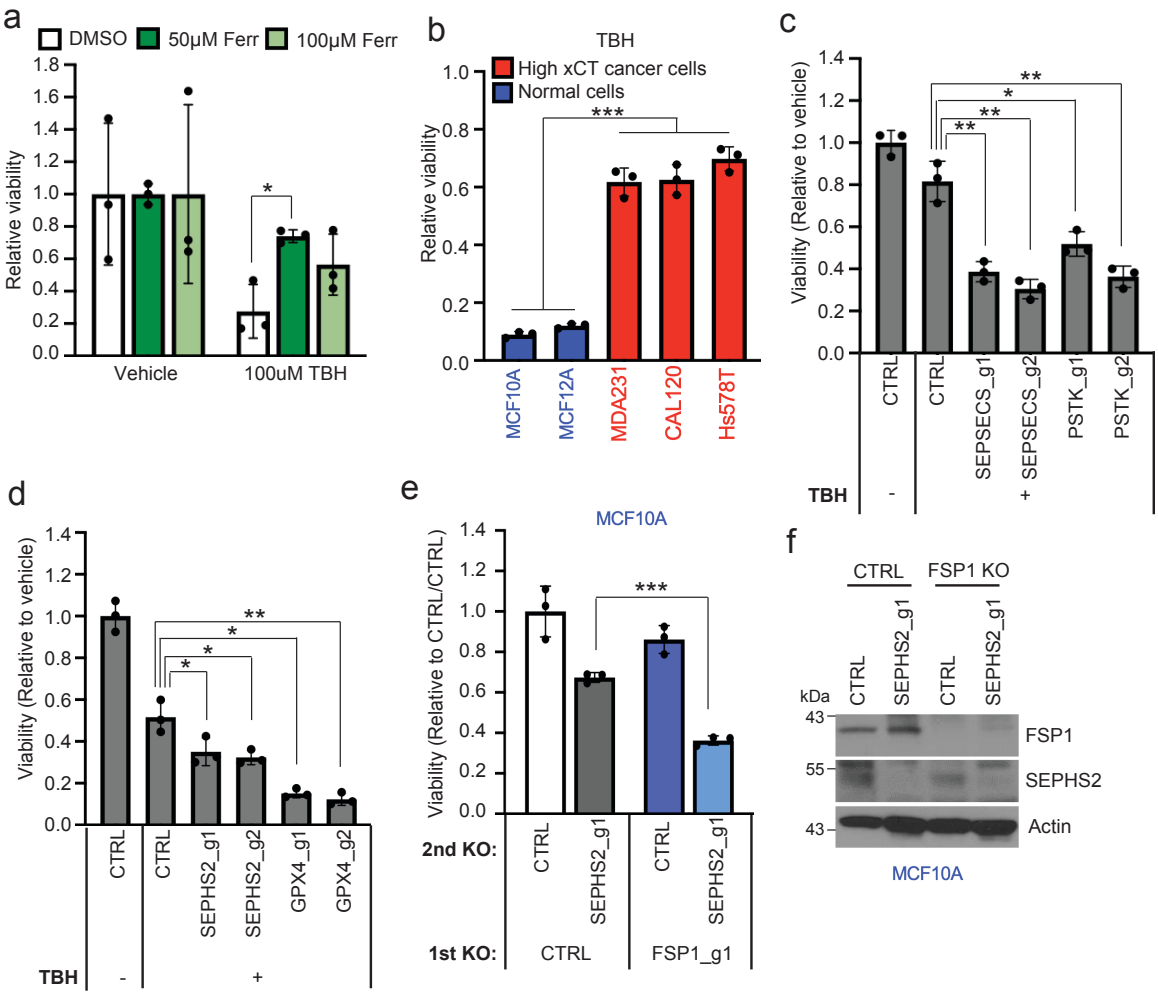

Figure 2.16 – SLC7A11 mediated selenium uptake protects against ferroptosis
a. Viability of MDA231 cells pretreated with ferrostatin (Ferr) for 3 hours and then with vehicle or 100 μM TBH for 48 hours. Values are relative to viability of cells from the same line treated with vehicle.
b. Viability of selenophilic cancer cell lines (red) and non-selenophilic normal lines (blue) treated with 100 μM TBH for 24 hours. Values are relative to viability of cells from the same lines treated with vehicle.
c. Viability of MDA231 cells subjected to KO with gRNAs against *SEPSECS* or *PSTK* for 5 days, then treated with vehicle or 50 μM TBH for 6 hours. Values are relative to viability of cells from the same line treated with vehicle.
d. Viability of MDA231 cells subjected to KO with gRNAs against *SEPHS2* or *GPX4* for 5 days and then treated with vehicle or 250 μM TBH for 24 hours. Values are relative to viability of cells from the same line treated with vehicle.
e. Viability of MCF10A cells subjected to sequential gene KO as shown. Values are relative to viability of cells from the same line subjected to CTRL KO and then to CTRL KO.

f. Immunoblots of FSP1 and SEPHS2 from **e**. FSP1 expression did not substantially differ between SEPHS2-sensitive lines and SEPHS2-insensitive lines (Fig. 2.17e). For all panels, $*P < 0.05$, $**P < 0.01$ and $***P < 0.001$ (Student's two-tailed *t*-test).

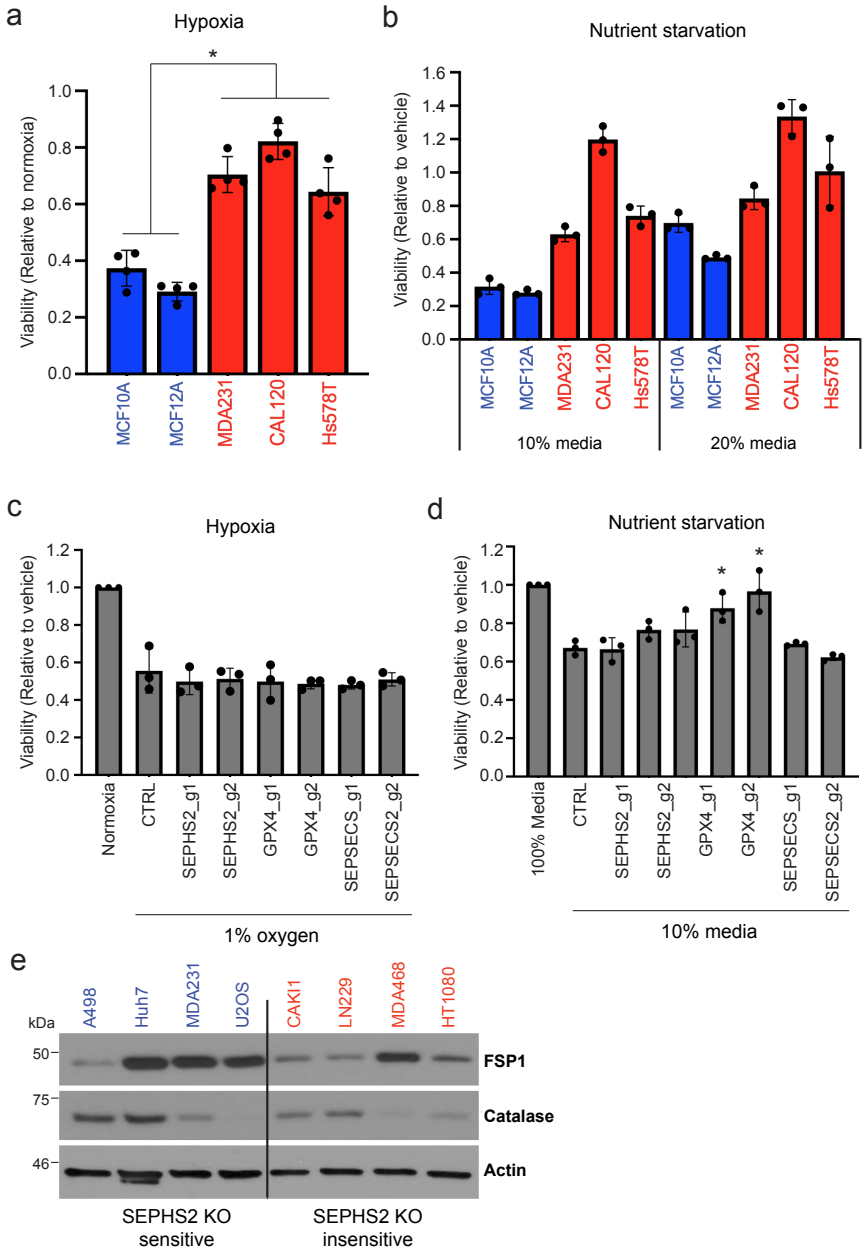

Figure 2.17 – Effects of hypoxia or nutrient-starved stresses on normal and selenophilic cancer cells

a. Viability of non-transformed (blue bars) and selenophilic cancer (red bars) cells under hypoxia (1% O_2) for 48 hours. Values are relative to cells cultured under normoxic condition (20% O_2), set at 1.0.

b. Viability of non-transformed (blue bars) and selenophilic cancer (red bars) cells under nutrient starved conditions (10% or 20% growth media) for 48 hours. Values are relative to cells cultured in 100% growth media, set at 1.0.

c. Viability of control, SEPHS2, GPX4, and SEPSECS deficient MDAMB231 cells after being cultured in hypoxic condition (1% O_2) for 48 hours. Values are relative to the cells cultured in normoxic condition (20% $O_{2)}$, set at 1.0.
d. Viability of control, SEPHS2, GPX4, and SEPSECS deficient MDAMB231 cells under nutrient starved conditions (10% growth media) for 48 hours. Values are relative to the cells cultured in 100% growth media, set at 1.0.
e. Immunoblot of FPS1 and catalase in SEPHS2 KO sensitive and insensitive cell lines. For all panels, $*p < 0.05$ (student's two-tailed t test)

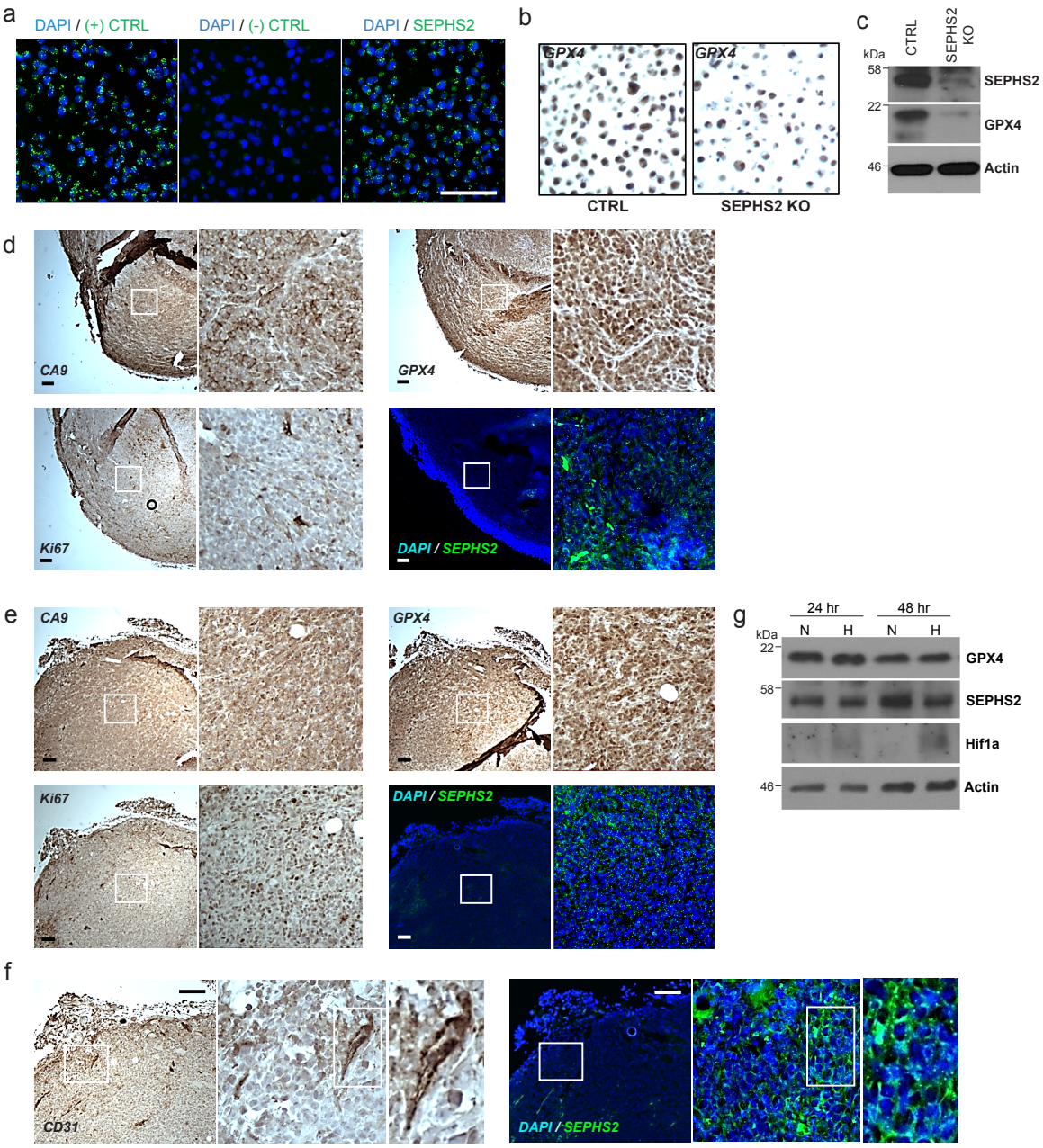

Figure 2.18 – SEPHS2 and GPX4 expression in tumor microenvironments
a. Validation of SEPHS2 RNA probe by RNAscope in situ hybridization in MDA231 cell pellet block samples. Scale bar=100μm.
b. Validation of specificity of GPX4 antibody in CTRL and SEPHS2 KO MDAMB231 cell pellet block by immunohistochemistry.
c. SEPHS2 immunoblots from the cells used in **b**.
d, **e.** Micrographs of serial xenograft tumor sections stained with CA9, GPX4, KI67 antibodies and in situ hybridized with SEPHS2 RNA probe. The right hand panels are

magnifications of the regions outlined by the white square. **d**, shows a hypoxic region as indicated by membrane staining of CA9, and with a low Ki67 index. **e**, shows a nonhypoxic region (as indicated by only background nonspecific stain in CA9) with a high Ki67 index. Scale bar is 100μm.
f. Micrographs of serial human tumor sections stained with CD31 antibody and in situ hybridized with SEPHS2 RNA probe, showing vasculature. Scale bar is 100μm.
g. Immunoblots of GPX4, SEPHS2 and Hif1a in MDAMB231 cells subjected to hypoxia (1% O_2) for 48hrs

SLC7A11-driven selenophilicity provides a protective advantage against ferroptosis through selenoprotein (GPX4) production, but we hypothesized that it will also introduce a requirement for the detoxification of selenium, in particular of the pathway intermediate selenide. Evidencing this double-edged aspect of selenium, increasing doses of selenite supplementation in the selenophilic MDA231 cells resulted in a dose-dependent increase in GPX4 levels (Fig. 2.19a). However, at higher doses, GPX4 expression plateaued, along with the formation of reactive oxygen species (ROS), which is a predicted product of selenide in aqueous solutions[67]. Furthermore, overexpression of catalase (CAT), which decomposes one form of ROS (H_2O_2), partially rescued SEPHS2 toxicity (Fig. 2.19c–e). These results suggest that SEPHS2 and the selenocysteine biosynthesis pathway sequesters free intracellular selenium (such as that in the form of selenide) to form beneficial selenoproteins, but beyond a threshold, the free intracellular selenium not incorporated into selenoproteins can harm cells via ROS formation. Further supporting this notion, selenium delivered via selenocysteine-containing peptides[131] similarly induced GPX4 expression but did not induce ROS formation (Fig. 2.19a,b).

Essentiality of SEPHS2 in cancer cells is due to its role as a selenide detoxifying enzyme

To directly examine whether SLC7A11 makes cells dependent on SEPHS2, we preemptively knocked out or pharmacologically inhibited SLC7A11 prior to SEPHS2

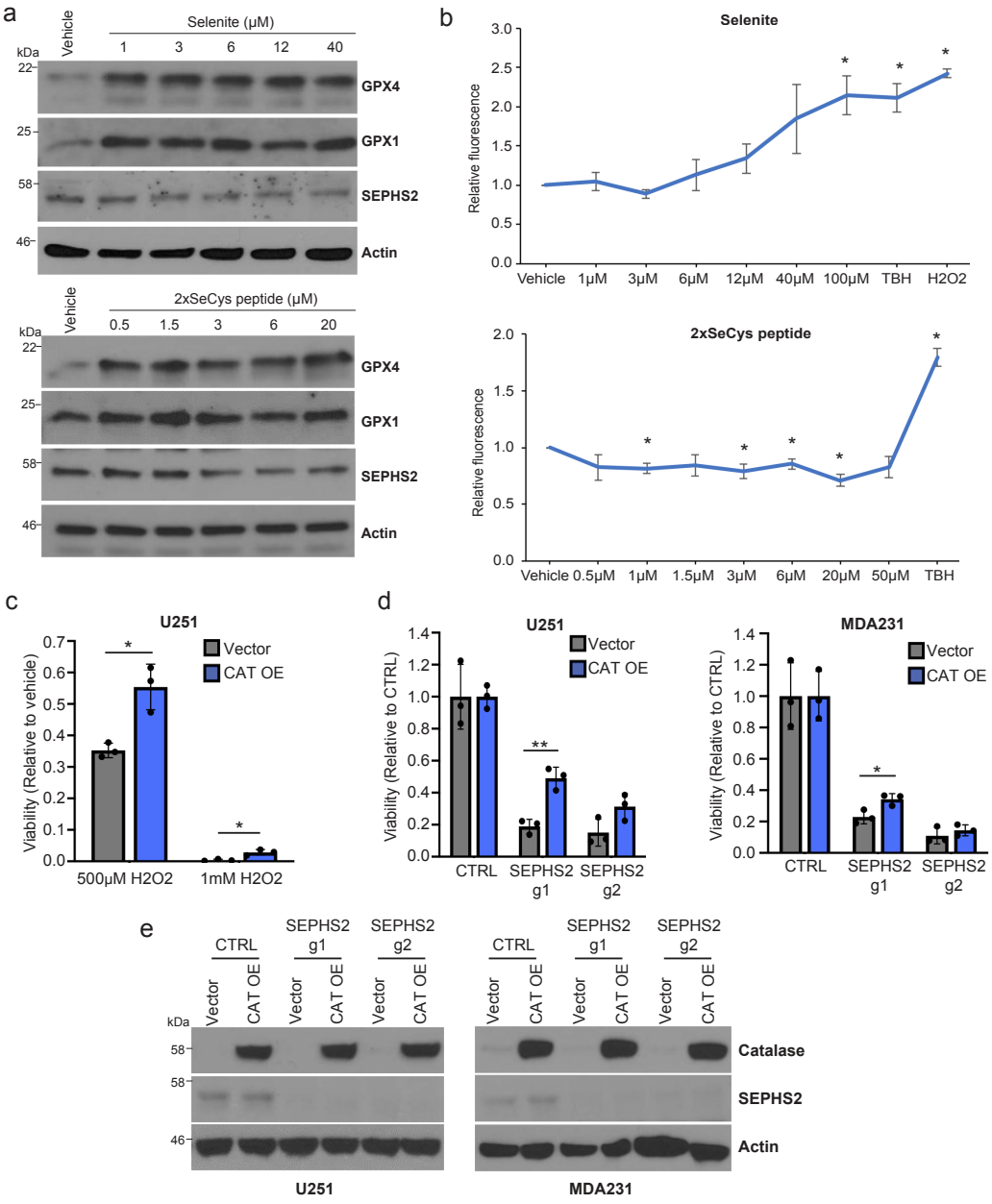

Figure 2.19 – Reactive oxygen species production by excess selenium and implications in SEPHS2 KO toxicity

a. Selenoprotein immunoblots of MDAMB231 cells at 24 hr recovery after 2 hr sodium selenite treatment or treated with 2-selenocysteine-containing peptide for 24 hr.

b. ROS quantification of cells treated with indicated concentrations of sodium selenite or 2xselenocysteine containing peptide, 250 μM TBH, or 500μM H_2O_2 for 45 mins.

c. Viability of U251 cells overexpressing vector or CAT treated with vehicle or H_2O_2 for 48 hr.

d. Viability of U251, and MDAMB231 cells overexpressing blank vector or CAT and subjected to KO with guides against SEPHS2 for 9 days.
e. Immunoblots of CAT and SEPHS2 in U251 and MDAMB231 cells overexpressing blank vector or CAT and subjected to KO with guides against SEPHS2 for 9 days.
For all panels, *$p < 0.05$ and **$p < 0.01$ (student's two-tailed t test).

KO (Fig. 2.20a and Fig. 2.15e-g). We found that not only could cells tolerate SLC7A11 loss, but also this fully prevented the toxicity of subsequent SEPHS2 KO, demonstrating that SLC7A11 directly causes a dependency on SEPHS2 and indicating a gain-of-function mode of toxicity. To further determine whether SEPHS2 has a function that is independent of its role in selenoprotein synthesis, we took advantage of the fact that KO of the other selenocysteine biosynthesis components PSTK or SEPSECS can also eliminate selenoprotein production, including that of SEPHS2. We constructed a mutant SEPHS2 (SEPHS2-U60C) with a selenocysteine-to-cysteine mutation that is predicted to decrease, but not eliminate, catalytic activity[132] while allowing the protein to be expressed even when selenocysteine biosynthesis is halted owing to SEPSECS or PSTK KO. We demonstrated that this enzyme is functional, as it rescued SEPHS2 KO in our earlier experiment (Fig. 2.6b). Expression of this construct was found to rescue the toxicity of SEPSECS or PSTK KO despite the cells' inability to express any other selenoprotein (Fig. 2.20b,c), which demonstrates that (1) SEPSECS and PSTK KO are toxic because of the loss of SEPHS2 that they cause, and (2) SEPHS2 impacts viability even when all selenoprotein biosynthesis has ceased. The rescue was not complete, indicating that loss of other selenoprotein(s) such as GPX4[132] may have partially contributed to the toxicity. Collectively, these data demonstrate that SEPHS2 is required in cancer cells for a reason other than production of selenoproteins.

We next examined whether SEPHS2 is required in cancer cells to detoxify the selenide produced by the selenocysteine biosynthesis pathway. Supporting this model, overexpression of SEPHS2 protected cancer cells against the toxicity of

selenite, whereas loss of SEPHS2 created a synergistic effect with selenite (Fig. 2.20d,e). As selenide is volatile and cannot be detected by conventional liquid chromatography–mass spectrometry (LC–MS) methods[133,134] nor treated as a conventional toxic drug, we had to develop a system for treating selenide to cells in a controlled manner, as well as a method for directly detecting selenide. First, we dissolved sodium selenide (Na_2Se) in an acidic (3.7% HCl) solution, which is predicted to produce selenide (H_2Se) via replacement reaction (Fig. 2.21a). To detect whether selenide gas was produced, we embedded silver nitrate or lead acetate, which have been shown to react with selenide in aqueous solution to produce dark brown metal–selenium compounds[135], into polyvinylpirolidone (PVP) as an immobilizing matrix, and these spots were placed on the lid of 96-well plates at varying distances from the gas-producing compartment. A color change was observed that directly correlated with distance, suggesting the capture of volatile selenide in these spots (Fig. 2.21a). Importantly, inductively coupled plasma mass spectrometry (ICP-MS) of these spots indicated that selenium had a robust presence, verifying that we were capturing volatile selenide gas (Fig. 2.21b). When this reaction was conducted in the middle compartment of a 96-well plate confluent in each well with MDAMB231 cells, we observed toxicity that followed a radial pattern emanating from the gas source, with toxicity correlating with proximity (Fig. 2.21c). Using this treatment system, we directly tested the effects of disrupting or overexpressing SEPHS2 on cells plated at equal distances from the source of selenide gas (Fig. 2.21d). Disruption of SEPHS2 sensitized cancer cells to selenide (Fig. 2.21e), and overexpression

of SEPHS2 protected cancer cells against it (Fig. 2.21f). Therefore, these results clearly demonstrate that SEPHS2 has a selenide-detoxification function.

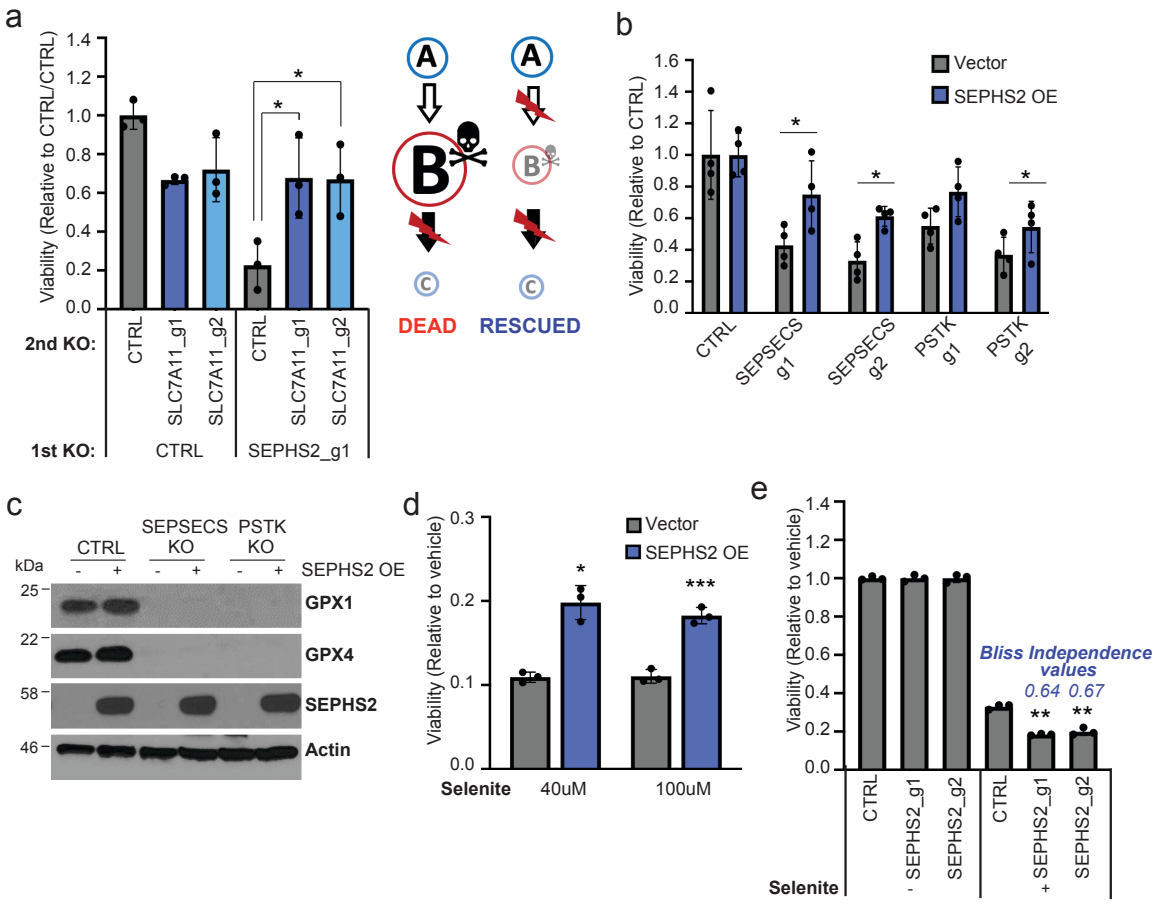

Figure 2.20 – Essentiality of SEPHS2 in cancer cells is due to selenide removal rather than downstream selenoprotein biosynthesis

a. Viability of MDAMB231 cells subjected to sequential gene KO as shown, demonstrating that preemptive loss of SLC7A11 renders SEPHS2 dispensable. Values were normalized to those of cells from the same line subjected to CTRL KO and then subjected to CTRL KO.

b. Viability of U251 cells overexpressing (OE) blank vector or SEPHS2-U60C that were subjected to KO with gRNAs against *SEPSECS* or *PSTK* for 11 days.

c. Immunoblot of selenoproteins in U251 cells overexpressing blank vector or SEPHS2-U60C and subjected to KO with gRNAs against *SEPSECS* or *PSTK* for 11 days.

d. Viability of U251 cells overexpressing blank vector or SEPHS2-U60C and treated with sodium selenite for 48 hours. Values are relative to that of cells from the same line treated with vehicle.

e. Viability of U251 cells subjected to KO with gRNAs against *SEPHS2* or controls and then treated with 12 μM sodium selenite for 72 hours. Bliss independence values were calculated with the formula $E_C = E_A + E_B - E_A \times E_B$, for which a value below 1.0 indicates a synergistic effect.

For all panels, *$p < 0.05$, **$p < 0.01$, and ***$p < 0.001$ (student's two-tailed t test)

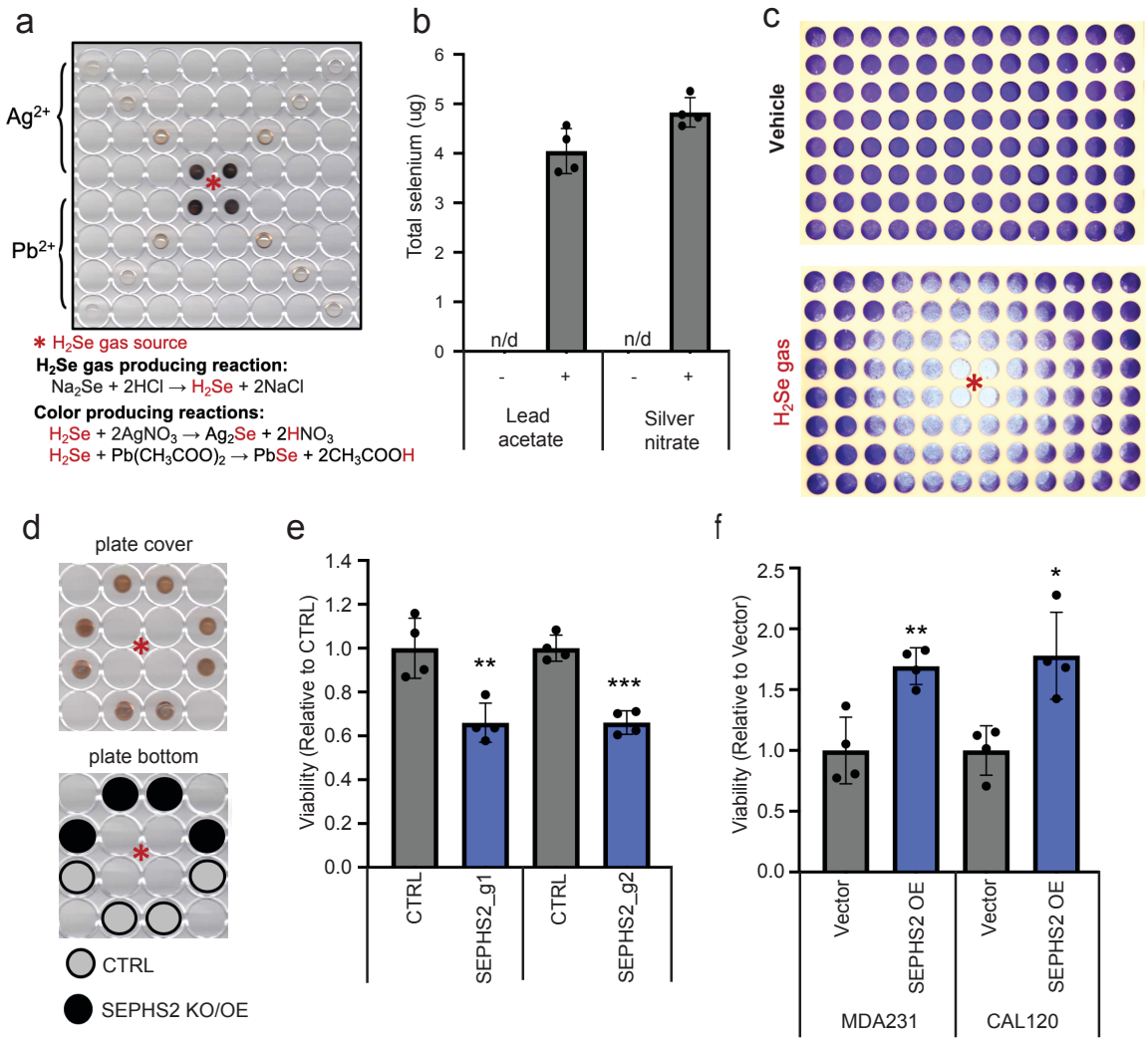

Figure 2.21 – SEPHS2 plays a selenium detoxification role in in cancer cells
a. Scanned image of the polystyrene microplate cover spotted with PVP embedded with silver nitrate or lead acetate, used as a non-contact selenide-gas indicator, after selenide-gas exposure for 1 min.
b. Selenium quantification, measured by ICP-MS, of the spots of PVP embedded with silver nitrate or lead acetate, demonstrating the capture of volatile selenide. Four spots that were equidistant from the selenide source were measured. n/d, not determined.
c. Scanned image of crystal violet staining of the remaining MDAMB231 cells following vehicle or selenide-gas exposure for 24 hours. For **c** and **d**, the asterisk indicates the location of selenide-gas production.
d. Experimental layout for comparing sensitivity to selenide gas, via equidistant cell plating. Similar browning of silver nitrate–PVP spots indicates similar exposure levels to selenide gas.

e. Viability of SEPHS2-KO or control MDAMB231 cells under selenide-gas exposure for 24 hours. Values are normalized to the viability of cells transduced with non-targeting gRNAs.
f. Viability of MDAMB231 cells overexpressing SEPHS-U60C or blank vector under selenide-gas exposure for 48 hours. Values are normalized to the viability of empty-vector-transduced cells.
For all panels, $*P < 0.05$, $**P < 0.01$ and $***P < 0.001$ (two-tailed Student's *t*-test).

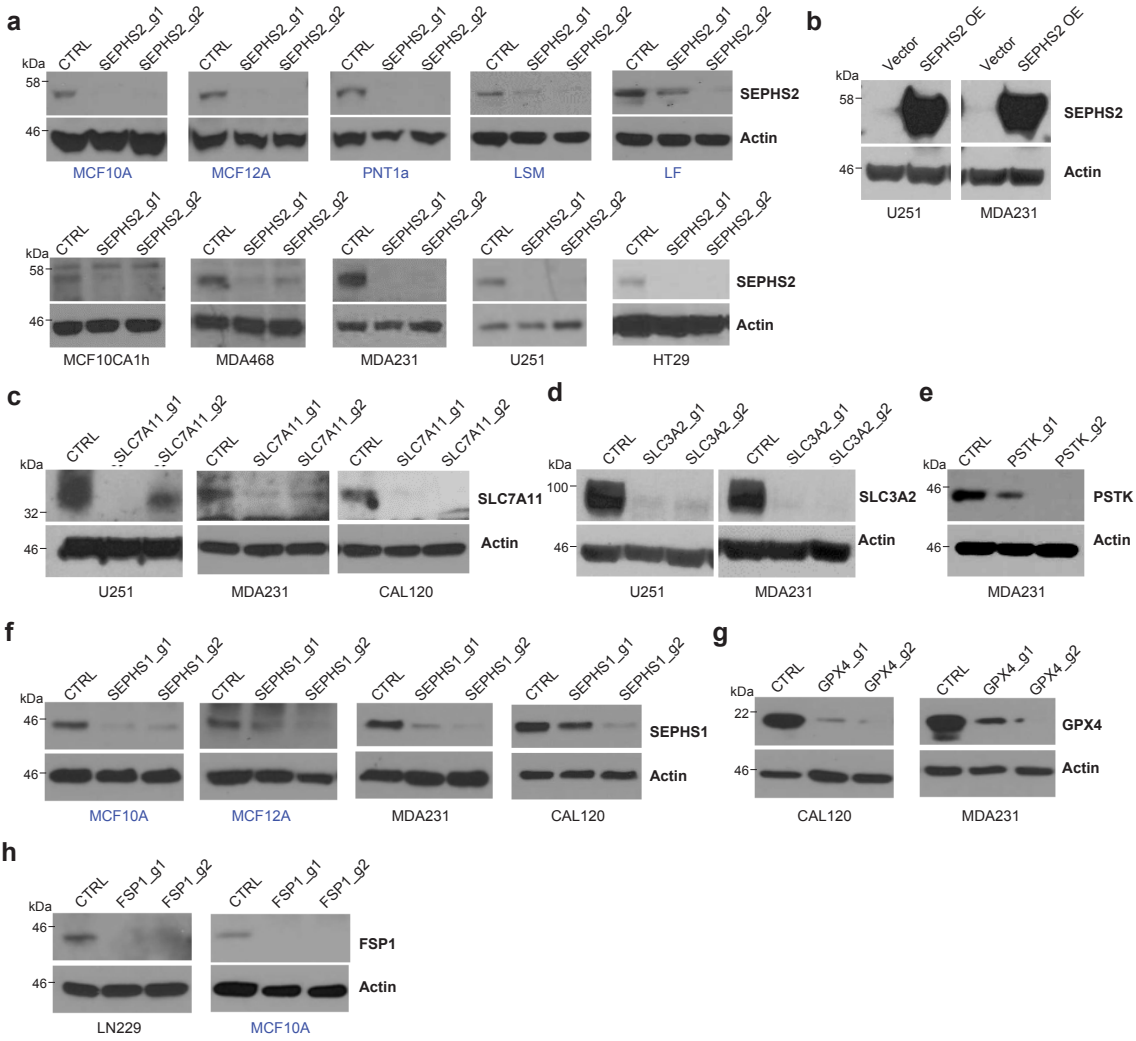

Figure 2.22 – Confirmation of gene knockout or overexpression after lentiviral transduction

a. Immunoblots of SEPHS2 in 5 non-transformed (blue) and 5 transformed (black) cell lines transduced with Cas9/sgRNAs against SEPHS2, and control (non-targeting sgRNA).

b. Immunoblots of SEPHS2 in cells transduced with CRISPR resistant SEPHS2_U60C and control (empty vector).

c. Immunoblots of SLC7A11 in cells transduced with Cas9/sgRNAs targeting SLC7A11 or non-targeting sgRNA.

d. Immunoblots of SLC3A2 in cells transduced as indicated

e. Immunoblots of PSTK in cells transduced as indicated.

f. Immunoblots of SEPHS1 in 2 non-transformed and 2 cancer cells transduced as indicated.

g. Immunoblots of GPX4 in cells transduced as indicated.

h. Immunoblots of FSP1 in cancer cells transduced as indicated.

All samples were lysed between 7-8 days after viral transduction.

DISCUSSION

In summary, we have shown how selenium uptake and selenocysteine biosynthesis are aberrantly activated in a subset of cancer cells owing to SLC7A11/xCT, and how this necessitates selenide detoxification by SEPHS2. The identification of selenophilic subsets of cancer cells has important implications in cancer biology that future investigative efforts can address, as selenium uptake drives the expression of selenoproteins implicated in processes such as ferroptosis, drug resistance and endoplasmic-reticulum stress[84,92,128]. While upregulation of selenoprotein production via the SLC7A11–SEPHS2 axis is likely to impact various aspects of cancer biology, we demonstrate that the most urgent requirement in these cancer cells is the detoxification of selenide, an endogenously produced metabolite that shows high volatility and toxicity. Indeed, our functional demonstration of selenide as the toxic intermediate of selenocysteine biosynthesis explains the longstanding paradox of how selenium, an essential micronutrient, can be toxic and anticarcinogenic. Targeting the selenide detoxifier SEPHS2 allows us to kill cancer cells with efficacy and precise selectivity, serving as a blueprint for future studies to exploit other pathways containing toxic metabolites.

EXPERIMENTAL PROCEDURES

Cell lines and cell culture

All cell lines were cultured at 37 °C under 5% CO2 and atmospheric oxygen unless otherwise indicated.

Molecular cloning of expression constructs

SEPHS2 was PCR-amplified from complementary DNA produced from WM115 cells, using forward and reverse primers containing BamH1 and NOT1 sites, respectively. The verified amplicon sequence corresponded exactly to the published consensus sequence for SEPHS2 (CDS ID: CCDS42150.1). The amplicon was cloned into pLV-EF1α-IRES-Blast vector. SEPHS2-U60C was constructed with a region (c.180A>C for p.U60C, and 5′-GGAGGGACGGCAGTGACCGGTGG-3′ (616–638 bp) was replaced by 5′-GGAGGGACCGCCGTTACTGGTGG-3′ for SEPHS2 CRISPR g1 resistance) mutated by site-directed mutagenesis for CRISPR resistant SEPHS2-U60C. Wild-type SEPHS2 has a UGA codon (amino-acid position 60), which acts to encode selenocysteine due to the presence of a stem-loop structure in the 3′ untranslated region called the selenocysteine insertion sequence (SECIS). In our SEPHS2-U60C construct, the codon is mutated to cysteine and the SECIS removed to allow expression independently of selenocysteinyl-tRNA availability, and four silent mutations are present in the guide-recognition site for SEPHS2_g1.

Lentivirus production and CRISPR–Cas9-mediated genome editing in cell lines.

Optimal gRNA sequences were obtained from a published guide sequence library[136]. Pseudotyped lentivirus was produced by cotransfecting pLentiCRISPR v2-containing guide sequences of interest7 with the VSV-G envelope plasmid and the Delta-Vpr packaging plasmids into HEK293T cells using X-tremeGENE 9 Transfection Reagent (Roche). Lentivirus-containing supernatant was collected at 24 h after replacement with fresh medium. The virus was directly used without being concentrated. Target cells were infected with freeze and thawed viral supernatant in the presence of 10 μg ml–1 polybrene for 24 h and then replaced in medium with puromycin (typically at 1 μg ml–1) or blasticidin (typically, 20 μg ml–1) to select for transduced cells. The titer for each virus was determined, and cells were infected at sub-one multiplicity of infection to prevent non-specific toxicity that can occur from superinfection leading to excessive expression of Cas9 and guide.

Determining relative cell viability following CRISPR–Cas9 KO.

Varying numbers of cells for each cell line (between 1,000 and 5,000 cells per well in each 96-well plate) were plated, and 1day after plating, cells were infected with lentivirus and polybrene. As the cell lines have differing growth rates, infectivity to pseudotyped lentivirus and sensitivity to puromycin, each of these parameters had to be optimized for each cell line. Briefly, the goal was to adjust the starting number of cells and the amount of virus for each cell line such that, after 3 days of puromycin selection, roughly 100–200 infected cells survived selection and were visible in the well. This low number ensured a low multiplicity of infection, and that cells did not reach confluency

before the end of the experiment, which would introduce noise. For each CRISPR guide–cell line combination, we measured cell viability (using CellTiter-Glo) at two points following infection and selection (day 5 and day 9). For each combination, the relative growth, as measured by fold-change increase of CellTiter-Glo signal between these two time points, was calculated and compared with the growth rate of that cell line transduced with non-targeting (CTRL) guide. For example, if U2OS cells grew by 5-fold under CTRL gRNA between day 4 and day 9 and U2OS cells grew by 2.5-fold under guide X, then guide X would have a relative viability score of 0.5. This system allowed us to precisely control for both the different growth rates and infectivity of different cell lines, as well as variabilities in starting number of infected cells, which arise even with titered virus. In this manner, the effects of KO for each of the 12 candidate detoxifying enzymes, 3 guides each, were determined across 11 different cells lines for the initial analyses (Fig. 2.3b). As we expanded to examine SEPHS2 KO effect in more cell lines (Fig. 2.3c), we utilized two guides (SEPHS2_g1 and SEPHS_g2). The individual guides are averaged to represent SEPHS2 effect.

Monitoring of long-term growth of MDAMB231 and MCF10A CRISPR–Cas9 KO lines.

MDAMB231 and MCF10A cells were infected with lentivirus to transduce them with CRISPR–Cas9 gRNAs against CTRL or SEPHS2 (guide 1), each in a 10-cm dish. The day after infection was counted as day 1. Every 4 days, cell counts were obtained and recorded, and 500,000 cells were replated onto a new 10-cm dish, to have

sufficient cells to continue the experiment and to allow monitoring of the growth rate of these 500,000 cells over the next 4 days. Leftover cells that were not replated were lysed for western blot analyses as shown in Fig. 2.11c. This step was repeated every 4 days to continually monitor the growth rate of each cell line.

Colony-formation assay.

MDAMB231 cells expressing SEPHS2-U60C or blank vector, and MCF10A cells were infected with SEPHS2 KO or CTRL virus. After 6 days of selection, the cells were seeded at a density of 2,000 MDAMB231 cells or 500 MCF10A cells per well in 6-well plates with 2 ml medium; MCF10A cells were plated at a lower density because of their higher proliferation rate. Five hundred microliters of medium were added in each well every 4 days without medium change. Nine days after the initial cell seeding, cells were washed with PBS, and stained for 1 h with 0.5% crystal violet in 25% methanol/75% PBS solution. Plates were then washed twice with PBS to remove excess dye and were scanned.

Western blot analysis.

Briefly, cells were quickly washed with cold PBS and lysed in cold RIPA lysis buffer freshly supplemented with protease inhibitor (Roche). Supernatant was collected after centrifugation at 13,000g at 4 °C for 10 min. Protein concentration was determined by Bradford assay. Proteins were denatured in 6X Laemmli buffer (Boston Bioproducts) and boiled at 90 °C for 5 min. We found that not boiling the sample was

required for SLC7A11 detection. Equal amounts of total protein (typically, 15–25 μg depending on the experiment) were loaded per lane on a polyacrylamide gel and analyzed by standard immunoblotting. Primary antibody dilutions are provided in the Reporting Summary. Immunoblot signals were detected by ECL, Pico or diluted Femto substrate (Pierce).

Cell-viability assay.

Cell viability was measured by CellTiter-Glo Luminescent Assay (Promega) using a Beckman Coulter DTX880 Multimode plate reader. Luminescence capture was set at 1second. Crystal violet staining was performed to visualize surviving cells following exposure to hydrogen selenide gas in a 96-well plate (Fig. 2.21c). Briefly, 8,000 cells were plated in two 96-well plates. The next day, the reaction mixture, which produced hydrogen-selenide gas, was placed in the center of the plate, and the plate was tightly sealed in the plastic bag. The plate sealed in the plastic bag was placed in the CO2 incubator. After 24 hours of incubation, cells were washed with PBS, and stained for 1 hour with 0.5% crystal violet in 25% methanol/75% PBS solution. Plates were then washed twice with PBS to remove excessive dye and scanned.

Medium thiol quantification.

Cells were washed once with phenol-red-free growth medium, and 10,000 cells were plated with the 100 μl of phenol-red-free growth medium in a 96-well plate. One hundred microliters of conditioned medium was collected and directly mixed with

50 µl of 10 mM DTNB (5,5′-dithiobis-(2-nitrobenzoic acid) dissolved in DMSO after 24 hours of conditioning. Absorbance at 450 nm was measured spectrophotometrically in 5 min (DTX880, Beckman Coulter). The remaining cells in the same plate were subjected to CellTiter-Glo assay for normalization. The absorbance value of the blank was subtracted as background, and values were normalized to total viable cells as determined by CellTiter-Glo. Owing to the masking effect of phenol red on DTNB absorbance, created by reacting with thiols, phenol-red-free medium was used for all thiol quantifications.

Production of selenide.

Selenide gas was formed by mixing sodium selenide, at a final 50 mM concentration, into 3.7% hydrochloric acid solution. Because selenide gas is volatile, 100 µl of the mixture was added into the center of the 96-well plate immediately after mixing the sodium selenide with hydrochloride. Immediately following this, the plate was tightly sealed in a plastic bag. All procedures were performed in the safety hood because of the toxic and volatile nature of the selenide that was produced.

Selenide detection.

PVP (5% wt/vol) solution was mixed with 1 M silver nitrate or lead acetate at a ratio of 9:1, yielding final concentrations of 100 mM of silver nitrate or lead acetate, and 4.5% PVP. Reagents were freshly prepared for each experiment. The solutions were mixed well by pipetting. Next, 15 µl of metal–PVP mixture was carefully spotted on the

inside of the cover of a 96-well plate. The cover was dried at room temperature for at least 1 hour, to form a coating membrane. This cover containing the ‘detector spots’ was placed above the wells, in which selenide gas was produced in the center of the plate. Upon immediate reaction with the selenide gas, the spots produced silver selenide or lead selenide, which are brown in color whereas the original spot was clear. Spots were developed for up to 1 min. The plate was imaged, and the spots were subjected to acid digestion for further ICP-MS analysis.

Total selenium measurement by ICP-MS analysis.

Cells were plated into 15-cm dishes, and medium was changed at 75% confluency and treated with 12 μM selenite 24 h after medium change. Cells were collected at 2 hours after selenite treatment, washed 3 times in cold PBS and weighed to a total cellular mass of 80–100 mg. The cell pellets were treated with 500 μl 1:1 H_2O_2/HNO_3 and were allowed to stand for 12 hours at room temperature with periodic venting. The samples were then sonicated at 35 kHz and 40 °C for 1 hour with periodic venting. The contents of the Eppendorf tube were transferred to a glass digestion tube with ASTM type I water (2 x 1 ml). The tubes were sealed and heated at 140 °C for 2 hours, cooled and diluted to 5 ml with ASTM type I water for analysis. All analyses were carried out with an Agilent 7500 A ICP-MS system fitted with a standard concentric nebulizer, a Peltier-cooled double-pass Scott-type spray chamber, a torch shield and standard Ni interface cones. The peristaltic pump was set to deliver 10 g l–1 yttrium as an internal standard, and masses at 77–78, 82, 83 and 89 were scanned using a spectrum

analysis with 20 points per mass, with 3 repetitions. Interference correction was conducted on the mass at 82 amu using standard environmental correction for bromine (82 = 82–83). Following each analytical sample, the probe-sample introduction system was rinsed with 10% nitric acid for 1 min to minimize carry-over. Calibration curves were prepared using standard solutions of Se (Ultra Scientific) and quality-control samples using a multielement standard from Environmental Express. In addition, mock samples were prepared for each calibration level and subjected to the sample preparation described previously to assure adequate recovery. In all cases, the recoveries were 100 ± 10% (data not shown). The calibration solutions were analyzed without background subtraction using the 89 internal standard peak. In all cases, the linear regression afforded an $r \geq 0.996$. The relative concentrations based on the use of the 77 and 82 isotopes were examined and found to agree within ±10%, so the average concentration was reported.

Measurement of selenium uptake by fluorometric assay.

Total selenium content was measured via fluorometric assay[137]. Cells were plated into 10-cm dishes, medium was changed at 75% confluency and was treated with vehicle or 12 μM selenite at 24 hours after medium change. Cells were collected 2 hours after selenite treatment, washed three times in cold PBS, and counted to 5 million then resuspended in 100 μl MiliQ H_2O and added to borosilicate glass tubes. Then, 500 μl of a 4:1 mixture of HNO_3 and $HClO_4$ was added to the glass tube and incubated on a heat block overnight at 130 °C. Next, 500 μl of HCl was then added and incubated at 130 °C for 1 hour. Tubes were removed and allowed to cool to room temperature before addition

of 2 ml of 2.5 mM ETDA, 500 µl of 6.3 mM 2,3-diaminonapthalene-HCl in ultrapure water and 1 ml of cyclohexane. Tubes were capped and incubated for 30 min at 60 °C. Samples were placed in a shaker for 5 min, and then 150 µl of the upper phase was aliquoted in technical triplicates into a 96-well plate. The plate was read for fluorescence emission on a DTX880 (Beckman Coulter) plate reader with excitation at 360 nm and emission at 528 nm. Values for selenite supplemented cells were normalized to basal values of intracellular selenium, giving a relative selenium uptake measurement.

Orthotopic xenograft studies.

Eight-week-old female wild-type nude athymic nu–/nu– mice were purchased from Charles River Laboratories and raised in an animal facility at University of Massachusetts Medical School (UMMS). Littermate controls were not used. To compare tumor growth between control and SEPHS2-KO cell lines in vivo, at 10 days after viral transduction, the cells (1×10^6) were resuspended in 1× PBS with Matrigel basement membrane matrix at a 1:1 ratio (total volume, 35 µl) and were subcutaneously injected into the area between the upper right second and third mammary fat pads of the nude mice. Tumor sizes were measured using a Vernier caliper, and volumes were determined according to the formula $4/3\pi \times ((L \times W \times D)/2)$, where L is the measurement parallel to the midline of the supine animal and W is perpendicular to the midline, and D is the distance from chest to the top of the tumor. Mice were euthanized at 7 weeks after injection, and the solid tumors were isolated. Mouse orthotopic xenografts were set up with 7 mice per cohort, as we have previously obtained statistically significant results

with this number of mice using this cell-line model in previous experiments that projected a >50% difference in cell viability. Mice were randomly assigned to be injected with SEPHS2 KO MDAMB231 cells or CTRL KO MDAMB231 cells. The researchers who carried out injection and tumor measurements were blinded to groups (SEPHS2 KO versus CTRL KO tumors). Our experiments complied with all ethical regulations and were approved by the Institute Animal Care and Use Committee (IACUC) of University of Massachusetts Medical School.

Processing of human breast tissues for SEPHS2 protein quantification.

All human breast-cancer samples and normal breast tissues were obtained with informed consent from the University of Massachusetts Medical School Biorepository and Tissue Bank using procedures conducted under an Institutional Review Board (IRB)-approved protocol. After their surgical removal, fresh tumors and normal tissues were partly snap-frozen in liquid nitrogen immediately and stored at −80 °C. The frozen section was homogenized in RIPA buffer with complete protease inhibitor cocktail, and was then centrifuged at 13,000g at 4 °C for 10 min. Then SDS–polyacrylamide gel electrophoresis was performed as described in the 'Western blot analysis' section. A strong non-specific band that appeared in breast tissues required the use of a 10% gel and long electrophoresis to separate SEPHS2 protein from the non-specific band (labelled with an asterisk in Fig. 2.10a). Protein levels of SEPHS2 and actin were quantified using ImageJ. Scanned films were inverted, and the intensity of each band was measured, and then the background value was subtracted. The intensity value of

the SEPHS2 protein band for each sample was normalized to the intensity value for actin protein.

Survival analysis.

Kaplan–Meier curves was used to analyze tumor-free survival in mouse experiments and for overall survival of human participants. The R survival package[138,139] was used to generate Kaplan–Meier survival plots and to compare the survival distributions of people with low SEPHS2 and those with high SEPHS2. The survival data 'brca_tcga_pub2015_all'[140] was downloaded from cBioportal[141]. People were divided into high and low groups on the basis of their SEPHS2 expression level (top 25% or bottom 25% in the cohort).

Transporter CRISPR screen.

We infected U251 cells with two CRISPR guides for each transporter target. Cells were replated in 12 μM selenite medium after full selection of the CRISPR guides, typically for 5 days. We measured cell viability (using CellTiter-Glo) at 3 points post selenite treatment: 24, 48 and 72 h. For each guide, the relative growth was measured by fold-change increase of CellTiter-Glo signal between selenite-treated cells and untreated controls.

Double-KO rescue assay.

MDAMB231 cells were infected with pLentiCRISPR V2-based lentivirus to deliver the first KO (CTRL, SLC7A11_g1, SLC7A11_g2) and were selected with puromycin. Cells were secondarily infected with pMD154 lentivirus to allow expression of the second gRNAs (CTRL or SEPHS2_g1) 6–7 days after initial infection, and were subsequently selected with 500 μg/ml hygromycin. These cells were selected for 5 days before being plated in triplicate in 96-well plates, with 200 cells per well and with duplicate plates. One plate was assayed for viability after overnight incubation, and the second plate was read after 5 days of growth to determine the relative growth rate of double-KO cells in comparison to controls.

Immunohistochemistry

Immunohistochemical detection of CD31, Ki67, CA9 and GPX4 in serial tumor samples was performed using formalin-fixed and paraffin-embedded tissue sections. After deparaffinization in xylene for 20 min, rehydrated tissue sections were subjected to antigen retrieval by boiling in Borg Decloaker solution (Biocare Medical) for 5 min. Slides were blocked with 5% horse serum and then incubated with antibodies for 1 h at room temperature. After incubation, biotinylated secondary antibodies plus streptavidin were used to stain the samples, with DAB chromogen as substrate, and hematoxylin solution for nuclear counterstaining. The section samples were imaged by QCapture Suite 2.98.2.

Immunocytochemistry.

Cell were seeded on cover slips coated with poly-d-lysine and collagen, fixed with 4% paraformaldehyde in PBS, permeabilized by incubation with 0.1% Triton X-100 in PBS and subsequently blocked with 1% BSA in PBS for 1 hour. To quantify the level of cells expressing cleaved ecaspase-3, the cells were incubated with a rabbit antibody against cleaved caspase-3 (Asp175) (Cell Signaling, 9664) in the cold room overnight. The cells were washed with PBS 3 times and were incubated with anti-rabbit Alexa Fluor 488 (Invitrogen) for 1 hour at room temperature in the dark. The cells were subsequently washed with PBS and mounted with Gold Antifade Reagent with DAPI (Invitrogen, P36935).

RNAscope in situ hybridization.

For SEPHS2 mRNA staining, fluorescent RNAscope in situ hybridization (ISH) was performed on the paraffin-embedded serial tumor sections using the RNAscope protocol (Advanced Cell Diagnostics, RNAscope Multiplex Fluorescent Reagent Kit v2 Assay User Manual, document number; 323100-USM); all reagents were provided by the RNAscope fluorescent reagent kit. After deparaffinization in xylene for 20 min and rehydration with serial 100%, 95% and 70% ethanol for 5 min each, tissue sections were treated with hydrogen peroxide for 10 min and heated at 99 °C in target-retrieval solution for 20 min. After target retrieval, sections were treated with protease plus at 40 °C in the hybridization oven for 30 min and hybridized with 3-plex positive control RNA probe, 3-plex negative control RNA probe and SEPHS2 RNA probe for 2 hours at 40 °C in the oven. The section samples were incubated with 3 different

amplifiers, AMP1 (30 min), AMP2 (30 min) and AMP3 (15 min), at 40 °C to amplify hybridization signals. After amplification steps, sections were treated with horseradish peroxidase C1 for 15 min at 40 °C and incubated with diluted TSA plus fluorescein (1:50 in TSA buffer) for 30 min at 40 °C in the oven. The section samples were counterstained and mounted with Vectashield antifade mounting medium with DAPI and were imaged by Lionheart LX Automated microscope (BioTek). Images were processed by Gen5 software (BioTek).

Cell-death analysis.

Cell death was measured using a FITC Annexin V Detection Kit (BD Biosciences, 556547). Cell lines treated with selected concentrations of sodium selenite or cell lines following KO with guides against SEPHS2 were stained with propidium iodide and annexin V–FITC. The stained cells were analyzed using the BD LSR II flow cytometer (BD Biosciences). The data were analyzed by FlowJo 10. Detection of ROS. ROS were detected using DCFDA Cellular ROS Detection Assay Kit (Abcam, ab113851). MDAMB231 cells were seeded at 2,000 cells per well, and 24 hours later were stained with DCF reagent and then treated with various selenite concentrations for 45 min. For SeCys peptide treatment, MDAMB231 cells were seeded at 2,000 cells per well and, 24 hours later, were treated with various concentrations of SeCys peptide for 24 hours before DCF staining. Fluorescence was measured using 485-nm excitation and 535-nm emission filters with a Beckman Coulter DTX880 Multimode plate reader. Values were normalized to those of DCF background and vehicle treatment.

Medium conditioning, selenide uptake and ferroptosis.

We have established that selenite uptake is highly reliant on the presence of extracellular thiols (Fig. 2.14a,b). Therefore, we observe that the toxicity of selenite treatment is highly modulated by whether the medium has been preconditioned for a period of time, which increases toxicity, or whether selenite has been added along with a fresh medium change, which conversely requires a longer time for selenium uptake and toxicity to occur. We note that in the experiments for Figs. 2.14c, 2.15a,b,e,f and 2.20d,e selenite was added to the medium that had already been conditioned since the seeding of the cells; in Fig. 2.13a and Fig. 2.19b, selenite was added along with fresh medium. Owing to the need to prestain cells for the DCFDA assay in Fig. 2.19b, selenite was added with 75 μM reduced glutathione in assay buffer to provide reduced thiols because conditioned medium could not be used for this assay. We found that a second factor that affected toxicity in some of our experiments was whether the virally transduced cells were 'in place' for the duration of the experiment, or for practical reasons if trypsin detached and then reattached during the experiment, for example when cells were virally transduced and selected in 6-well format and then replated in 96-well format for CellTiter-Glo assays. In the latter case, we found that disruption of selenocysteine biosynthesis pathway (such as via SEPHS2 KO) did induce a small degree of toxicity even in the insensitive cells, which we think was due to detachment and reattachment being a mild ferroptotic stimulus. The MCF10A cells from Fig. 2.5a and Fig. 2.16e show this effect, compared with the same cells in Fig. 2.5b, which were not detached and reattached.

Statistics and reproducibility.

Tumor-free survival in mice was compared between CTRL and SEPHS2-KO groups using the Kaplan–Meier method, and significant differences in curves were assessed using the log-rank test. Results of the viability assay and Ellman's test and total selenium measurement were analyzed using a two-tailed Student's t-test. $P < 0.05$ was considered statistically significant, and data marked with one (*), two (**) or three (***) asterisks indicate P values of < 0.05, < 0.01 and < 0.001, respectively. All experiments were repeated at least three times with the following exceptions: focused candidate detoxifying-enzyme screen was carried out in 11 cell lines in Fig. 2.3b, effects of SEPHS2 KO on tumor growth (Fig. 2.8), focused screen for selenium uptake mediator (Fig. 2.13a), SEPHS2 protein measurements human tumors versus normal tissues (Fig. 2.10a,b), imaging for cleaved caspase-3 in SEPHS2 KO cells (Fig. 2.4c,d), selenium ICP-MS quantification of captured spots (Fig. 2.21b), validation of SEPHS2 expression KO (Figure 2.22) and validations of drug efficacy (Figs. 2.15g and 2.16a), which were performed once. The following experiments were repeated twice: SEPHS2 KO in multiple cell lines (Fig. 2.3c, d), SEPHS1 KO in multiple cell lines (Fig. 2.7a), SEPHS2/ GPX4/SEPSECS KO cell treatment with hypoxia and nutrient starvation (Fig. 2.17c,d) and erastin treatment of SEPHS2 KO (Fig. 2.15g). In all experiments, all attempts at replication were successful. Bliss independence values (Fig. 2.20e) were calculated using standard formula of $EC = EA + EB – EA \times EB$. EA is the effect of SEPHS2 KO alone, EB is the effect of selenite treatment alone, and EC is the expected theoretical

combination of SEPHS2 KO and selenite treatment. A Bliss independence score of <1 indicates a synergistic effect.

ACKNOWLEDGEMENTS

We thank M. Green, E. Baehrecke, A. Mercurio, D. Sabatini, C. Haynes, D. Guertin, B. Bible, K. Krupczak, K. Luk, C. Brown, A. Jaferi and S. Deibler for advice, assistance and feedback. We thank D. Sabatini, S. Wolfe, M. Lee, A. Mercurio and K. -Y. Choi for materials including vectors and cell lines. We thank O. Kwon for illustrations, and C. -C. Hsieh for assistance with statistics. This work was supported by the Suh Kyungbae Foundation (SUHF) Young Investigator Award to D.K.; NIH T32 CA130807-8 to M.E.S.; Searle Scholars Program, Rita Allen Foundation, Whitehall Foundation, Smith Family Foundation, and NIH/NIA DP2 AG067490-01 to P.L.G; and R01 CA229910 to L.M.S.

CHAPTER III:

DISCUSSION

Summary of Findings

In this study we have shown that the production of selenocysteine is not only the rate limiting factor in selenoprotein biosynthesis, but also creates a cancer specific vulnerability in that it requires the formation of a toxic intermediate, selenide, as a selenium donor. Disruption of SEPHS2, the downstream processing enzyme, results in an increase in selenide, which poisons cancer cells but leaves nontransformed cells virtually unharmed. Cancer cells are selenophilic, meaning that they take up selenium more readily than normal cells. The more selenium is fed into the selenocysteine biosynthesis pathway, the more selenide that accumulates when SEPHS2 is disrupted. Therefore, this increase in selenium uptake results in the cancer specific toxicity of SEPHS2 KO.

We studied the effect of SEPHS2 KO in cancer cells *in vitro* and in an *in vivo* mouse model and determined the increased expression of SEPHS2 in *ex vivo* human breast tumor samples. We tested numerous cancer and normal cell lines to determine their sensitivity to SEPHS2 KO. Normal cell lines derived from multiple tissues, both immortalized and primary, were significantly less effected by SEPHS2 KO in comparison to various cancer cell lines. *In vivo* characterization involved an orthotopic xenograft model, where tumors engrafted with SEPHS2 KO breast cancer cells resulted in significantly fewer and smaller tumors in comparison to control tumors. Additional studies of patient breast tumor samples and survival data revealed increased SEPHS2 expression in tumors in comparison to normal breast tissue, and survival data analysis indicated that higher levels of SEPHS2 in patient tumors resulted in significantly lower overall survival.

The normal endogenous function of SEPHS2 is that it catalyzes the reaction between selenide and phosphate from ATP to create selenophosphate, which is used in the formation of selenocysteine. Selenocysteine is then incorporated into selenoproteins. We have found that SEPHS2 has an additional critical role in cancer cells in that it detoxifies selenide. In the nontransformed line MCF10A, SEPHS2 was dispensable over the course of 28 days of culture. SEPHS2 KO cells continued to have a similar growth rate to those of control, even though selenoprotein expression was completely abolished. This indicates that normal cells do not require SEPHS2 or selenoprotein production for their survival and proliferation under basal conditions.

We discovered that xCT/SLC7A11 is involved in the selenocysteine biosynthesis pathway by increasing the levels of total thiols, which creates a reducing environment that facilitates uptake of selenium, as selenite is converted to the volatile selenide. xCT can therefore be characterized as the upstream regulator of the selenocysteine biosynthesis pathway, as SLC7A11 KO results in decreased expression of selenoproteins. Due to this regulation, selenophilic cancer cells have increased selenium uptake and therefore more resistance to tert-butyl hydrogen peroxide (TBH) induced ferroptosis. Knockout of selenocysteine biosynthesis pathway enzymes SEPHS2, SEPSECS, PSTK, as well as ferroptosis regulator GPX4 significantly sensitized cells to ferroptosis under TBH stress. This indicates a mechanism for why cells would be selenophilic, as increased selenium leads to more selenocysteine biosynthesis and therefore antioxidant selenoproteins such as GPX4.

We also demonstrated that SEPHS2 KO cancer cells die due to selenide poisoning. Dual KO of SEPHS2 and the selenium uptake mediator SLC7A11 resulted in rescue of the SEPHS2 KO toxicity phenotype, due to lack of selenium uptake that occurs with SLC7A11 KO. Referring back to the kitchen sink analogy in Chapter I, SLC7A11 KO results in the selenium "faucet" being turned off, meaning that there is no need to drain away the built-up selenide via SEPHS2 processing. We were able to separate the two proposed functions of SEPHS2, selenide detoxification and selenoprotein production, by overexpressing SEPHS2 in cells where the direct selenocysteine production enzymes, SEPSECS and PSTK, were knocked out. Cells that had increased levels of SEPHS2 had a significantly higher viability in comparison to cells that only had SEPSECS KO, which is due to the selenide detoxifying function of SEPHS2 independently of selenoprotein production. We further established the selenide detoxification function of SEPHS2 by treating cells with a "cloud" of selenide gas. SEPHS2 KO sensitized cells to selenide treatment, and SEPHS2 overexpression rescued viability, both in comparison to control cells. These data show the selenide detoxification function of SEPHS2.

Selenium as a Nutrient and a Poison

In the context of cancer, selenium functions as both a nutrient that is essential for selenoprotein production as well as a toxic compound that needs to be readily processed by SEPHS2. The selenium that is taken up in our diet contributes to the production of important antioxidants such as TXNRD1 and GPX4. Selenium has been described as a nutrient that has a small window between nutritional and toxic doses[67]. Our study,

described in Chapter II, provides some important insights into this nutrition/toxicity gap—the amount of selenide that can be processed by SEPHS2 contributes to beneficial antioxidant selenoproteins, but selenide that supersedes SEPHS2 processing capacity would be toxic. This can explain why high doses of selenite can be toxic as they increase the intracellular selenide pool past the detoxification capacity of SEPHS2. We show that the reductive conversion of the nutritional selenium compound selenite to selenide is critical to its toxicity, as preventing its reduction via SLC7A11 KO prevents its toxicity. Therefore, selenium is toxic precisely because it is processed by the selenocysteine biosynthesis machinery.

We have established that cancer cells take up more selenium than normal cells, and that this increase in selenium is protective against oxidative stress that leads to ferroptosis. However, the higher levels of selenium in cancer cells leads to a vulnerability— these cells can be poisoned by selenide buildup that results from SEPHS2 KO. Selenium therefore can be viewed as an essential nutrient that leads to the production of important antioxidants, as well as a poison when built up in a cell.

SEPHS2 as a Selenium Detoxifier

SEPHS2 had previously been identified as a selenium processing enzyme in the human selenocysteine biosynthesis pathway[51]. Our study demonstrates that SEPHS2 is the sole enzyme that produces selenophosphate, as SEPHS2 KO significantly reduces selenoprotein expression. In agreement with previous studies discussed in Chapter I, we were also able to validate that SEPHS1 cannot compensate for SEPHS2 disruption.

The focus of previous studies has primarily been on the selenophosphate that SEPHS2 produces and its downstream contributions to selenocysteine biosynthesis. In this study, we instead concentrate on the selenide that it uses as a substrate, effectively consuming and detoxifying it. When the function of SEPHS2 is disrupted, selenide accumulates to toxic levels and results in cell death. Selenide accumulation is toxic in cancer cells because it functions as a pro-oxidant. Reports have shown that selenide reacts with water to form hydroxyl radicals and elemental selenium[142]. We have also established that cancer cells treated with selenite, which is reduced to selenide by xCT, leads to a significant increase in cellular ROS (Fig. 2.19b). Additionally, we directly examine the selenide detoxification function of SEPHS2 by treating with selenide gas, which is the first published example of direct gene KO or overexpression sensitizing or protecting (respectively) against selenide gas. A group has reported the deleterious effects of increased selenium and ROS, which can signal for apoptosis via DNA damage and ferroptosis through lipid peroxidation[125]. We have shown that SEPHS2 KO induced cell death is partially rescued by ferroptosis inhibitors, indicating that both increase in selenide and the loss of GPX4 sensitizes cells to ferroptosis. The obvious assumption of SEPHS2 function is that of a selenocysteine biosynthesis pathway enzyme that contributes to the production of selenoproteins. While this is true, in this study we describe a second, important function of SEPHS2. The ability for SEPHS2 to process and detoxify selenide is essential for cancer cell survival.

xCT and Selenophilicity

In this study we have determined that xCT is an upstream regulator of selenocysteine biosynthesis and selenoprotein expression. xCT has a well-defined role as a cystine/glutamate antiporter, and this function increases the level of extracellular thiols[33]. This creates a reduced extracellular environment, which contributes to the reduction of selenocompounds into selenide. This reduction is directly related to the uptake of selenium, indicating that selenide is the form of selenium that is most readily taken up by cells. The direct mechanism of transport is yet to be determined. It has been reported that hydrogen sulfide uptake occurs by simple diffusion across the plasma membrane[143]. Due to the atomic similarities between selenium and sulfur, it is possible that hydrogen selenide is taken up by cells via a similar mechanism.

Increased selenium uptake in tumors has been observed since the 1960s as reported by radioactive selenite being used as a tumor labelling agent. Our findings likely explain this phenomenon, as selenium accumulates in cancer cells due to xCT expression, which we characterize as selenophilicity. The two functions of xCT are elegantly coordinated to create an antioxidant system that supports redox homeostasis. Import of cystine is necessary for the cellular production of glutathione, and uptake of selenium is important for the production of glutathione peroxidase selenoproteins. Glutathione peroxidases function as antioxidants by using glutathione as a substrate, so both components are necessary for antioxidant activity. This dual function of xCT, in mediating both the production of glutathione and selenophilicity, benefits the cancer cells by regulating both the substrate and enzymes that reduce levels of ROS.

We have determined that selenophilicity is directly related to xCT activity. xCT is regulated by the redox sensitive transcription factor NF E2 Related Factor 2 (NRF2)[144]. Hydrogen peroxide treatment, a commonly used oxidative stressor for *in vitro* studies, increased nuclear translocation of NRF2 as well as xCT mRNA and extracellular glutamate release in breast cancer cells[144]. Kelch-like ECH-associated protein 1 (KEAP1) targets NRF2 for ubiquitination, and overexpression of KEAP1 results in decreased xCT protein levels[144]. Therefore, activity of NRF2 increases xCT expression and activity in response to oxidative stress. The authors relate this upregulation to an increase in glutathione synthesis. Due to the "moonlighting" role of xCT as a mediator of selenium import, these cells also have the capability to produce more selenoprotein glutathione peroxidases that can use this glutathione as a substrate for antioxidant reactions. Therefore, our findings indicate the scenario where cancer cells that encounter an oxidative stressor activate NRF2 resulting in a higher expression of xCT and increased selenophilicity, which benefits the cells by increasing antioxidant selenoprotein production to protect against the oxidative insult.

The tumor microenvironment also contributes to the need for defense against oxidative stress. Solid tumors grow quickly and often times lack the angiogenesis necessary to deliver oxygen and nutrients to the central cells. These hypoxic conditions result in tumor cells activating transcription factors that allow cells to survive and grow under these harsh conditions. Hypoxia-inducible factor 1 (HIF-1) is well studied and reported to be a major transcription factor that promotes angiogenesis and changes to cellular metabolism[145]. Emerging research, however, points to the coordinated response

of both HIF-1 and NRF2 to the oxidative stress of a hypoxic environment[146]. Cells that encounter a hypoxic environment and activate NRF2 will have the benefit of increased xCT activity resulting in higher levels of glutathione and selenoprotein antioxidants to restore redox homeostasis. We postulate that the environment of the tumor triggers the mechanism of increased selenophilicity via NRF2 upregulation of xCT, which is advantageous to cancer cells.

Another likely benefit of cancer cell selenophilicity may lie in protection against chemotherapeutics. Many chemotherapeutic treatments result in an increase in ROS. For example, procarbazine is used to treat Hodgkin's lymphoma and glioblastoma multiforme. Procarbazine is readily oxidized into its azo derivative, increasing ROS which induces oxidative DNA damage and stimulates apoptosis[147]. It has been reported that xCT expression correlates with increased protection against chemotherapy[128]. We propose that this may be due in part to increased selenium uptake and more robust expression of selenoprotein antioxidants such as GPX1 which has been shown to protect against chemotherapy[112]. If some cells within a tumor have the capacity to evade chemotherapeutic treatment, they will expand to repopulate the tumor once treatment has ended. In this way, selenophilic cancer cells may be able to survive chemotherapeutic induced clonal selection.

SEPHS2 as a Potential Therapeutic Target in Cancer

Selenophilic cancer cells express higher levels of xCT and take up more selenium in comparison to non-selenophilic cells. This increase in the intracellular selenium pool

creates a unique vulnerability. Disruption of the selenide processing enzyme SEPHS2 results in an increase in intracellular selenide, which is toxic to cells. Selenophilic cancer cells are more sensitive to SEPHS2 KO, as the higher level of selenium influx poisons these cells more efficiently than cells that have less selenium uptake. It is for this reason that we suspect that SEPHS2 KO is a more efficient cancer target in selenophilic cancer types than others. Additionally, SEPHS2 may be a particularly good target for chemoresistant cancer types that upregulate xCT[128]. It is important to note that the synergistic effect of SEPHS2 KO treated with selenite *in vitro* is a promising indicator that SEPHS2 KO and selenium supplementation may be an interesting combination therapy. In important factor when considering an entire system inhibition, as in a cancer patient, is that the essentiality of SEPHS2 from the Cancer Cell Line Encyclopedia is highly differential in cancer cell lines[148]. Some cell lines are sensitive to SEPHS2 KO and others are not, which is a strong indicator that SEPHS2 is not an enzyme that is pan-essential for all cell types. This, when considered alongside the data that all of the tested normal cell lines were insensitive to SEPHS2 KO, is promising in regard to the cancer specificity of a SEPHS2 inhibitor.

In the lab we have studied SEPHS2 disruption using CRISPR/Cas9 technology. While this is a robust and efficient tool for *in vitro* studies, the system has not been optimized for use in direct treatment of human cancer. Another method of inhibition will have to be employed to study the effect of SEPHS2 disruption in human cancer patients. Two methods of enzyme inhibition to consider are 1) small molecule inhibitors and 2) RNA inhibition (RNAi). RNAi technology is developing quickly into a promising new

field of therapeutic inhibition. However, issues arise concerning the limitation of coverage – in an RNA based therapy only a subset of cells will receive the inhibitor. This technology must be improved before this is a viable option for cancer therapy targeting SEPHS2. Small molecule compounds, however, have been well studied as inhibitors for enzymes due to their ability to bind and inactivate an enzyme's active site. SEPHS2 homologs that have reported secondary structures lead us to infer that SEPHS2 may have a hydrophobic groove that suggests druggability. I will further discuss work that has been done in regard to a small molecule SEPHS2 inhibitor in Appendix A.

The stratification of tumors as high or low xCT expression, therefore more or less selenophilic, will be an important factor to consider when treating cancer patients with a SEPHS2 inhibitor. Our study has shown that cancer cell lines can vary widely in their expression of xCT. If this phenomenon is reflected in human tumors as well, there will be varying degrees of selenium uptake and therefore sensitivity to SEPHS2 inhibition or selenium treatment. It is possible that not considering a tumor's ability to take up selenium was a complicating factor in early selenite trials. Although there are numerous promising studies as mentioned in Chapter I, they have not yet lead to successful clinical application. A selenite treatment clinical trial that stratifies patients based on the selenophilicity of their tumors would shed light on whether selenite treatment alone is a viable chemotherapeutic option. However, our study indicates that combining selenite treatment with a SEPHS2 inhibitor creates a synergistic level of toxicity in cancer cells, so this may be the most effective method of treatment in humans.

There are numerous cancer subtypes that tend to be more selenophilic than others. For example, our study mainly used triple negative breast cancer cell lines to investigate the effect of SEPHS2 KO. It is important to note that multiple breast cancer cell lines also show low levels of selenium import, so there is likely variability in any subtype. Gene expression profile analysis of SLC7A11 expression in tumor types using the Gene Expression Profiling Interactive Analysis (GEPIA) software revealed significantly higher SLC7A11 levels in cancer vs normal tissue in numerous cancer subtypes including colon and rectum adenocarcinoma, esophageal carcinoma, lung squamous cell carcinoma, and uterine corpus endometrial carcinoma[149]. SEPHS2 expression is also a good indicator of flux through the selenocysteine biosynthesis pathway. Therefore, higher SEPHS2 expression in patient tumor samples, as seen in the GEPIA analysis included in this study, also indicates a potential for selenophilicity. SEPHS2 expression is increased in cancer in relation to normal tissue in breast invasive carcinoma, diffuse large B-cell lymphoma, and pancreatic carcinoma. All of these subtypes have the potential to be more selenophilic, and therefore may be good candidates for selenite and SEPHS2 inhibition treatments. In a personalized medicine approach, by examining *SLC7A11* gene or xCT protein expression in tumor biopsies for example, one may be able to prescribe future SEPHS2 inhibitors for high xCT expression tumor patients.

An important point regarding xCT expression in human tumors is the complicating factor of tumor heterogeneity. Tumors often consist of different clonal subpopulations that exhibit different genetic variations, marker expression and importantly, drug sensitivity[150]. For example, it is possible that a tumor that generally expresses higher

levels of xCT would have a subpopulation of cells that have little or no xCT expression. Then, when treated with a SEPHS2 inhibitor, it is possible that only the high xCT cells would be sensitive, leaving a subpopulation unharmed. This resistant population could then repopulate the tumor with SEPHS2 inhibitor resistant cells. However, it is possible to target these less-sensitive cells by "pushing the system" with a combination therapy of sodium selenite treatment with a SEPHS2 inhibitor. Then, even cells with lower xCT expression would be flooded with selenium, increasing the probability of cell death due to selenide buildup.

Another important facet of tumor heterogeneity lies in the existence of cancer stem cells (CSCs). Cancer stem cells are self-renewing and differentiate into cancer progenitors or mature cancer cells and are often difficult to target with chemotherapeutics due to their quiescent nature[150]. Some human tumors, such as triple negative breast cancer, have been characterized as containing higher numbers of cancer stem cells in comparison to other tumor types[151]. Studies have shown that selenium compounds, such as toxic selenide, can interfere with important CSC signaling pathways such as Wnt/β-catenin[150]. Therefore, selenium-based treatments may be efficient in targeting the normally therapy evasive CSCs.

In regard to the tumor microenvironment (TME), there are multiple factors to consider when discussing SEPHS2 inhibition as a potential cancer therapy. The TME consists of numerous cell types, including invading immune cells. Inflammation is promoted by cancer cell activation of transcription factors such as HIF1-α and NF-κB and the resulting production of cytokines that signal to recruit immune cells[152]. An influx

of selenium in tumors, such as with sodium selenite treatment or SEPHS2 inhibition, may be additionally deleterious to cancer cells outside of the direct cell death mechanisms. Selenium induced oxidation of polythiols on the surface of cancer cells has been reported to activate the ability of natural killer (NK) cells to recognize the tumor cell as foreign and begin an immune response[153,154]. This indicates an interesting compound response of both intracellular increase in ROS and activation of immune cells in the tumor microenvironment with selenium-based treatment.

Patient survival data is another indicator of the potential of selenium-based treatment in cancer. Not only is SEPHS2 increased in tumor cells versus normal cells in breast invasive carcinoma, but this phenotype is also observed in patients that have a significantly decreased overall survival. Analysis of The Cancer Genome Atlas database reveals that patients with higher expression of SEPHS2 survived for significantly shorter time than those with tumors that had less SEPHS2 expression. This links SEPHS2 expression and selenophilicity to tumor progression and patient mortality. SEPHS2 inhibition is therefore a possible treatment method to decrease tumor progression and extend patient life.

Limitations and Outstanding Questions

While we provide extensive data indicating that selenide is accumulating in SEPHS2 KO cells and that selenide accumulation is the cause of toxicity, there has yet to be a method developed that can directly quantify endogenous intracellular selenide levels. In this study we used both acid digestion and inductively coupled plasma mass spectrometry

(ICP-MS) to determine the levels of intracellular selenium. These assays degrade samples with concentrated acid and heat or ionize them, respectively. This separates the selenium atoms from any other components of selenocompounds. However, this will affect all intracellular selenium atoms including all forms of inorganic selenocompounds as well as selenocysteine and selenomethionine containing proteins. While we were able to detect exogenously produced selenide gas using the PVP dot method described in the study, there was no detectable signal produced when PVP dots were exposed to SEPHS2 KO cells treated with selenite, indicating that the method is not sensitive enough to detect the quantities of selenide formed endogenously from cells. Further optimization of the sensitivity of the PVP dot method of selenide detection may allow researchers to detect gaseous selenide at endogenous levels. This may be possible with advances in ICP-MS technology to improve sensitivity to very small quantities of selenide.

Another optimization that would improve the study of selenium metabolism is a robust selenocysteine detection mechanism. In this study we relied on selenoprotein expression to monitor the downstream effects of SEPHS2 and SLC7A11 disruption. It is important to note that as discussed in Chapter I, it is not possible to directly incorporate selenocysteine from protein degradation. Selenocysteine must be produced *de novo* via the function of SEPHS2, PSTK and SEPSECS. Therefore, selenocysteine production can be used as a direct readout of selenocysteine biosynthesis pathway activity. While probing for multiple selenoproteins is a valid method to determine the selenoprotein expression landscape, measuring selenocysteine would be an even more direct way to monitor selenocysteine biosynthesis. A few studies have proposed the use of a UGA

mutated luciferase with the addition of an SECIS element to be one method for selenocysteine monitoring[155,156]. In this case, selenocysteine would be incorporated by the SECIS to the growing luciferase polypeptide chain during translation, allowing for the protein to be expressed. Adding the luciferin substrate would then give a measurable luminescent readout of luciferase expression directly related to the levels of selenocysteine. This method is advantageous in comparison to monitoring selenoprotein expression due to complex translation regulatory factors and protein stability. This method may be worth further pursuit to directly quantify the activity of the selenocysteine biosynthesis pathway.

The study in Chapter II shows promising data for the *in vivo* relevance of SEPHS2 KO. However, the study does not address SLC7A11 mediation of the selenocysteine biosynthesis pathway *in vivo*. Previous studies have exemplified how xCT can regulate the extracellular environment. For example, the efflux of glutamate from glioma cells expressing xCT can damage neurons in the peritumoral space and advance glioma growth[157,158]. The cystine/glutamate antiporter function of xCT has been studied in *in vivo* models,[159] however, there has yet to be any investigation into the regulation of selenium import by xCT *in vivo*. It is difficult to predict how the dynamics of extracellular thiol accumulation seen in the cell culture system would be translated *in vivo* when taking into account factors such as blood flow and oxygen levels. Modulation of selenium import by xCT in an *in vivo* setting would be an important factor to consider when attempting to stratify patients for SEPHS2 inhibition treatment. The patients that would respond best to a SEPHS2 inhibitor would be those with tumors that are expressing high levels of xCT,

therefore they are selenophilic. It is important to investigate the regulation of selenium import *in vivo*, perhaps by pharmacologically inhibiting xCT in a SEPHS2 KO xenograft model. Will xCT inhibition rescue the growth deficit phenotype *in vivo*, as shown in *vitro*? This is an interesting outstanding question.

An additional limitation of the study is the *in vivo* orthotopic xenograft model. While xenografts can be a powerful tool for studying tumors in an animal model system, genetically manipulating the cancer cells pre-implantation may affect the tumor growth results. For example, it is possible that the SEPHS2 KO cells that were implanted in mouse mammary tissue were already dying, and therefore could skew the results of tumor implantation and growth. Instead, using doxycycline induced CRISPR KO expressing cancer cells and allowing the tumors to grow before induction and then comparing tumor growth to control induced tumors would be an efficient method for determining the effect of SEPHS2 KO in existing tumors. This is a more clinically relevant model, as the effect of SEPHS2 disruption in existing tumors is more reflective of human cancer treatment. An additional clinically relevant assay would be the use of patient derived xenografts (PDXs), in which tumor samples from human cancers are propagated *in vivo*. While genetic manipulation of PDX cells is possible, this assay may be more robust and informative with a future SEPHS2 inhibitor. These additional assays should be performed to confirm the deleterious effect of SEPHS2 KO *in vivo*.

In this study we show data that indicates that xCT is not the direct transporter of selenide. In Figure 2.14c, SLC3A2 KO cells are treated with selenite and reduced glutathione (GSH) to mimic the extracellular reduction function of xCT. These cells have

significantly lower viability than SLC3A2 KO treated with selenite, showing that selenium is still entering the cells in the absence of xCT. This suggests the role of xCT as a mediator of selenide uptake while not being the direct transporter. One outstanding question is how selenide is getting into the cells. It is possible that there is another transporter mediating selenide entry. However, we hypothesize that due to the volatile nature of selenide and its similarities to hydrogen sulfide (discussed in Chapter I), no transporter is necessary as it diffuses across the plasma membrane.

Significance of Findings

The toxic metabolite theory was first established in a study that described how excess glycine is metabolized into toxic metabolites aminoacetone and methylglyoxal when the downstream enzyme is disrupted[120]. The study in Chapter II further describes the potential toxicity of endogenously produced metabolites in cancer. Our study started with a targeted screen, inhibiting enzymes that were reported to process potentially toxic metabolites. The building of the endotoxome, a list cross-referencing endogenously produced metabolites with toxicological databases, will help inform future targeted screening. We discovered that SEPHS2 KO significantly impaired cancer cell viability during the initial screen. Further investigation of the mechanism of toxicity of SEPHS2, as well as investigation of upstream regulators and cancer specificity allowed us to conclude that SEPHS2 was a novel cancer target. This approach outlines a roadmap for future investigations, as it is possible that other cancer specific detoxifying enzymes can be identified using the methods outlined in Chapter II.

This study is significant in that it demonstrates increased activity of selenocysteine biosynthesis pathway in cancer for the first time and establishes selenophilicity as the mechanism for this upregulation. This will likely lead to follow up studies further investigating the details of selenocysteine biosynthesis pathway function in cancer cells. Importantly, this study provides important insights into why excess selenium is toxic. Selenium toxicity has been observed for hundreds of years in livestock and in rare cases of selenosis in humans as well. We have found that the conversion of a form of dietary selenium, selenite, to selenide is a critical step in its toxicity. This can have important implications in understanding selenium toxicity in livestock and human disease, as well as using selenium for selective killing of cancer cells.

The xCT antiporter has been characterized as a transporter of extracellular cystine into the cell and therefore a direct mediator of glutathione production[94]. In this study we characterize the moonlighting role of xCT as a mediator of extracellular thiols, therefore providing a reducing environment for selenocompounds and the resulting selenium uptake. xCT therefore regulates production of glutathione which is the substrate for selenoprotein glutathione peroxidases that are expressed using selenium from the intracellular selenide pool that xCT also indirectly mediates. This is an elegantly coordinated method to produce the components (glutathione and GPX4, for example) necessary to counter oxidative stressors such as lipid peroxidation and evade cell death via ferroptosis.

The significance of SEPHS2 as a potential cancer target is evident in our study. There are two strong pieces of evidence of the therapeutic potential of SEPHS2

disruption. First, our *in vitro* studies of SEPHS2 KO show no toxicity in normal immortalized and primary cell lines, which is a strong indicator of cancer specificity. In the case that we are able to find a strong and selective small molecule inhibitor for SEPHS2, these data indicate that the side effects related to SEPHS2 disruption in normal tissue may be negligible. Second, SEPHS2 KO cancer cell toxicity was applicable to an orthotopic xenograft model. This indicates that SEPHS2 disruption has deleterious effects to cancer cells in a tumor model as well as *in vitro*. It is important to monitor these effects in a xenograft system, as the tumor microenvironment differs significantly from that of tissue culture. These data together lead us to conclude that SEPHS2 is a novel and promising cancer target.

Future Directions

Selenocysteine biosynthesis is just one example of a metabolic pathway that has increased activity in cancer cells compared to normal cells. There are likely to be many examples of these pathways where targeting the detoxifying enzyme ends up hurting cancer cells more than normal cells due to their overexpression. This study acts as a blueprint for future toxic metabolite studies as it outlines methods for treating upstream metabolites to enhance toxicity (Fig. 2.20e) and characterizing loss of viability effects as toxic metabolite accumulation or loss of downstream products (Fig. 2.20b). Development of further targeted screening assays and characterization of these detoxifying enzymes may lead to additional interesting and valuable cancer targets.

This study can be used to inform future clinical decisions as well. For example, stratifying cancer patients who are treated with selenite as an anti-tumor agent based on the level of xCT expression in their tumors may greatly inform the results. This would also be true for future testing of a SEPHS2 inhibitor. As tumors with high xCT rely more heavily on the selenocysteine biosynthesis pathway than normal cells, it would also be a valuable model for targeting the antioxidant selenoproteome. While our study has focused on the selenide toxicity aspect of SEPHS2 KO, it cannot be discounted that disruption of antioxidant selenoproteins such as GPX4 would be additionally deleterious to cancer cells. While GPX4 is considered a valuable cancer target by itself, our study has shown that inhibiting SEPHS2 in cancer results in loss of not only GPX4 but the entire selenoproteome. This means that cancer cells will be deprived of other important antioxidant selenoproteins such as TXNRD1 and GPX1, while also being poisoned by the accumulation of selenide. This is a potentially powerful combination of significantly depleting cellular antioxidants while flooding the cells with ROS.

The next steps in characterizing SEPHS2 as a suitable cancer target consists of characterizing the recombinant enzyme and screening for a small molecule inhibitor. After successful propagation and purification of the recombinant enzyme, one would have to develop a suitable assay to monitor SEPHS2 activity. The activity assay optimization is key for the use in a small molecule screen, to determine significance of decrease in SEPHS2 activity in the presence of potential inhibitors. If a promising inhibitor were to be identified, further studies characterizing the effect of pharmacological SEPHS2 disruption would be necessary. It would be important to ensure

that the pharmacological inhibition of SEPHS2 results in a similar *in vitro* phenotype to SEPHS2 KO, i.e. the selective toxicity to cancer cells in comparison to normal cell lines. Further studies include pharmacological toxicity testing in model organisms before determining the ability to reduce tumor xenograft growth. These lines of investigation should be pursued with the understanding that changes to the compound structure may be necessary to increase SEPHS2 inhibition selectivity as well as create pharmacological stability in a model organism (e.g. *mus musculus* and *rattus norvegicus*) system. The work described can identify and characterize a small molecule inhibitor for SEPHS2 that may have the potential to enter the clinical testing system and become a chemotherapeutic.

APPENDIX A

Characterizing recombinant SEPHS2_U60C for small molecule inhibitor screening

In this section I will discuss the work that has been completed in regard to identifying a small molecule SEPHS2 inhibitor. It is important to note that in this set of experiments we use a mutated form of SEPHS2 that replaces the selenocysteine with cysteine. This is the same overexpression construct we used in the study described in Chapter II (Fig. 2.6), without the CRISPR/Cas9 resistance mutations. The change of selenocysteine to cysteine is necessary for the efficient propagation of SEPHS2 in bacterial culture, as *E. coli* do not have the correct elongation factors to incorporate selenocysteine at the UGA codon and therefore are unable to efficiently express wild-type SEPHS2[160]. We hypothesize, based on evidence from selenocysteine to cysteine mutated GPX4, that this change to the catalytic active site would decrease the activity of SEPHS2[132]. Nonetheless, mutant SEPHS2_U60C can be considered to be functionally equivalent to WT SEPHS2 as we have shown that overexpression of this construct can rescue the deleterious effects of SEPHS2 KO (Fig. 2.6b). During the course of these investigations we determined that SEPHS2_U60C can be robustly expressed in BL21 bacteria, then purified using a combination of nickel affinity column and ion exchange chromatography. Importantly, we were able to determine that SEPHS2_U60C has a consistently measurable level of activity.

The propagation of 6X HIS tagged SEPHS2_U60C recombinant protein is performed in BL21 bacteria using an inducible pET30a+ vector. After transformation, the bacteria are grown in a starter culture overnight and then transferred to a larger propagation culture. While monitoring the optical density (OD), the vector is induced with isopropyl β- d-1-thiogalactopyranoside (IPTG) and cultured at low temperatures overnight. Both

the induction with IPTG and the low culture temperatures result in SEPH2_U60C being preferentially expressed over the endogenous bacterial proteins. After harvest, cells are lysed, centrifuged and run through a nickel affinity column. This column is packed with nickel coated agarose beads that preferentially bind to the 6X HIS tag that is expressed at the N-terminal of SEPHS2_U60C. The column is washed with buffers that have increasing concentrations of imidazole in HEPES buffer, a compound that competitively binds to the nickel beads, effectively releasing contaminating bacterial proteins at lower concentrations and then eluting SEPHS2_U60C at the highest concentration. Each fraction from the nickel affinity column, as well as the whole cell lysate, were analyzed via SDS-PAGE and Coomassie staining (Figure A.1).

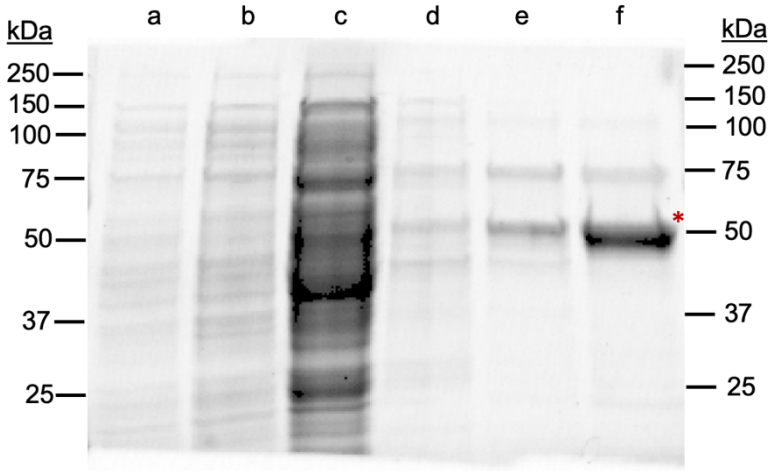

Figure A.1 – Coomassie stained SDS-PAGE gel image of the nickel column aliquots
a. Whole cell lysate of BL21 expressing SEPHS2-U60C, diluted 1:50 in 1X SDS
b. Flow-through from nickel-HIS binding, diluted 1:50 in 1X SDS
c. First wash with HEPES buffer containing 20mM imidazole
d. Second wash with HEPES buffer containing 50mM imidazole
e. Third wash with HEPES buffer containing 75mM imidazole
f. Elution fraction of concentrated SEPHS2-U60C. Red asterisk marks SEPHS2-U60C. All other bands in this fraction are bacterial protein contaminants.

While the nickel column is a robust system for concentrating SEPHS2_U60C expression into one aliquot of buffer, the recombinant enzyme was still contaminated with bacterial proteins. To fully purify SEPHS2_U60C, we performed ion exchange chromatography using a fast protein liquid chromatography (FPLC) system. The isoelectric point of SEPHS2_U60C was calculated to be 5.45, which means it has a net negative charge (is anionic) at neutral pH. Because of this, we used a quaternary amine (Q) column which is packed with positively charged resin and is a strong anion exchanger. We found that SEPHS2_U60C bound to this column and was eluted as set of pure fractions at approximately 15% Buffer B as 1M NaCl, or 150mM NaCl (Figure A.2a). Fractions from the ion exchange column were analyzed via SDS-PAGE and Coomassie staining to determine which fractions contained pure SEPHS2_U60C (Figure A.2b,c). The pure enzyme fraction was then concentrated using a centrifuge filter, the concentration was determined, and the enzyme was aliquoted and frozen to store for long term use.

a

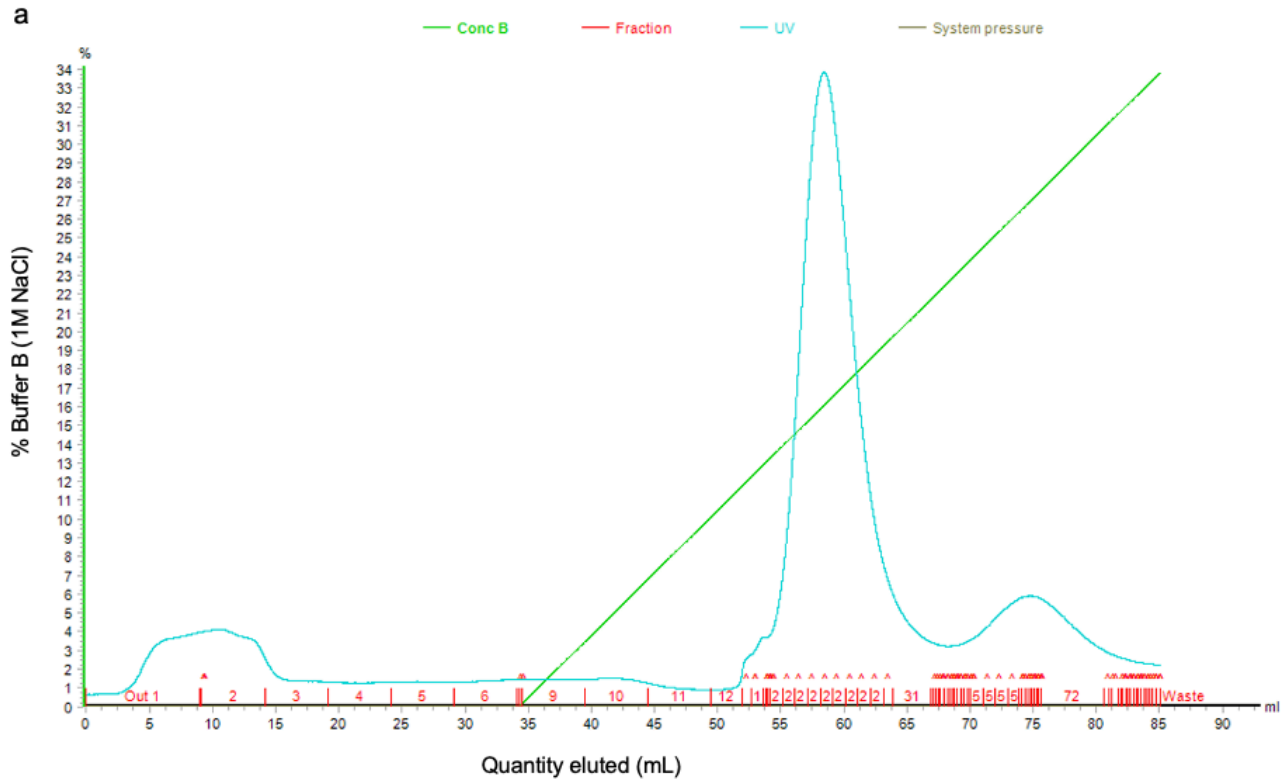
Conc B
Fraction
UV
System pressure
%
% Buffer B (1M NaCl)
Out 1
Waste
ml
Quantity eluted (mL)

b

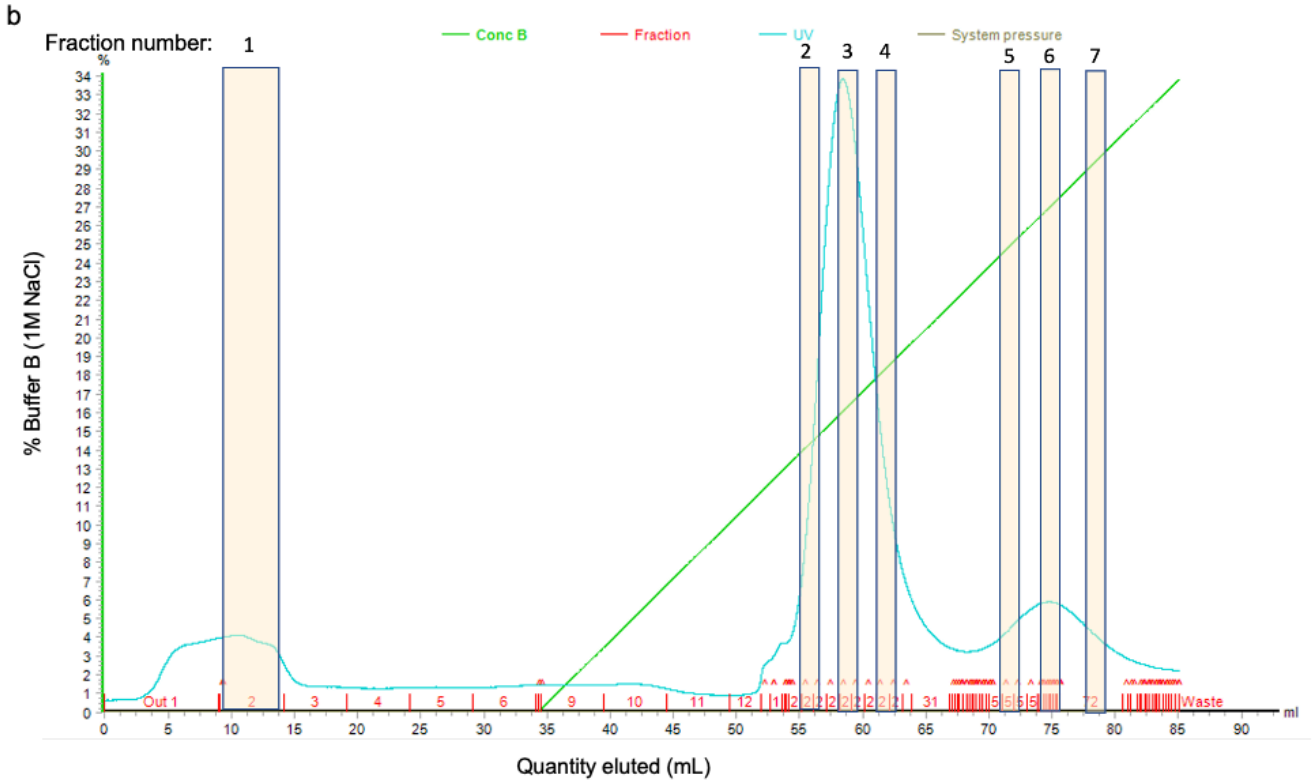
Fraction number:
1
2
3
4
5
6
7
Conc B
Fraction
UV
System pressure
%
% Buffer B (1M NaCl)
Out 1
Waste
ml
Quantity eluted (mL)

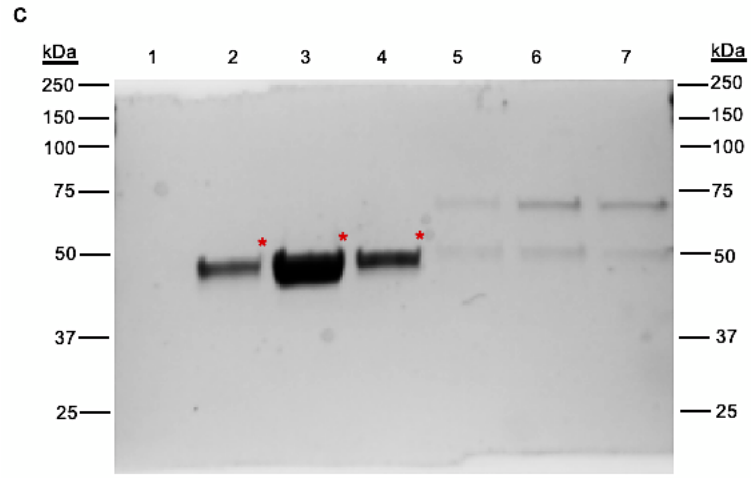

Figure A.2 – Ion exchange chromatography-based purification of recombinant SEPHS2_U60C

a. Ion exchange chromatogram of UV absorbance detected for each fraction

b. Ion exchange chromatogram with analyzed fractions highlighted

c. Coomassie stained SDS-PAGE gel image of fractions. Fraction 1 was not detectable via Coomassie staining. Fractions 2-4 contain pure SEPHS2-U60C, denoted with a red asterisk. Fractions 5-7 contain a contaminating bacterial proteins as well as small amounts of SEPHS2_U60C.

We then analyzed the activity of recombinant SEPHS2_U60C. Although another group has proposed an activity assay for SEPHS2_U60C, their assay was unable to successfully be translated to a format that is conducive to high throughput screening[161]. SEPHS2 functions as an enzyme that uses ATP, hydrogen selenide and water as substrates to produce AMP, inorganic phosphate, and selenophosphate (Fig. A.3a). We were able to determine the activity of SEPHS2_U60C utilizing AMP-glo, which is a luminescence-based assay that detects AMP produced by the ATPase function of SEPHS2_U60C. Included in the reaction were also magnesium salts and DTT, as magnesium has been reported as a cofactor for SEPHS2 homologues in other species and DTT is important to keep the reactive cysteine in a reduced state[56,162]. We have been able to detect a robust luminescent signal related to SEPHS2_U60C activity, and the level of AMP produced also tracks linearly with enzyme concentration with a slight plateau between 2.5μM and 5μM. This assay appears to be a robust method for determining recombinant SEPHS2_U60C activity (Figure A.3b,c).

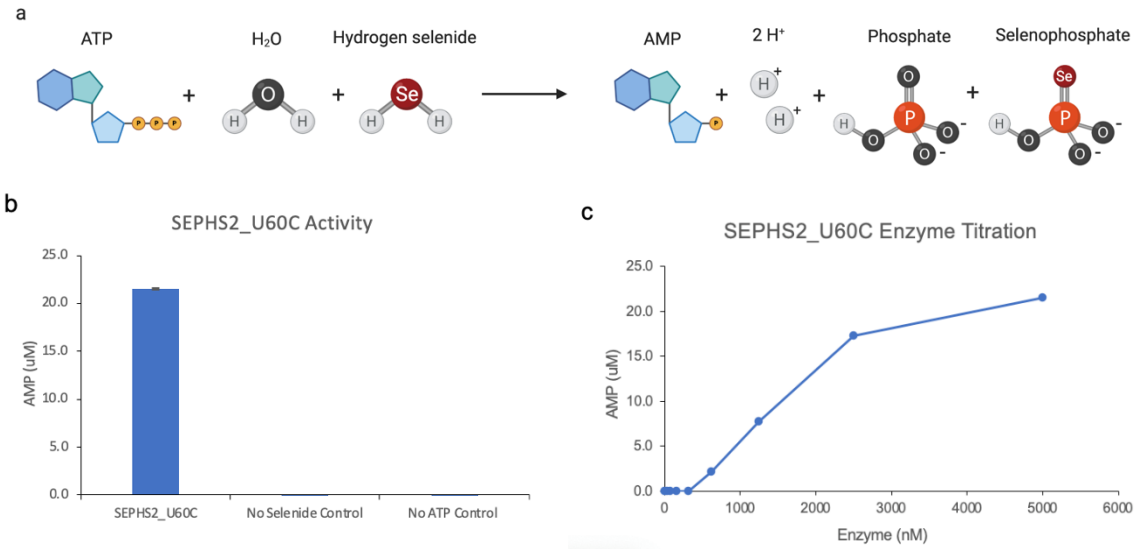

Figure A.3 – Characterization of SEPHS2_U60C activity
a. Diagram of SEPHS2 reaction. Created with BioRender.com
b. AMP produced with 5µM SEPHS2_U60C at 37°C in 30 min.
c. AMP produced with variable concentrations of SEPHS2_U60C at 37°C in 30 min.

Further work on developing this assay for small molecule screening consists of miniaturizing the assay for use with an automated small molecule library testing system. Characterization of any promising SEPHS2_U60C inhibitors would then also have to be applied to a recombinant wild type SEPHS2 system. Recombinant wild-type SEPHS2 propagation and isolation in mammalian cells would then be followed by characterization using the AMP-glo system. After this characterization, any potential inhibitors could be applied to the reaction to assess enzyme inhibition. As discussed in Chapter III, further investigation of any small molecule SEPHS2 inhibitor compounds would consist of assessment of the *in vitro* phenotype in comparison to CRISPR/mediated SEPHS2 KO in cancer cell lines, followed by application to an *in vivo* xenograft model or genetic model for breast cancer. There are numerous steps to follow down the road of SEPHS2 inhibitor discovery. The potential to find an inhibitor that could be used to treat cancer one day is worth the journey.

BIBLIOGRAPHY

1 Surveillance Research Program, N. C. I. *SEER*Explorer: An interactive website for SEER cancer statistics*.

2 Hanahan, D. & Weinberg, R. A. Hallmarks of cancer: the next generation. *Cell* **144**, 646-674, doi:10.1016/j.cell.2011.02.013 (2011).

3 Warburg, O. On the origin of cancer cells. *Science* **123**, 309-314, doi:10.1126/science.123.3191.309 (1956).

4 Vander Heiden, M. G., Cantley, L. C. & Thompson, C. B. Understanding the Warburg effect: the metabolic requirements of cell proliferation. *Science* **324**, 1029-1033, doi:10.1126/science.1160809 (2009).

5 Yang, L., Venneti, S. & Nagrath, D. Glutaminolysis: A Hallmark of Cancer Metabolism. *Annu Rev Biomed Eng* **19**, 163-194, doi:10.1146/annurev-bioeng-071516-044546 (2017).

6 Swinnen, J. V., Brusselmans, K. & Verhoeven, G. Increased lipogenesis in cancer cells: new players, novel targets. *Curr Opin Clin Nutr Metab Care* **9**, 358-365, doi:10.1097/01.mco.0000232894.28674.30 (2006).

7 Currie, E., Schulze, A., Zechner, R., Walther, T. C. & Farese, R. V., Jr. Cellular fatty acid metabolism and cancer. *Cell Metab* **18**, 153-161, doi:10.1016/j.cmet.2013.05.017 (2013).

8 Fauman, E. B., Rai, B. K. & Huang, E. S. Structure-based druggability assessment--identifying suitable targets for small molecule therapeutics. *Curr Opin Chem Biol* **15**, 463-468, doi:10.1016/j.cbpa.2011.05.020 (2011).

9 Xu, D., Jalal, S. I., Sledge, G. W. & Meroueh, S. O. Small-molecule binding sites to explore protein-protein interactions in the cancer proteome. *Mol Biosyst* **12**, 3067-3087, doi:10.1039/c6mb00231e (2016).

10 DeBerardinis, R. J. & Chandel, N. S. Fundamentals of cancer metabolism. *Sci Adv* **2**, e1600200, doi:10.1126/sciadv.1600200 (2016).

11 Robinson, A. D., Eich, M. L. & Varambally, S. Dysregulation of de novo nucleotide biosynthetic pathway enzymes in cancer and targeting opportunities. *Cancer Lett* **470**, 134-140, doi:10.1016/j.canlet.2019.11.013 (2020).

12 Locasale, J. W. *et al.* Phosphoglycerate dehydrogenase diverts glycolytic flux and contributes to oncogenesis. *Nat Genet* **43**, 869-874, doi:10.1038/ng.890 (2011).

13 Farber, S. & Diamond, L. K. Temporary remissions in acute leukemia in children produced by folic acid antagonist, 4-aminopteroyl-glutamic acid. *N Engl J Med* **238**, 787-793, doi:10.1056/NEJM194806032382301 (1948).

14 Cantor, J. R. *et al.* Physiologic Medium Rewires Cellular Metabolism and Reveals Uric Acid as an Endogenous Inhibitor of UMP Synthase. *Cell* **169**, 258-272 e217, doi:10.1016/j.cell.2017.03.023 (2017).

15 Wexler, P. TOXNET: an evolving web resource for toxicology and environmental health information. *Toxicology* **157**, 3-10 (2001).

16 Kim, S. *et al.* PubChem Substance and Compound databases. *Nucleic Acids Res* **44**, D1202-1213, doi:10.1093/nar/gkv951 (2016).

17 Burgos-Barragan, G. *et al.* Mammals divert endogenous genotoxic formaldehyde into one-carbon metabolism. *Nature* **548**, 549-554, doi:10.1038/nature23481 (2017).
18 Blau, N., van Spronsen, F. J. & Levy, H. L. Phenylketonuria. *Lancet* **376**, 1417-1427, doi:10.1016/S0140-6736(10)60961-0 (2010).
19 Blackburn, P. R. *et al.* Maple syrup urine disease: mechanisms and management. *Appl Clin Genet* **10**, 57-66, doi:10.2147/TACG.S125962 (2017).
20 Kanehisa, M. & Goto, S. KEGG: kyoto encyclopedia of genes and genomes. *Nucleic Acids Res* **28**, 27-30, doi:10.1093/nar/28.1.27 (2000).
21 Possemato, R. *et al.* Functional genomics reveal that the serine synthesis pathway is essential in breast cancer. *Nature* **476**, 346-350, doi:10.1038/nature10350 (2011).
22 Gondi, C. S. *et al.* Downregulation of uPA, uPAR and MMP-9 using small, interfering, hairpin RNA (siRNA) inhibits glioma cell invasion, angiogenesis and tumor growth. *Neuron Glia Biol* **1**, 165-176, doi:10.1017/s1740925x04000237 (2004).
23 Sanjana, N. E., Shalem, O. & Zhang, F. Improved vectors and genome-wide libraries for CRISPR screening. *Nat Methods* **11**, 783-784, doi:10.1038/nmeth.3047 (2014).
24 Lentsch, E. *et al.* CRISPR/Cas9-Mediated Knock-Out of Kras(G12D) Mutated Pancreatic Cancer Cell Lines. *Int J Mol Sci* **20**, doi:10.3390/ijms20225706 (2019).
25 Schwarz, K. & Foltz, C. M. SELENIUM AS AN INTEGRAL PART OF FACTOR 3 AGAINST DIETARY NECROTIC LIVER DEGENERATION. *Journal of the American Chemical Society* **79**, 3292-3293, doi:10.1021/ja01569a087 (1957).
26 Weeks, M. E. The discovery of the elements. VI. Tellurium and selenium. *Journal of Chemical Education* **9**, 474, doi:10.1021/ed009p474 (1932).
27 Chun, O. K. *et al.* Estimation of antioxidant intakes from diet and supplements in U.S. adults. *J Nutr* **140**, 317-324, doi:10.3945/jn.109.114413 (2010).
28 Filippini, T. *et al.* Diet composition and serum levels of selenium species: A cross-sectional study. *Food Chem Toxicol* **115**, 482-490, doi:10.1016/j.fct.2018.03.048 (2018).
29 Sager, M. Selenium in agriculture, food, and nutrition. *Pure and Applied Chemistry* **78**, 111-133, doi:https://doi.org/10.1351/pac200678010111 (2006).
30 Thomson, C. D. & Robinson, M. F. Urinary and fecal excretions and absorption of a large supplement of selenium: superiority of selenate over selenite. *Am J Clin Nutr* **44**, 659-663, doi:10.1093/ajcn/44.5.659 (1986).
31 Vendeland, S. C., Deagen, J. T., Butler, J. A. & Whanger, P. D. Uptake of selenite, selenomethionine and selenate by brush border membrane vesicles isolated from rat small intestine. *Biometals* **7**, 305-312, doi:10.1007/BF00144126 (1994).
32 Esaki, N. *et al.* Enzymatic synthesis of selenocysteine in rat liver. *Biochemistry* **20**, 4492-4496, doi:10.1021/bi00518a039 (1981).

33 Olm, E. *et al.* Extracellular thiol-assisted selenium uptake dependent on the x(c)-cystine transporter explains the cancer-specific cytotoxicity of selenite. *Proc Natl Acad Sci U S A* **106**, 11400-11405, doi:10.1073/pnas.0902204106 (2009).

34 Guimaraes, M. J. *et al.* Identification of a novel selD homolog from eukaryotes, bacteria, and archaea: is there an autoregulatory mechanism in selenocysteine metabolism? *Proc Natl Acad Sci U S A* **93**, 15086-15091, doi:10.1073/pnas.93.26.15086 (1996).

35 Xu, X.-M. *et al.* Selenophosphate synthetase 2 is essential for selenoprotein biosynthesis. *Biochemical Journal* **404**, 115-120, doi:10.1042/BJ20070165 (2007).

36 Xu, X. M. *et al.* Biosynthesis of selenocysteine on its tRNA in eukaryotes. *PLoS Biol* **5**, e4, doi:10.1371/journal.pbio.0050004 (2007).

37 Hatfield, D. & Portugal, F. H. Seryl-tRNA in mammalian tissues: chromatographic differences in brain and liver and a specific response to the codon, UGA. *Proc Natl Acad Sci U S A* **67**, 1200-1206, doi:10.1073/pnas.67.3.1200 (1970).

38 Berry, M. J. *et al.* Recognition of UGA as a selenocysteine codon in type I deiodinase requires sequences in the 3' untranslated region. *Nature* **353**, 273-276, doi:10.1038/353273a0 (1991).

39 Fagegaltier, D., Lescure, A., Walczak, R., Carbon, P. & Krol, A. Structural analysis of new local features in SECIS RNA hairpins. *Nucleic Acids Res* **28**, 2679-2689, doi:10.1093/nar/28.14.2679 (2000).

40 Tujebajeva, R. M. *et al.* Decoding apparatus for eukaryotic selenocysteine insertion. *EMBO Rep* **1**, 158-163, doi:10.1093/embo-reports/kvd033 (2000).

41 Copeland, P. R., Fletcher, J. E., Carlson, B. A., Hatfield, D. L. & Driscoll, D. M. A novel RNA binding protein, SBP2, is required for the translation of mammalian selenoprotein mRNAs. *EMBO J* **19**, 306-314, doi:10.1093/emboj/19.2.306 (2000).

42 Fletcher, J. E., Copeland, P. R., Driscoll, D. M. & Krol, A. The selenocysteine incorporation machinery: interactions between the SECIS RNA and the SECIS-binding protein SBP2. *RNA* **7**, 1442-1453 (2001).

43 Fagegaltier, D. *et al.* Characterization of mSelB, a novel mammalian elongation factor for selenoprotein translation. *EMBO J* **19**, 4796-4805, doi:10.1093/emboj/19.17.4796 (2000).

44 Donovan, J., Caban, K., Ranaweera, R., Gonzalez-Flores, J. N. & Copeland, P. R. A novel protein domain induces high affinity selenocysteine insertion sequence binding and elongation factor recruitment. *J Biol Chem* **283**, 35129-35139, doi:10.1074/jbc.M806008200 (2008).

45 Maciel-Dominguez, A., Swan, D., Ford, D. & Hesketh, J. Selenium alters miRNA profile in an intestinal cell line: evidence that miR-185 regulates expression of GPX2 and SEPSH2. *Mol Nutr Food Res* **57**, 2195-2205, doi:10.1002/mnfr.201300168 (2013).

46 Chavatte, L., Brown, B. A. & Driscoll, D. M. Ribosomal protein L30 is a component of the UGA-selenocysteine recoding machinery in eukaryotes. *Nat Struct Mol Biol* **12**, 408-416, doi:10.1038/nsmb922 (2005).

47 Budiman, M. E. *et al.* Eukaryotic initiation factor 4a3 is a selenium-regulated RNA-binding protein that selectively inhibits selenocysteine incorporation. *Mol Cell* **35**, 479-489, doi:10.1016/j.molcel.2009.06.026 (2009).

48 Burk, R. F., Hill, K. E. & Motley, A. K. Plasma selenium in specific and non-specific forms. *Biofactors* **14**, 107-114, doi:10.1002/biof.5520140115 (2001).

49 Mihara, H., Kurihara, T., Watanabe, T., Yoshimura, T. & Esaki, N. cDNA cloning, purification, and characterization of mouse liver selenocysteine lyase. Candidate for selenium delivery protein in selenoprotein synthesis. *J Biol Chem* **275**, 6195-6200, doi:10.1074/jbc.275.9.6195 (2000).

50 Esaki, N., Nakamura, T., Tanaka, H. & Soda, K. Selenocysteine lyase, a novel enzyme that specifically acts on selenocysteine. Mammalian distribution and purification and properties of pig liver enzyme. *J Biol Chem* **257**, 4386-4391 (1982).

51 Xu, X. M. *et al.* Selenophosphate synthetase 2 is essential for selenoprotein biosynthesis. *Biochem J* **404**, 115-120, doi:10.1042/BJ20070165 (2007).

52 Na, J. *et al.* Selenophosphate synthetase 1 and its role in redox homeostasis, defense and proliferation. *Free Radic Biol Med* **127**, 190-197, doi:10.1016/j.freeradbiomed.2018.04.577 (2018).

53 Peyroche, G. *et al.* Sodium selenide toxicity is mediated by O2-dependent DNA breaks. *PLoS One* **7**, e36343, doi:10.1371/journal.pone.0036343 (2012).

54 Kern, J. C. & Kehrer, J. P. Free radicals and apoptosis: relationships with glutathione, thioredoxin, and the BCL family of proteins. *Front Biosci* **10**, 1727-1738, doi:10.2741/1656 (2005).

55 UniProt, C. UniProt: a worldwide hub of protein knowledge. *Nucleic Acids Res* **47**, D506-D515, doi:10.1093/nar/gky1049 (2019).

56 Wang, K. T., Wang, J., Li, L. F. & Su, X. D. Crystal structures of catalytic intermediates of human selenophosphate synthetase 1. *J Mol Biol* **390**, 747-759, doi:10.1016/j.jmb.2009.05.032 (2009).

57 Noinaj, N. *et al.* Structural insights into the catalytic mechanism of Escherichia coli selenophosphate synthetase. *J Bacteriol* **194**, 499-508, doi:10.1128/JB.06012-11 (2012).

58 Nunziata, C. *et al.* Structural analysis of human SEPHS2 protein, a selenocysteine machinery component, over-expressed in triple negative breast cancer. *Sci Rep* **9**, 16131, doi:10.1038/s41598-019-52718-0 (2019).

59 World Health, O., Food & Agricultural Organization of the United, N. 341 (World Health Organization and Food and Agriculture Organization of the United Nations, 2004).

60 Navarro-Alarcon, M. & Cabrera-Vique, C. Selenium in food and the human body: a review. *Sci Total Environ* **400**, 115-141, doi:10.1016/j.scitotenv.2008.06.024 (2008).

61 Combs, G. F., Jr. Food system-based approaches to improving micronutrient nutrition: the case for selenium. *Biofactors* **12**, 39-43, doi:10.1002/biof.5520120107 (2000).

62 Chen, X. *et al.* Studies on the relations of selenium and Keshan disease. *Biol Trace Elem Res* **2**, 91-107, doi:10.1007/BF02798589 (1980).

63 Beck, M. A. *et al.* Selenium deficiency increases the pathology of an influenza virus infection. *FASEB J* **15**, 1481-1483 (2001).

64 Moghaddam, A. *et al.* Selenium Deficiency Is Associated with Mortality Risk from COVID-19. *Nutrients* **12**, doi:10.3390/nu12072098 (2020).

65 Forceville, X. *et al.* Selenium, systemic immune response syndrome, sepsis, and outcome in critically ill patients. *Crit Care Med* **26**, 1536-1544, doi:10.1097/00003246-199809000-00021 (1998).

66 Marsden, W. *The travels of Marco Polo (1271-1285)*. (The Heritage Press, 1962).

67 Spallholz, J. E. On the nature of selenium toxicity and carcinostatic activity. *Free Radic Biol Med* **17**, 45-64 (1994).

68 Alderman, L. C. & Bergin, J. J. Hydrogen selenide poisoning: an illustrative case with review of the literature. *Arch Environ Health* **41**, 354-358, doi:10.1080/00039896.1986.9935778 (1986).

69 Chawla, R. *et al.* Exposure to a high selenium environment in Punjab, India: Biomarkers and health conditions. *Sci Total Environ* **719**, 134541, doi:10.1016/j.scitotenv.2019.134541 (2020).

70 Nuttall, K. L. Evaluating selenium poisoning. *Ann Clin Lab Sci* **36**, 409-420 (2006).

71 Morris, J. S. & Crane, S. B. Selenium toxicity from a misformulated dietary supplement, adverse health effects, and the temporal response in the nail biologic monitor. *Nutrients* **5**, 1024-1057, doi:10.3390/nu5041024 (2013).

72 Banerjee, B. D., Dwivedi, S. & Singh, S. Acute hydrogen selenide gas poisoning admissions in one of the hospitals in Delhi, India: case report. *Hum Exp Toxicol* **16**, 276-278, doi:10.1177/096032719701600508 (1997).

73 Schecter, A., Shanske, W., Stenzler, A., Quintilian, H. & Steinberg, H. Acute hydrogen selenide inhalation. *Chest* **77**, 554-555 (1980).

74 Health, N. I. f. O. S. a. (NIOSH Publications, Cincinnati, Ohio, 2007).

75 Friberg L, N. G., Vouk VB. *Handbook on the toxicology of metals*. p. 568 (Elsevier North Holland, 1979).

76 Cone, J. E., Del Rio, R. M., Davis, J. N. & Stadtman, T. C. Chemical characterization of the selenoprotein component of clostridial glycine reductase: identification of selenocysteine as the organoselenium moiety. *Proc Natl Acad Sci U S A* **73**, 2659-2663, doi:10.1073/pnas.73.8.2659 (1976).

77 Bock, A. *et al.* Selenocysteine: the 21st amino acid. *Mol Microbiol* **5**, 515-520, doi:10.1111/j.1365-2958.1991.tb00722.x (1991).

78 Gromer, S. *et al.* Active sites of thioredoxin reductases: why selenoproteins? *Proc Natl Acad Sci U S A* **100**, 12618-12623, doi:10.1073/pnas.2134510100 (2003).

79 Snider, G. W., Ruggles, E., Khan, N. & Hondal, R. J. Selenocysteine confers resistance to inactivation by oxidation in thioredoxin reductase: comparison of selenium and sulfur enzymes. *Biochemistry* **52**, 5472-5481, doi:10.1021/bi400462j (2013).

80 Taskov, K. *et al.* Nematode selenoproteome: the use of the selenocysteine insertion system to decode one codon in an animal genome? *Nucleic Acids Res* **33**, 2227-2238, doi:10.1093/nar/gki507 (2005).
81 Gobler, C. J. *et al.* The central role of selenium in the biochemistry and ecology of the harmful pelagophyte, Aureococcus anophagefferens. *ISME J* **7**, 1333-1343, doi:10.1038/ismej.2013.25 (2013).
82 Lobanov, A. V., Hatfield, D. L. & Gladyshev, V. N. Selenoproteinless animals: selenophosphate synthetase SPS1 functions in a pathway unrelated to selenocysteine biosynthesis. *Protein Sci* **17**, 176-182, doi:10.1110/ps.073261508 (2008).
83 Lobanov, A. V. *et al.* Evolutionary dynamics of eukaryotic selenoproteomes: large selenoproteomes may associate with aquatic life and small with terrestrial life. *Genome Biol* **8**, R198, doi:10.1186/gb-2007-8-9-r198 (2007).
84 Labunskyy, V. M., Hatfield, D. L. & Gladyshev, V. N. Selenoproteins: molecular pathways and physiological roles. *Physiol Rev* **94**, 739-777, doi:10.1152/physrev.00039.2013 (2014).
85 Short, S. P. & Williams, C. S. Selenoproteins in Tumorigenesis and Cancer Progression. *Adv Cancer Res* **136**, 49-83, doi:10.1016/bs.acr.2017.08.002 (2017).
86 Ursini, F. *et al.* Diversity of glutathione peroxidases. *Methods Enzymol* **252**, 38-53, doi:10.1016/0076-6879(95)52007-4 (1995).
87 Toppo, S., Flohe, L., Ursini, F., Vanin, S. & Maiorino, M. Catalytic mechanisms and specificities of glutathione peroxidases: variations of a basic scheme. *Biochim Biophys Acta* **1790**, 1486-1500, doi:10.1016/j.bbagen.2009.04.007 (2009).
88 Tamura, T. & Stadtman, T. C. A new selenoprotein from human lung adenocarcinoma cells: purification, properties, and thioredoxin reductase activity. *Proc Natl Acad Sci U S A* **93**, 1006-1011, doi:10.1073/pnas.93.3.1006 (1996).
89 Chu, F. F. *et al.* Expression and chromosomal mapping of mouse Gpx2 gene encoding the gastrointestinal form of glutathione peroxidase, GPX-GI. *Biomed Environ Sci* **10**, 156-162 (1997).
90 Choi, J. H. *et al.* Overexpression of mitochondrial thioredoxin reductase and peroxiredoxin III in hepatocellular carcinomas. *Anticancer Res* **22**, 3331-3335 (2002).
91 Dixon, S. J. *et al.* Ferroptosis: an iron-dependent form of nonapoptotic cell death. *Cell* **149**, 1060-1072, doi:10.1016/j.cell.2012.03.042 (2012).
92 Yang, W. S. *et al.* Regulation of ferroptotic cancer cell death by GPX4. *Cell* **156**, 317-331, doi:10.1016/j.cell.2013.12.010 (2014).
93 Sato, H., Tamba, M., Ishii, T. & Bannai, S. Cloning and expression of a plasma membrane cystine/glutamate exchange transporter composed of two distinct proteins. *J Biol Chem* **274**, 11455-11458, doi:10.1074/jbc.274.17.11455 (1999).
94 Sato, H. *et al.* Redox imbalance in cystine/glutamate transporter-deficient mice. *J Biol Chem* **280**, 37423-37429, doi:10.1074/jbc.M506439200 (2005).
95 Croteau, W., Davey, J. C., Galton, V. A. & St Germain, D. L. Cloning of the mammalian type II iodothyronine deiodinase. A selenoprotein differentially

expressed and regulated in human and rat brain and other tissues. *J Clin Invest* **98**, 405-417, doi:10.1172/JCI118806 (1996).

96 Jo, S. *et al.* Type 2 deiodinase polymorphism causes ER stress and hypothyroidism in the brain. *J Clin Invest* **129**, 230-245, doi:10.1172/JCI123176 (2019).

97 Fekkes, D., Hennemann, G. & Visser, T. J. Evidence for a single enzyme in rat liver catalysing the deiodination of the tyrosyl and the phenolic ring of iodothyronines. *Biochem J* **201**, 673-676, doi:10.1042/bj2010673 (1982).

98 Zhang, L., Zhu, J. H., Zhang, X. & Cheng, W. H. The Thioredoxin-Like Family of Selenoproteins: Implications in Aging and Age-Related Degeneration. *Biol Trace Elem Res* **188**, 189-195, doi:10.1007/s12011-018-1521-9 (2019).

99 Yan, J., Fei, Y., Han, Y. & Lu, S. Selenoprotein O deficiencies suppress chondrogenic differentiation of ATDC5 cells. *Cell Biol Int* **40**, 1033-1040, doi:10.1002/cbin.10644 (2016).

100 Zhuang, C. *et al.* Selenomethionine Suppressed TLR4/NF-kappaB Pathway by Activating Selenoprotein S to Alleviate ESBL Escherichia coli-Induced Inflammation in Bovine Mammary Epithelial Cells and Macrophages. *Front Microbiol* **11**, 1461, doi:10.3389/fmicb.2020.01461 (2020).

101 Zhang, Y. *et al.* Role of Selenoproteins in Redox Regulation of Signaling and the Antioxidant System: A Review. *Antioxidants (Basel)* **9**, doi:10.3390/antiox9050383 (2020).

102 Chen, B. *et al.* GPx3 promoter hypermethylation is a frequent event in human cancer and is associated with tumorigenesis and chemotherapy response. *Cancer Lett* **309**, 37-45, doi:10.1016/j.canlet.2011.05.013 (2011).

103 Saito, Y., Watanabe, Y., Saito, E., Honjoh, T. & Takahashi, K. Production and Application of Monoclonal Antibodies to Human Selenoprotein P. *Journal of Health Science* **47**, 346-352, doi:10.1248/jhs.47.346 (2001).

104 Burk, R. F. *et al.* Selenoprotein P and apolipoprotein E receptor-2 interact at the blood-brain barrier and also within the brain to maintain an essential selenium pool that protects against neurodegeneration. *FASEB J* **28**, 3579-3588, doi:10.1096/fj.14-252874 (2014).

105 Hill, K. E. *et al.* Production of selenoprotein P (Sepp1) by hepatocytes is central to selenium homeostasis. *J Biol Chem* **287**, 40414-40424, doi:10.1074/jbc.M112.421404 (2012).

106 Burk, R. F., Hill, K. E., Motley, A. K., Austin, L. M. & Norsworthy, B. K. Deletion of selenoprotein P upregulates urinary selenium excretion and depresses whole-body selenium content. *Biochim Biophys Acta* **1760**, 1789-1793, doi:10.1016/j.bbagen.2006.08.010 (2006).

107 Vinceti, M., Filippini, T., Cilloni, S. & Crespi, C. M. The Epidemiology of Selenium and Human Cancer. *Adv Cancer Res* **136**, 1-48, doi:10.1016/bs.acr.2017.07.001 (2017).

108 Muecke, R. *et al.* Multicenter, phase III trial comparing selenium supplementation with observation in gynecologic radiation oncology: follow-up analysis of the

survival data 6 years after cessation of randomization. *Integr Cancer Ther* **13**, 463-467, doi:10.1177/1534735414541963 (2014).

109 Karamali, M., Nourgostar, S., Zamani, A., Vahedpoor, Z. & Asemi, Z. The favourable effects of long-term selenium supplementation on regression of cervical tissues and metabolic profiles of patients with cervical intraepithelial neoplasia: a randomised, double-blind, placebo-controlled trial. *Br J Nutr* **114**, 2039-2045, doi:10.1017/S0007114515003852 (2015).

110 Panieri, E. & Santoro, M. M. ROS homeostasis and metabolism: a dangerous liason in cancer cells. *Cell Death Dis* **7**, e2253, doi:10.1038/cddis.2016.105 (2016).

111 Lu, Y. P. *et al.* Enhanced skin carcinogenesis in transgenic mice with high expression of glutathione peroxidase or both glutathione peroxidase and superoxide dismutase. *Cancer Res* **57**, 1468-1474 (1997).

112 Gan, X. *et al.* High GPX1 expression promotes esophageal squamous cell carcinoma invasion, migration, proliferation and cisplatin-resistance but can be reduced by vitamin D. *Int J Clin Exp Med* **7**, 2530-2540 (2014).

113 Wu, X. M., Lu, J., Li, B. R., Zhang, B. G. & Ru, R. P. [Therapeutic effects of epimeric glycyrrhizic acids on hepatic injury in rats]. *Zhongguo Yao Li Xue Bao* **13**, 370-374 (1992).

114 Perez, S., Talens-Visconti, R., Rius-Perez, S., Finamor, I. & Sastre, J. Redox signaling in the gastrointestinal tract. *Free Radic Biol Med* **104**, 75-103, doi:10.1016/j.freeradbiomed.2016.12.048 (2017).

115 Cavalieri, R. R., Scott, K. G. & Sairenji, E. Selenite (75Se) as a tumor-localizing agent in man. *J Nucl Med* **7**, 197-208 (1966).

116 Tobe, T., Ueda, K., Ando, M., Okamoto, Y. & Kojima, N. Thiol-mediated multiple mechanisms centered on selenodiglutathione determine selenium cytotoxicity against MCF-7 cancer cells. *J Biol Inorg Chem* **20**, 687-694, doi:10.1007/s00775-015-1254-6 (2015).

117 Lo, M., Wang, Y. Z. & Gout, P. W. The x(c)- cystine/glutamate antiporter: a potential target for therapy of cancer and other diseases. *J Cell Physiol* **215**, 593-602, doi:10.1002/jcp.21366 (2008).

118 Takeuchi, S. *et al.* Increased xCT expression correlates with tumor invasion and outcome in patients with glioblastomas. *Neurosurgery* **72**, 33-41; discussion 41, doi:10.1227/NEU.0b013e318276b2de (2013).

119 Shin, S. S. *et al.* Participation of xCT in melanoma cell proliferation in vitro and tumorigenesis in vivo. *Oncogenesis* **7**, 86, doi:10.1038/s41389-018-0098-7 (2018).

120 Kim, D. *et al.* SHMT2 drives glioma cell survival in ischaemia but imposes a dependence on glycine clearance. *Nature* **520**, 363-367, doi:10.1038/nature14363 (2015).

121 Burk, R. F. & Hill, K. E. Regulation of Selenium Metabolism and Transport. *Annu Rev Nutr* **35**, 109-134, doi:10.1146/annurev-nutr-071714-034250 (2015).

122 Amoedo, N. D., Obre, E. & Rossignol, R. Drug discovery strategies in the field of tumor energy metabolism: Limitations by metabolic flexibility and metabolic

resistance to chemotherapy. *Biochim Biophys Acta Bioenerg* **1858**, 674-685, doi:10.1016/j.bbabio.2017.02.005 (2017).

123 Strickland, L. B., Dawson, P. J., Santner, S. J. & Miller, F. R. Progression of premalignant MCF10AT generates heterogeneous malignant variants with characteristic histologic types and immunohistochemical markers. *Breast Cancer Res Treat* **64**, 235-240, doi:10.1023/a:1026562720218 (2000).

124 Cavalieri, R. R. & Scott, K. G. Sodium selenite Se 75. A more specific agent for scanning tumors. *JAMA* **206**, 591-595 (1968).

125 Jiang, C., Wang, Z., Ganther, H. & Lu, J. Distinct effects of methylseleninic acid versus selenite on apoptosis, cell cycle, and protein kinase pathways in DU145 human prostate cancer cells. *Mol Cancer Ther* **1**, 1059-1066 (2002).

126 Kim, J. Y. *et al.* Human cystine/glutamate transporter: cDNA cloning and upregulation by oxidative stress in glioma cells. *Biochim Biophys Acta* **1512**, 335-344, doi:10.1016/s0005-2736(01)00338-8 (2001).

127 Jiang, L. *et al.* Ferroptosis as a p53-mediated activity during tumour suppression. *Nature* **520**, 57-62, doi:10.1038/nature14344 (2015).

128 Hangauer, M. J. *et al.* Drug-tolerant persister cancer cells are vulnerable to GPX4 inhibition. *Nature* **551**, 247-250, doi:10.1038/nature24297 (2017).

129 Doll, S. *et al.* FSP1 is a glutathione-independent ferroptosis suppressor. *Nature* **575**, 693-698, doi:10.1038/s41586-019-1707-0 (2019).

130 Bersuker, K. *et al.* The CoQ oxidoreductase FSP1 acts parallel to GPX4 to inhibit ferroptosis. *Nature* **575**, 688-692, doi:10.1038/s41586-019-1705-2 (2019).

131 Alim, I. *et al.* Selenium Drives a Transcriptional Adaptive Program to Block Ferroptosis and Treat Stroke. *Cell* **177**, 1262-1279 e1225, doi:10.1016/j.cell.2019.03.032 (2019).

132 Ingold, I. *et al.* Selenium Utilization by GPX4 Is Required to Prevent Hydroperoxide-Induced Ferroptosis. *Cell* **172**, 409-422 e421, doi:10.1016/j.cell.2017.11.048 (2018).

133 Delafiori, J., Ring, G. & Furey, A. Clinical applications of HPLC-ICP-MS element speciation: A review. *Talanta* **153**, 306-331, doi:10.1016/j.talanta.2016.02.035 (2016).

134 Suzuki, K. T. & Ogra, Y. Metabolic pathway for selenium in the body: speciation by HPLC-ICP MS with enriched Se. *Food Addit Contam* **19**, 974-983, doi:10.1080/02652030210153578 (2002).

135 Dauplais, M., Lazard, M., Blanquet, S. & Plateau, P. Neutralization by metal ions of the toxicity of sodium selenide. *PLoS One* **8**, e54353, doi:10.1371/journal.pone.0054353 (2013).

136 Wang, T., Wei, J. J., Sabatini, D. M. & Lander, E. S. Genetic screens in human cells using the CRISPR-Cas9 system. *Science* **343**, 80-84, doi:10.1126/science.1246981 (2014).

137 Sheehan, T. M. & Gao, M. Simplified fluorometric assay of total selenium in plasma and urine. *Clin Chem* **36**, 2124-2126 (1990).

138 A Package for Survival Analysis in S. Version 2.38. (CRAN website - http//cran.r-project.org/package=survival, 2015).

139 Harrington, D. P. F., T. R. . A class of rank test procedures for censored survival data. *Biometrika*, doi:10.1093/biomet/69.3.553 (1982).
140 Ciriello, G. *et al.* Comprehensive Molecular Portraits of Invasive Lobular Breast Cancer. *Cell* **163**, 506-519, doi:10.1016/j.cell.2015.09.033 (2015).
141 Cerami, E. *et al.* The cBio cancer genomics portal: an open platform for exploring multidimensional cancer genomics data. *Cancer Discov* **2**, 401-404, doi:10.1158/2159-8290.CD-12-0095 (2012).
142 Spallholz, J. E. Free radical generation by selenium compounds and their prooxidant toxicity. *Biomed Environ Sci* **10**, 260-270 (1997).
143 Stefan, R. I., Aboul-Enein, H. Y. & Radu, G. L. Biosensors for the enantioselective analysis of S-enalapril and S-ramipril. *Prep Biochem Biotechnol* **28**, 305-312, doi:10.1080/10826069808010143 (1998).
144 Habib, E., Linher-Melville, K., Lin, H. X. & Singh, G. Expression of xCT and activity of system xc(-) are regulated by NRF2 in human breast cancer cells in response to oxidative stress. *Redox Biol* **5**, 33-42, doi:10.1016/j.redox.2015.03.003 (2015).
145 Wang, G. L. & Semenza, G. L. General involvement of hypoxia-inducible factor 1 in transcriptional response to hypoxia. *Proc Natl Acad Sci U S A* **90**, 4304-4308, doi:10.1073/pnas.90.9.4304 (1993).
146 Toth, R. K. & Warfel, N. A. Strange Bedfellows: Nuclear Factor, Erythroid 2-Like 2 (Nrf2) and Hypoxia-Inducible Factor 1 (HIF-1) in Tumor Hypoxia. *Antioxidants (Basel)* **6**, doi:10.3390/antiox6020027 (2017).
147 Renschler, M. F. The emerging role of reactive oxygen species in cancer therapy. *Eur J Cancer* **40**, 1934-1940, doi:10.1016/j.ejca.2004.02.031 (2004).
148 Ghandi, M. *et al.* Next-generation characterization of the Cancer Cell Line Encyclopedia. *Nature* **569**, 503-508, doi:10.1038/s41586-019-1186-3 (2019).
149 Tang, Z. *et al.* GEPIA: a web server for cancer and normal gene expression profiling and interactive analyses. *Nucleic Acids Res* **45**, W98-W102, doi:10.1093/nar/gkx247 (2017).
150 Murdolo, G. *et al.* Selenium and Cancer Stem Cells. *Advances in cancer research* **136**, 235-257, doi:10.1016/bs.acr.2017.07.006 (2017).
151 Park, S.-Y., Choi, J.-H. & Nam, J.-S. Targeting Cancer Stem Cells in Triple-Negative Breast Cancer. *Cancers* **11**, 965, doi:10.3390/cancers11070965 (2019).
152 Diwakar, B. T., Korwar, A. M., Paulson, R. F. & Prabhu, K. S. The Regulation of Pathways of Inflammation and Resolution in Immune Cells and Cancer Stem Cells by Selenium. *Advances in cancer research* **136**, 153-172, doi:10.1016/bs.acr.2017.07.003 (2017).
153 Lipinski, B. Rationale for the treatment of cancer with sodium selenite. *Med Hypotheses* **64**, 806-810, doi:10.1016/j.mehy.2004.10.012 (2005).
154 Zhong, W. & Oberley, T. D. Redox-mediated effects of selenium on apoptosis and cell cycle in the LNCaP human prostate cancer cell line. *Cancer Res* **61**, 7071-7078 (2001).
155 Latreche, L., Jean-Jean, O., Driscoll, D. M. & Chavatte, L. Novel structural determinants in human SECIS elements modulate the translational recoding of

UGA as selenocysteine. *Nucleic Acids Res* **37**, 5868-5880, doi:10.1093/nar/gkp635 (2009).

156 Banerjee, S., Yang, S. & Foster, C. B. A luciferase reporter assay to investigate the differential selenium-dependent stability of selenoprotein mRNAs. *J Nutr Biochem* **23**, 1294-1301, doi:10.1016/j.jnutbio.2011.07.010 (2012).

157 Savaskan, N. E. *et al.* Small interfering RNA-mediated xCT silencing in gliomas inhibits neurodegeneration and alleviates brain edema. *Nat Med* **14**, 629-632, doi:10.1038/nm1772 (2008).

158 Takano, T. *et al.* Glutamate release promotes growth of malignant gliomas. *Nat Med* **7**, 1010-1015, doi:10.1038/nm0901-1010 (2001).

159 Riegman, M. *et al.* Ferroptosis occurs through an osmotic mechanism and propagates independently of cell rupture. *Nat Cell Biol* **22**, 1042-1048, doi:10.1038/s41556-020-0565-1 (2020).

160 Arner, E. S., Sarioglu, H., Lottspeich, F., Holmgren, A. & Bock, A. High-level expression in Escherichia coli of selenocysteine-containing rat thioredoxin reductase utilizing gene fusions with engineered bacterial-type SECIS elements and co-expression with the selA, selB and selC genes. *J Mol Biol* **292**, 1003-1016, doi:10.1006/jmbi.1999.3085 (1999).

161 Kamada, S. *et al.* A non-radioactive assay for selenophosphate synthetase activity using recombinant pyruvate pyrophosphate dikinase from Thermus thermophilus HB8. *Biosci Biotechnol Biochem* **80**, 1970-1972, doi:10.1080/09168451.2016.1200458 (2016).

162 Crawhall, J. C. & Segal, S. Dithiothreitol in the study of cysteine transport. *Biochim Biophys Acta* **121**, 215-217, doi:10.1016/0304-4165(66)90380-1 (1966).